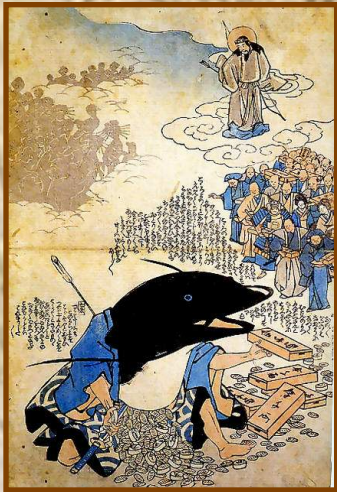


Earthquakes on Compressional Inversion Structures – Problems in Mechanics and in Hazard Assessment

Richard H. Sibson
University of Otago



**"WATER IS THE DRIVING FORCE
OF ALL NATURE"**

- Leonardo da Vinci

UNIVERSITY
of
OTAGO



Te Whare Wānanga o Ōtāgo

2016 SCEC Annual Meeting, Palm Springs, CA

SC ~~1~~ EC

Signals in Stone



20 cm

Fault-Infill Vein, Elandshoogte Mine, Sth. Africa

What Drives Fault Failure?

- *Shear Failure of Intact Rock (Coulomb Criterion)*

$$\tau = C_i + \mu_s(\sigma_n - P_f)$$

- *Griffith Failure Criterion*

$$\tau^2 = 4T_o(\sigma_n - P_f) + 4T_o^2$$

- *Reshear of Existing Faults*

$$\tau = c + \mu_s(\sigma_n - P_f)$$

- *Hydraulic Extension Fracturing*

$$P_f = \sigma_3 + T_o$$

when $(\sigma_1 - \sigma_3) < 4T_o$

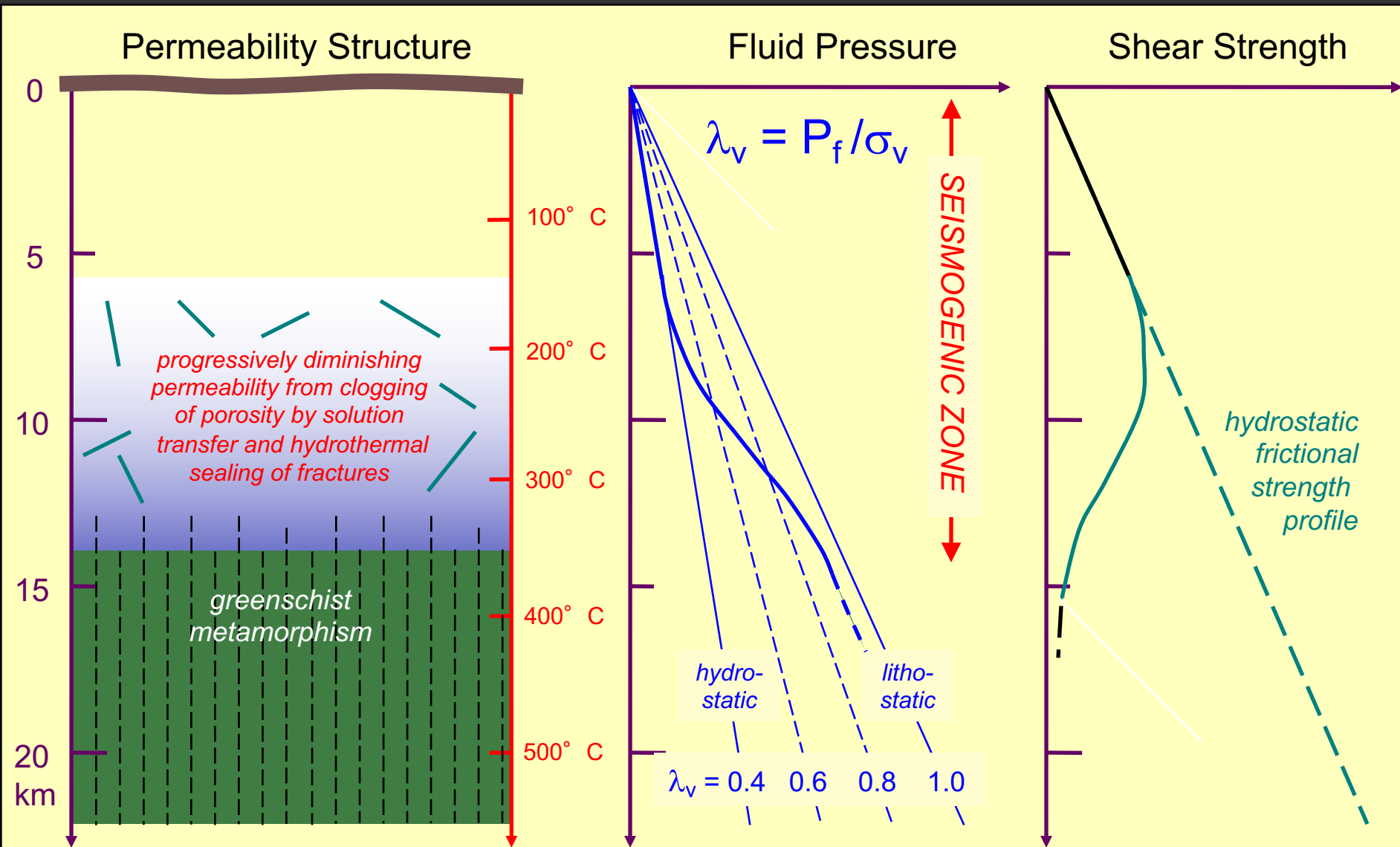
TWO drivers to failure - $\Delta(\sigma_1 - \sigma_3)$ and ΔP_f



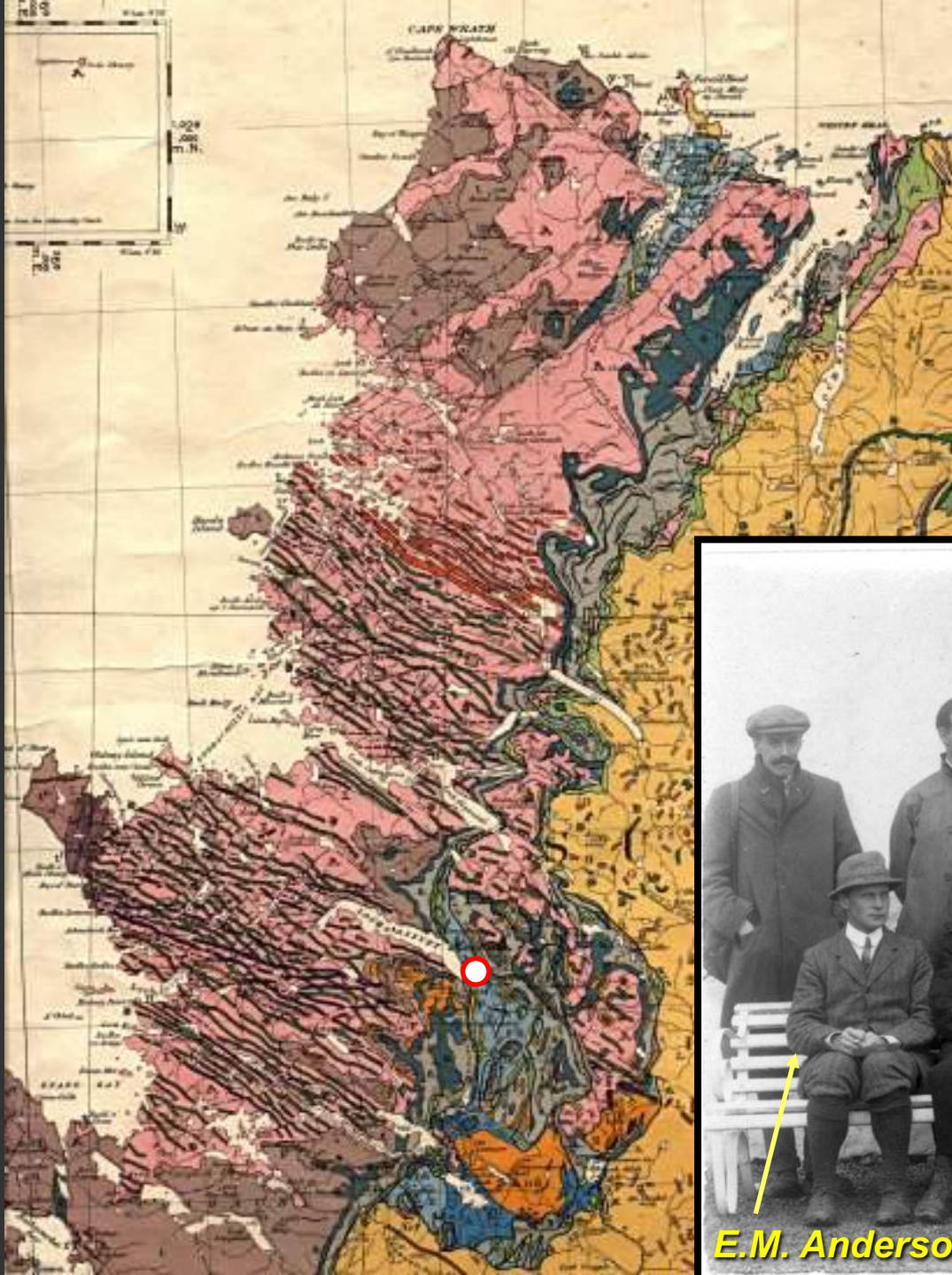
- increasing STRESS

- decreasing STRENGTH

Fluid Overpressure – Another Variable?



1. THE ORIGINAL FAULT MECHANIC



Mapping the Moine Thrust, NW Scotland c. 1885-1905



INCHNADAMPH
1912

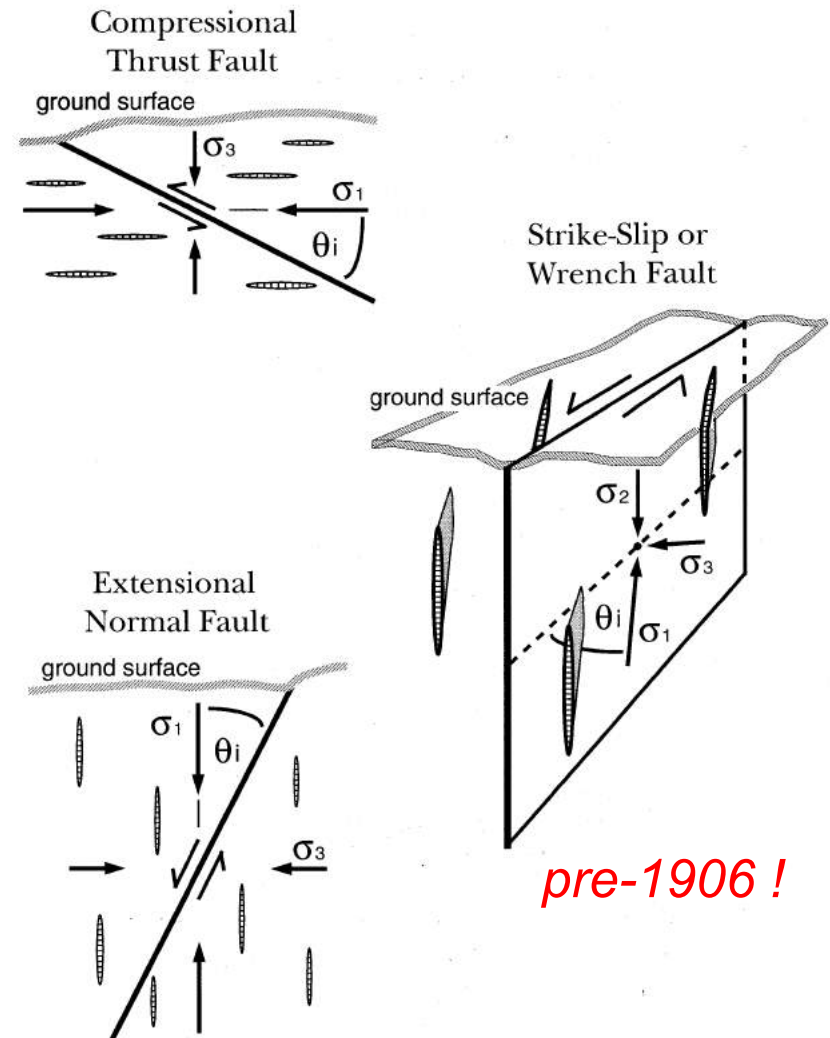
E.M. Anderson

- BGS Photo Archives

E.M. Anderson – 'The Dynamics of Faulting' (1905)

Trans. Geol. Soc. Edin. 8, 387-402 – foundation paper in frictional fault mechanics

- No shear stress along the rock-air interface at Earth's surface
- One principal stress subvertical – **stress trajectories generally vertical or horizontal**
- There are therefore **THREE fundamental stress regimes** in the Earth's crust depending whether $\sigma_v = \sigma_1$, σ_2 , or σ_3
- Faults develop in homogeneous, isotropic, intact crust in accordance with the Coulomb shear failure criterion, forming along planes containing σ_2 lying at c. $25-30^\circ$ to σ_1
- **THREE fundamental fault types: NORMAL Faults ($\sigma_v = \sigma_1$), THRUST Faults ($\sigma_v = \sigma_3$), and WRENCH (Strike-Slip) Faults ($\sigma_v = \sigma_2$).**



- relates to **fault initiation** – works well for **low-displacement faults**

Low-Displacement Reverse Faults Commonly Exhibit 'Andersonian' Relationships

Holocene Thrust, SE Iran



Minor Thrust, SE Otago, NZ



Quartz Veins associated with Thrust Fault, Oguf Gynfor, Anglesey



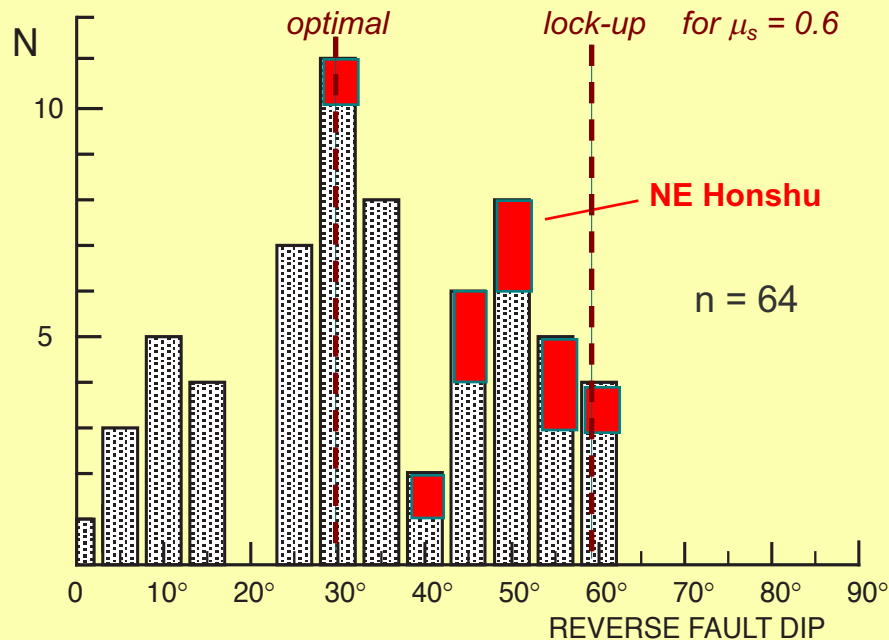
Conjugate Thrusts in Porous Sandstone, Pismo Beach, California



Non-Andersonian Steep Reverse Faults (dips $> 45^\circ$)



Global Dip Distribution for Intracontinental Reverse Fault Ruptures



- $M_w > 5.5$ reverse-slip ruptures
- slip vector within $\pm 30^\circ$ of dip direction
- positive discrimination of rupture plane from surface break, from aftershock distribution, or topography
- 3 clusters at dips of $30 \pm 5^\circ$, $50 \pm 5^\circ$, and $10 \pm 5^\circ$
- NO ruptures dipping $> 60^\circ$

Sibson, 2009: *Tectonophysics* 493, 404-416

- dip distribution consistent with $\mu_s \approx 0.6$
assuming horizontal σ_1

2. WHAT IS COMPRESSIONAL INVERSION?

*“Every valley shall be exalted
And every mountain and hill made low”*

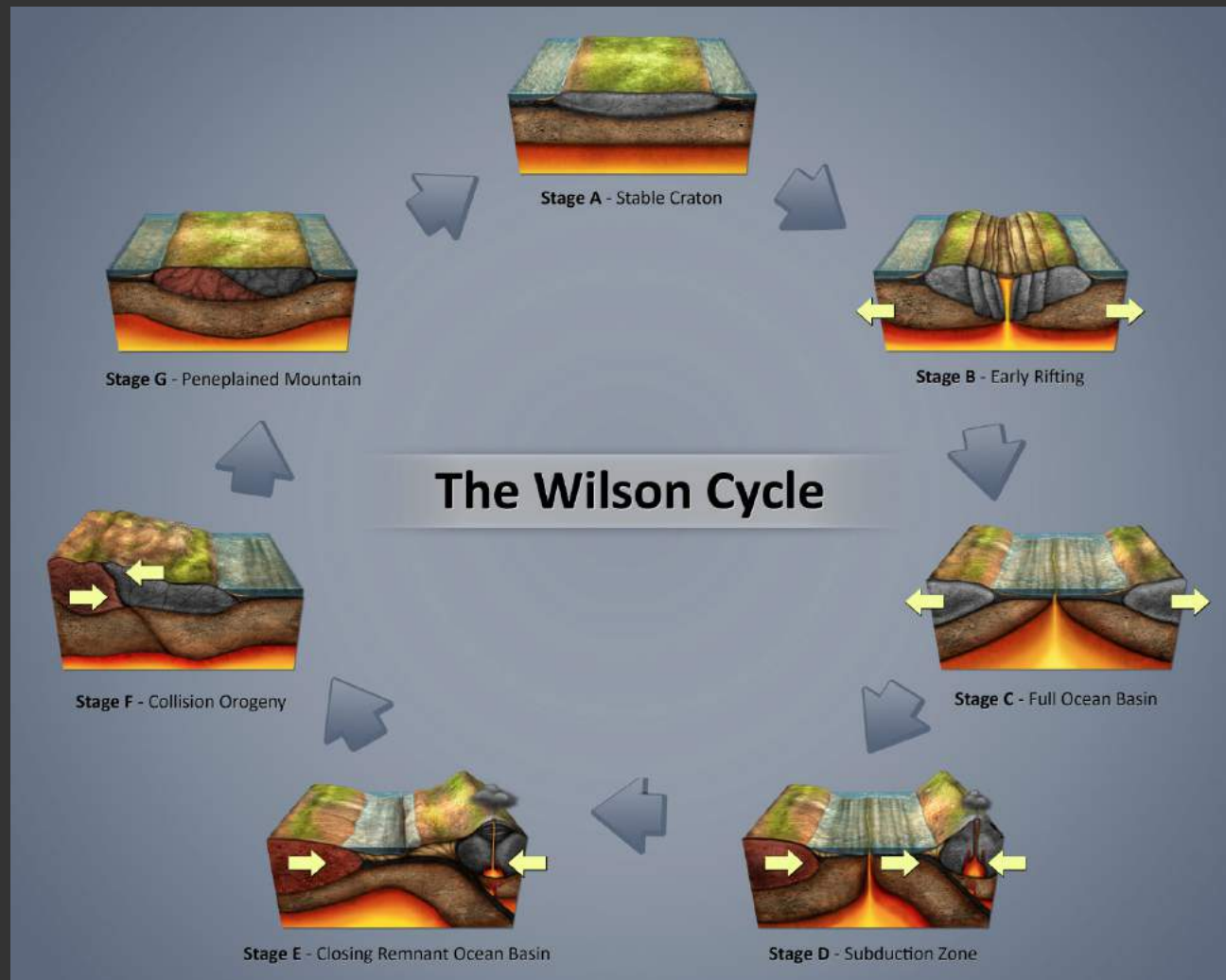
- Isaiah 40: 4

COMPRESSIONAL INVERSION – SHORTENING OF FORMERLY EXTENDED CRUST

– involves Reverse-Slip reactivation under compression of inherited Normal Faults

- Bert Bally (1983) - *Seismic Expression of Structural Styles* - reflection profiling shows compressional inversion is widespread
- Characteristic **Structural-Stratigraphic** signature – growth normal fault with abrupt thickening of syn-rift sediment on hanging-wall – **harpoon-head** structure
- PLANAR vs. LISTRIC faults?
- Coaxial vs. Non-Coaxial inversion - strike-slip component?
- Reactivation of inherited faults is **extremely selective**
- GSL Spec. Publ. 44 – *Inversion Tectonics* (1989)
GSL Spec. Publ. 88 – *Basin Inversion* (1995)

Compressional Inversion – Inevitable Consequence of Wilson Cycle of Ocean/Marginal-Sea Opening and Closure

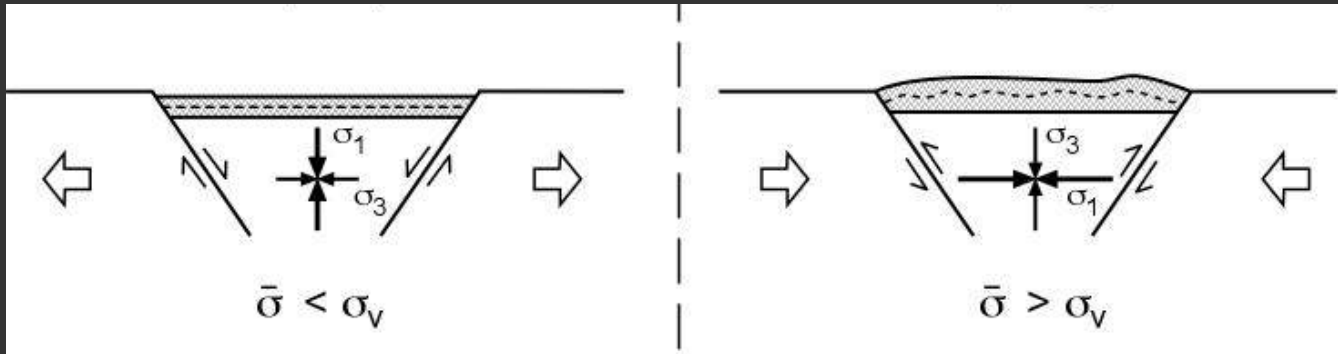


- easier to impose brittle structure during crustal extension

Compressional Inversion

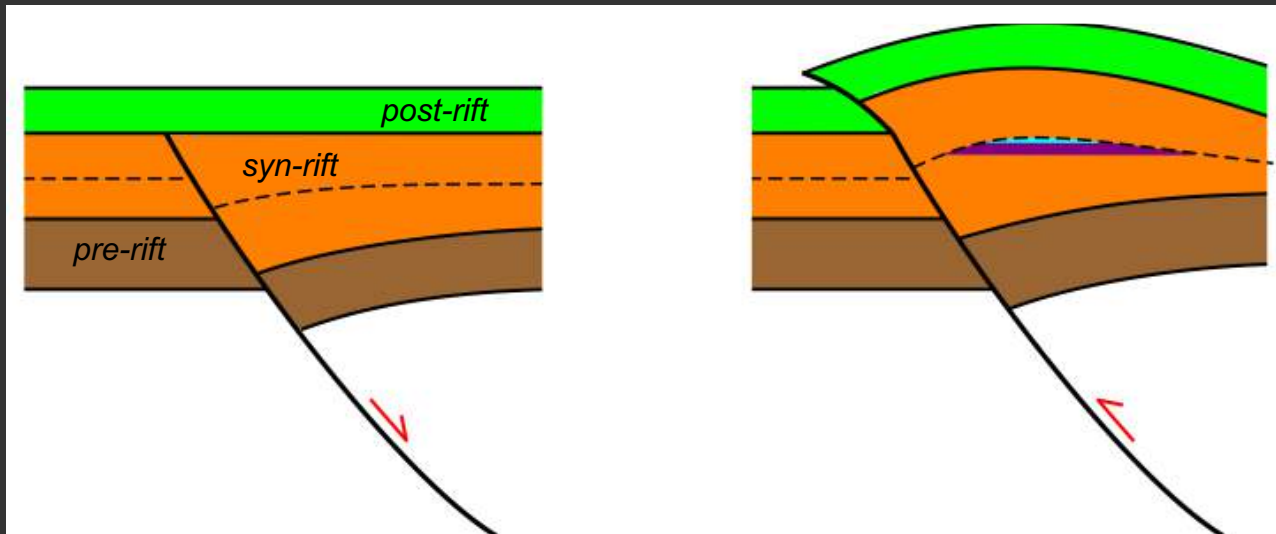
EXTENSIONAL RIFTING

COMPRESSIONAL INVERSION

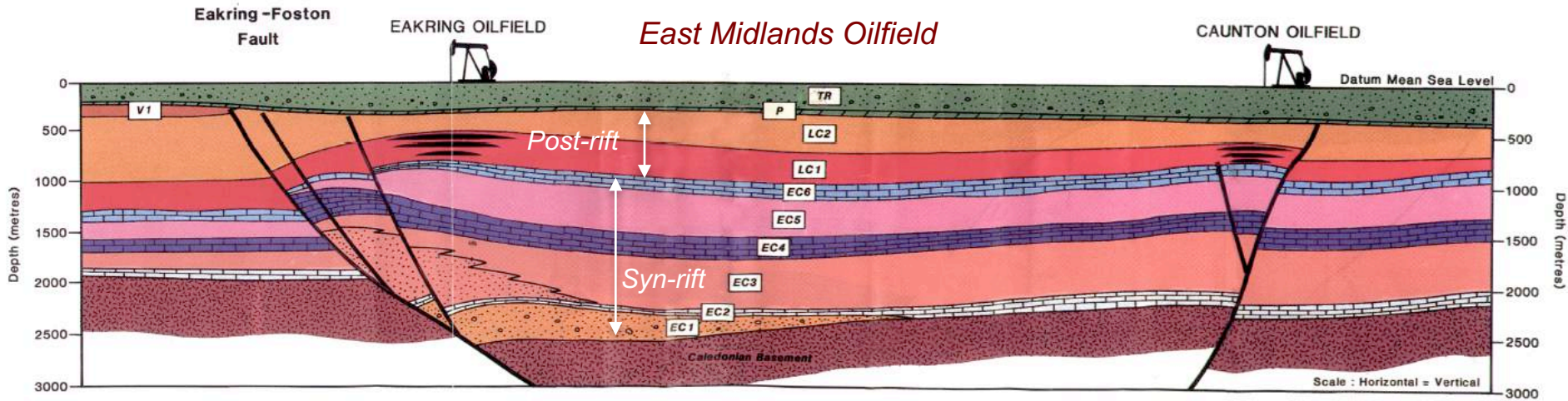


Growth Normal Fault

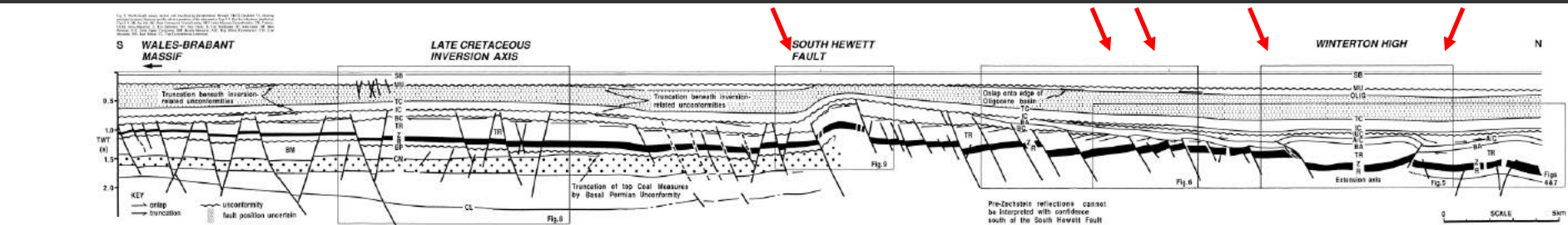
Inversion Oil-Gas Reservoir



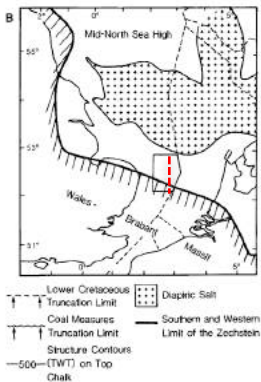
Characteristics of Compressional Inversion



Fraser, Nash, Steele & Ebdon 1990: *GSL Spec. Publ. 50*, 417-440

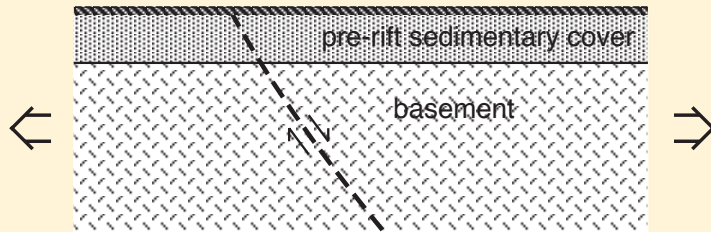


Selective Reverse-Slip Reactivation, southern North Sea

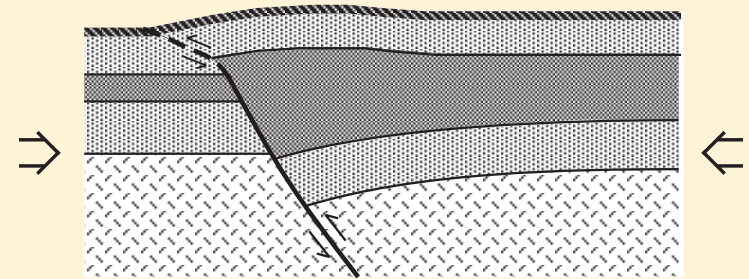


Badley, Price & Backshall, 1989: *GSL Spec. Publ. 44*, 201-219

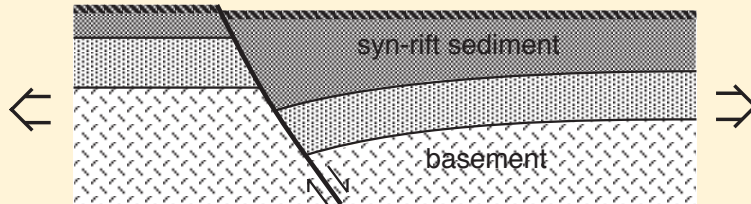
Structural / Stratigraphic Characteristics of Compressional Inversion Faults



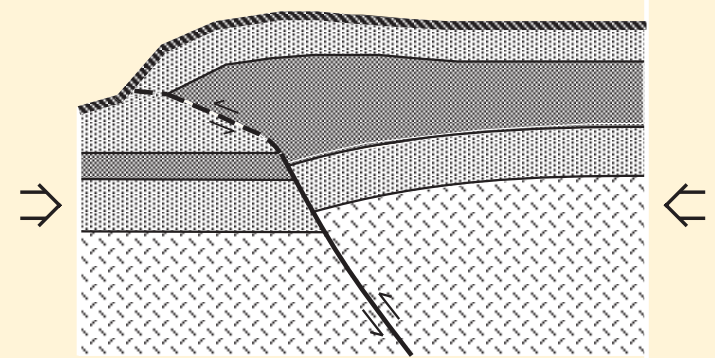
(1) Rift Initiation.



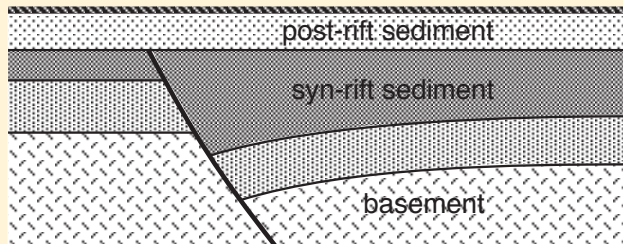
(4) Onset of compressional inversion - variable dip separations - optimal thrust forms in post-rift sediments.



(2) Progressive Extension with deposition of syn-rift sediments.



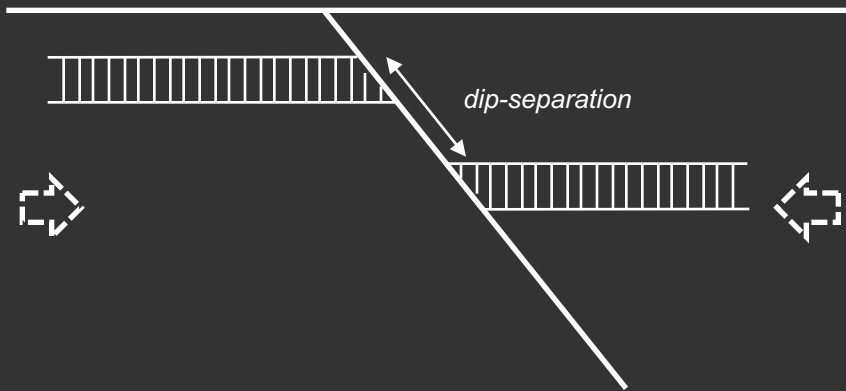
(5) Continued shortening - variable reverse separations.



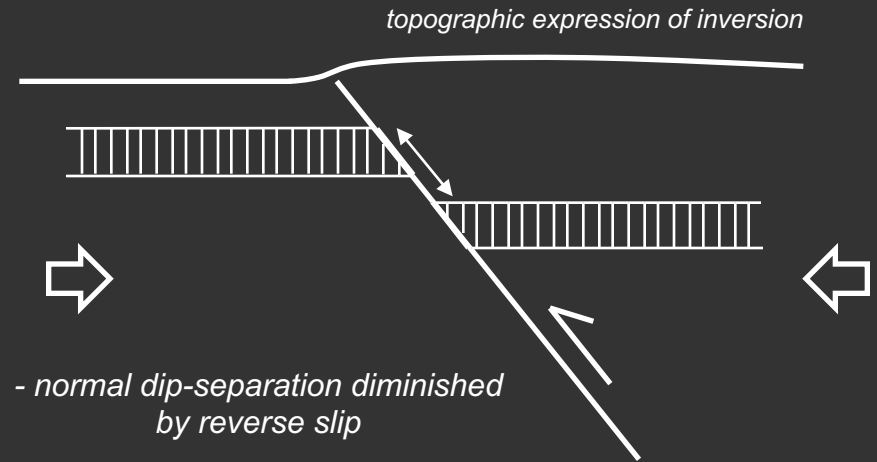
(3) Deposition of post-rift sediments during sag phase.

Misleading Dip-Separations

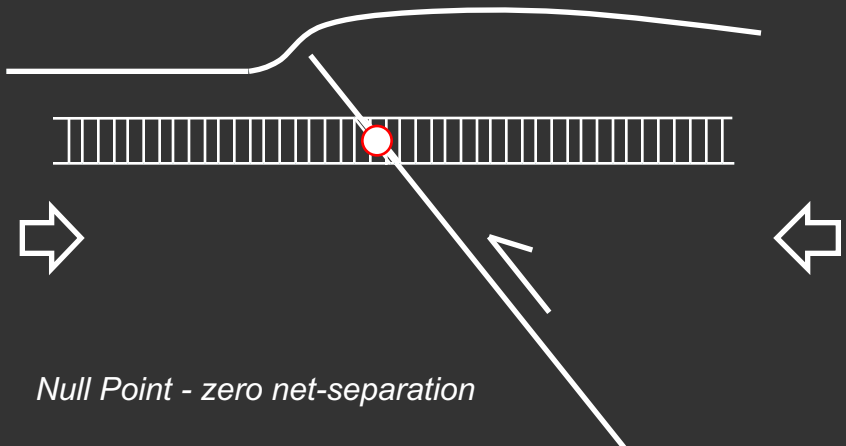
1) *Inherited Normal Fault*



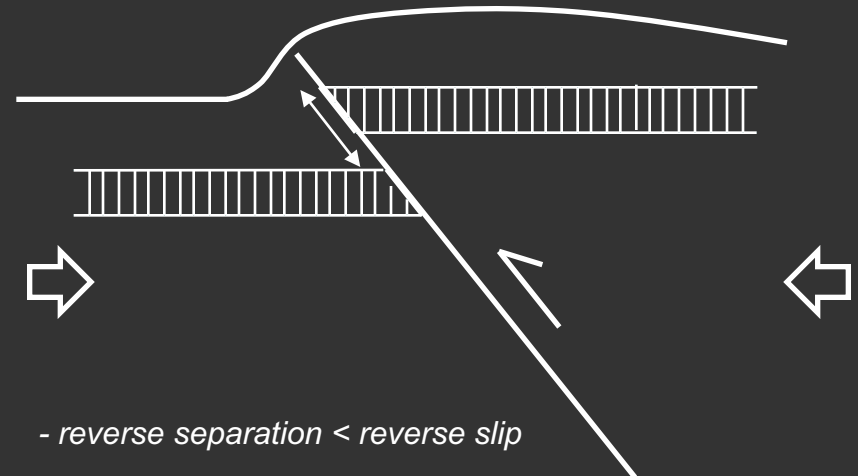
2) *Incipient Compressional Inversion*



3) *Ongoing Inversion*

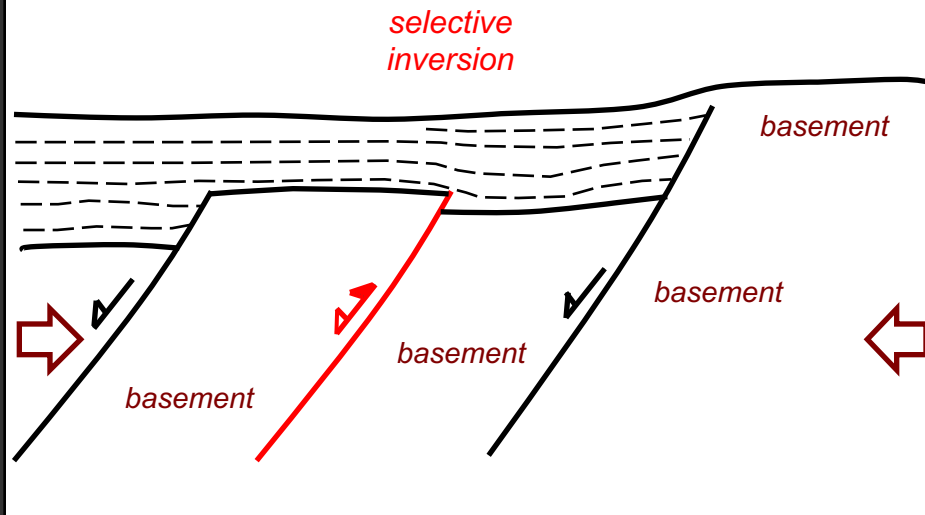


4) *Advanced Inversion*

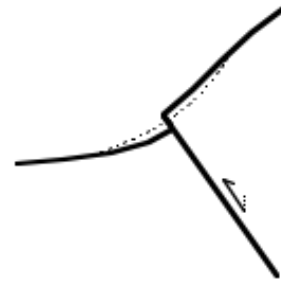


Near-Surface Structural Complications

Incipient Inversion – seismogenic structures ‘lurking’ below young sedimentary cover along margins of former extensional basins



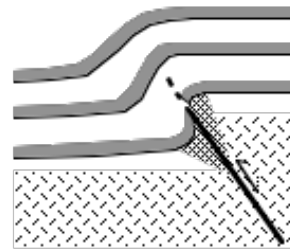
(a) Collapse of Rupture Scarp



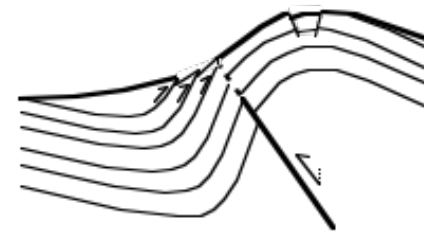
(b) Rockfalls & Landslides



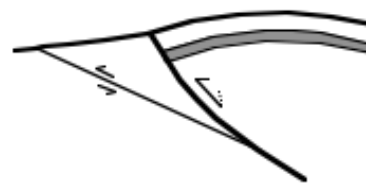
(c) Monoclinal Drape-Fold in Cover



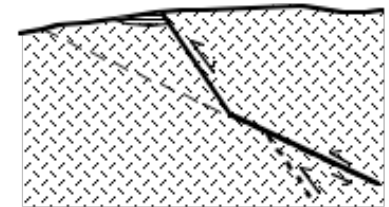
(d) Distributed Folding Deformation (flexural slip and bending) in Cover



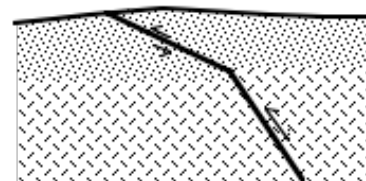
(e) Listric Reverse Fault - High-Level Folding with Development of a Footwall Short-Cut at Depth



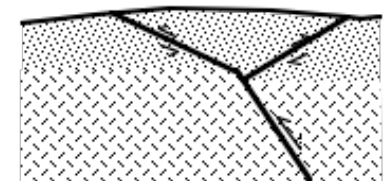
(f) Decapitation in Basement by Short-Cut Thrust



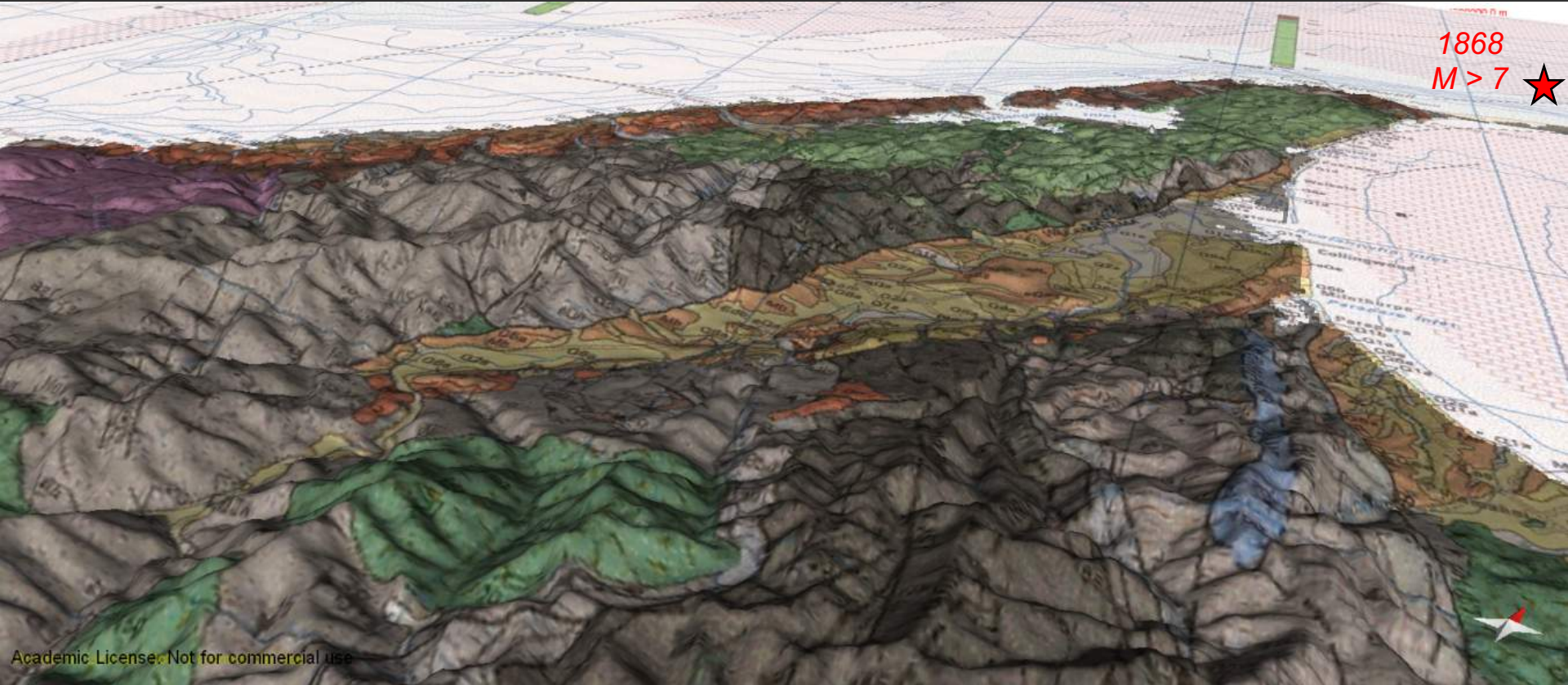
(g) Reverse-Fault Refracting to Low-Dip in Young Cover Sediment



(h) Reverse Fault ‘Pop-Up’ in Young Cover Sediment

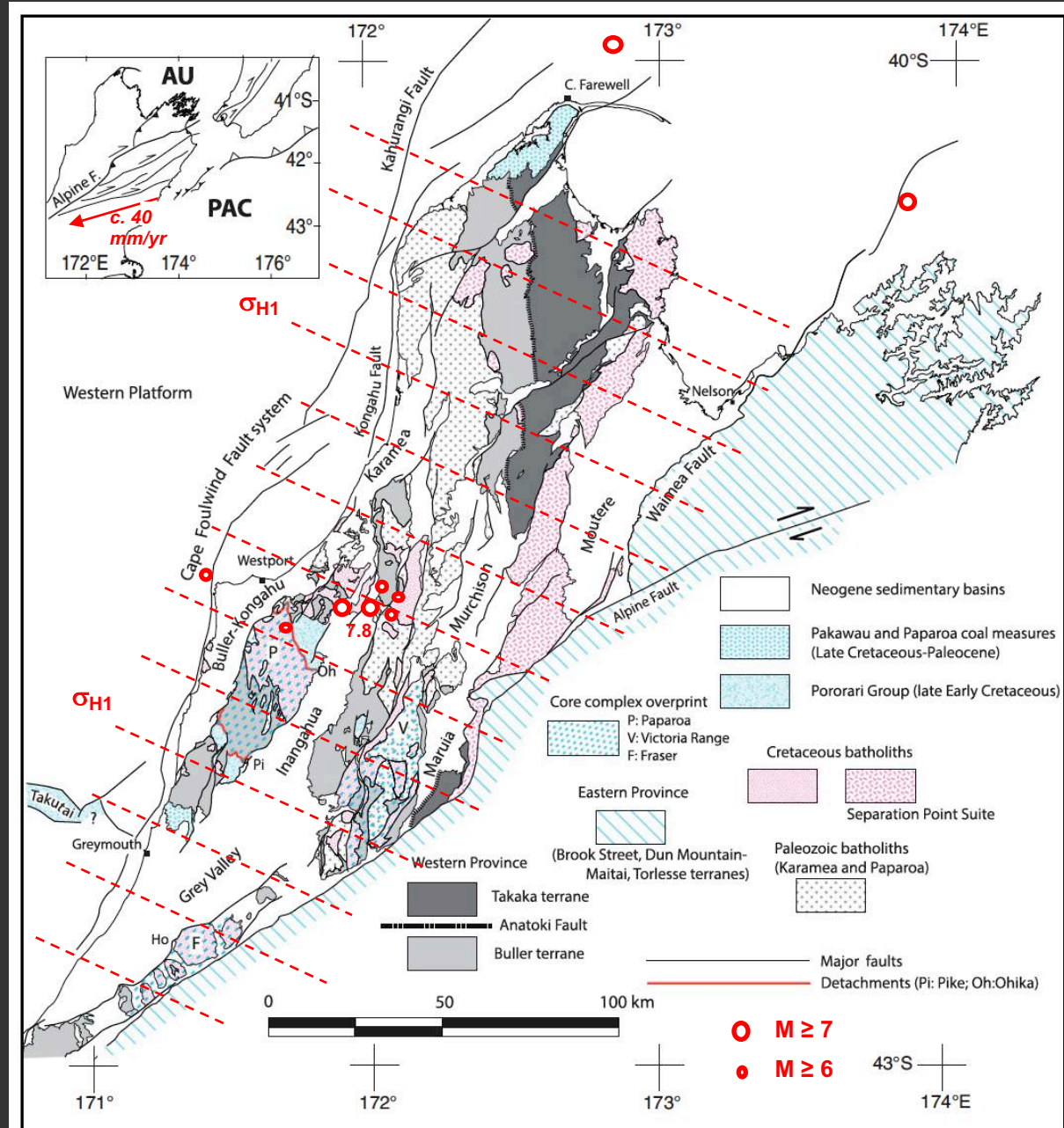


Wakamarama Fault Trace, NW South Island



Finite Strain from Compressional Inversion, NW South Island

- 'THICK-SKINNED' deformation involving basement as well as sedimentary cover
- WNW-ESE finite shortening locally <40% or more

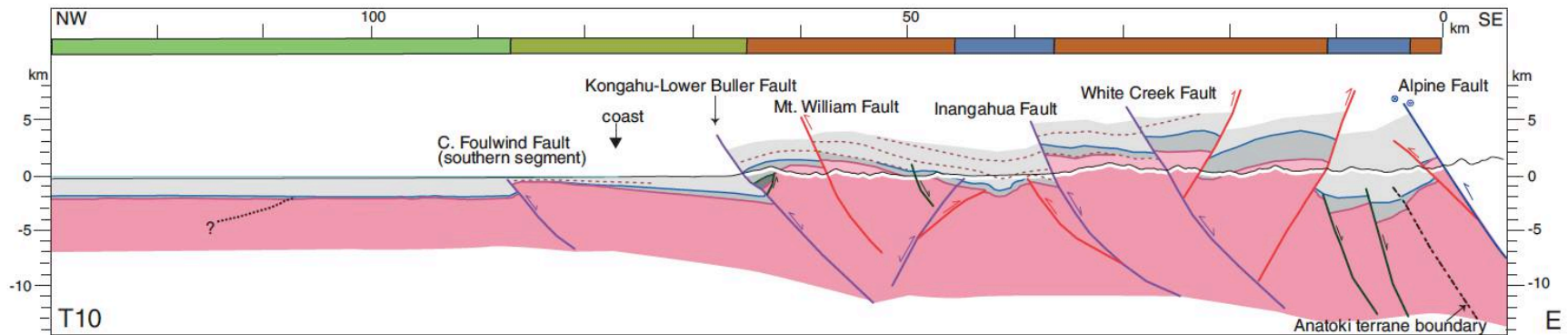
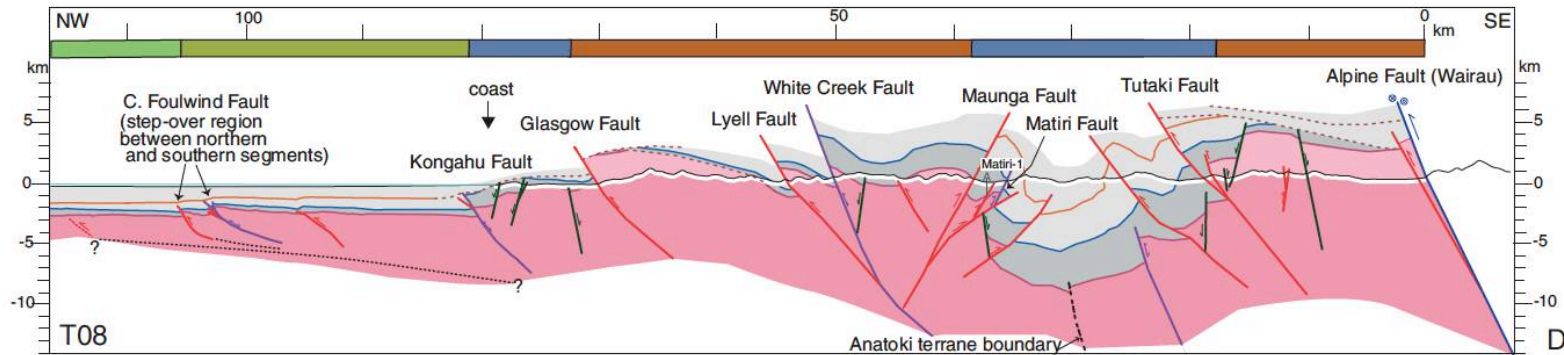
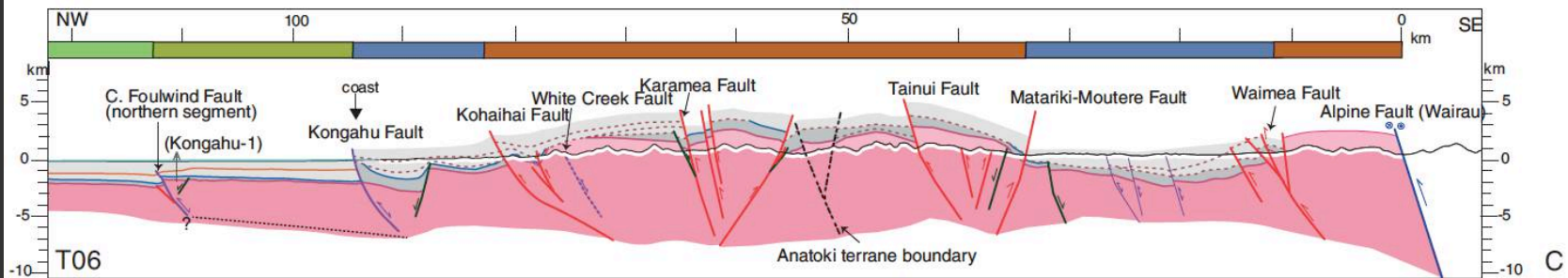


Ghisetti, Barnes & Sibson, 2014:
NZJGG 57 271-294

Inversion History, NW South Island

PERIOD	TECTONICS	ACTIVE STRUCTURES
6 - 0 Ma	Progressive E-W shortening of NW South Island following initiation of convergence across Alpine Fault and uplift of Southern Alps	REVERSE FAULTING & FOLDING
< 25 Ma	Initiation of ALPINE FAULT with ensuing dextral strike-slip	NE-SW Alpine Fault transform
45 – 35 Ma	Rifting and subsidence associated with opening of Emerald Basin	Enhancement of N-S to NNE-SSW NORMAL FAULT fabric
85 – 65 Ma	Rifting and subsidence accompanying opening of Tasman Sea between Zealandia & Australia	Imposition of N-S to NNE-SSW NORMAL FAULT fabric

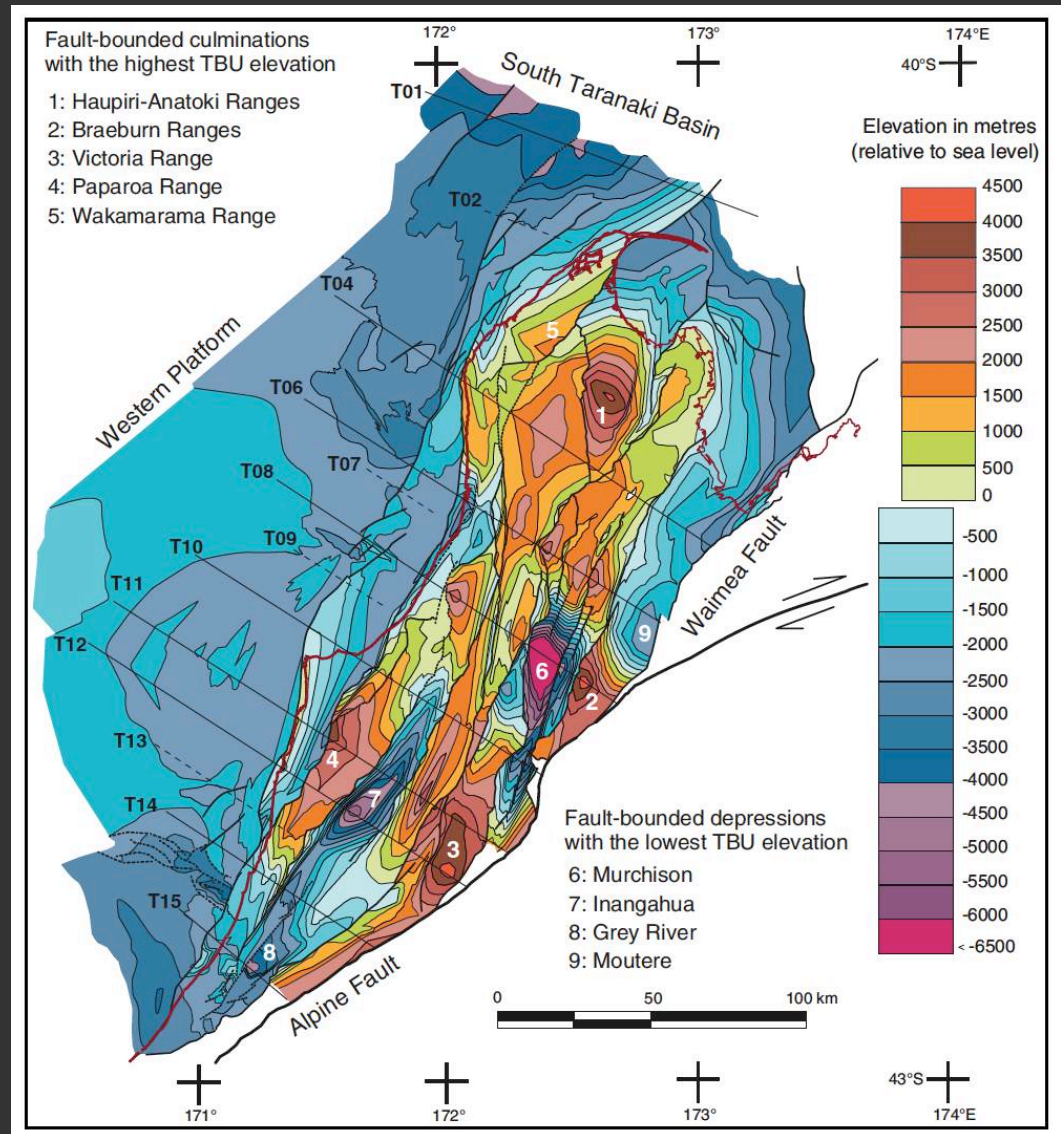
Structural Cross-Sections, NW South Island



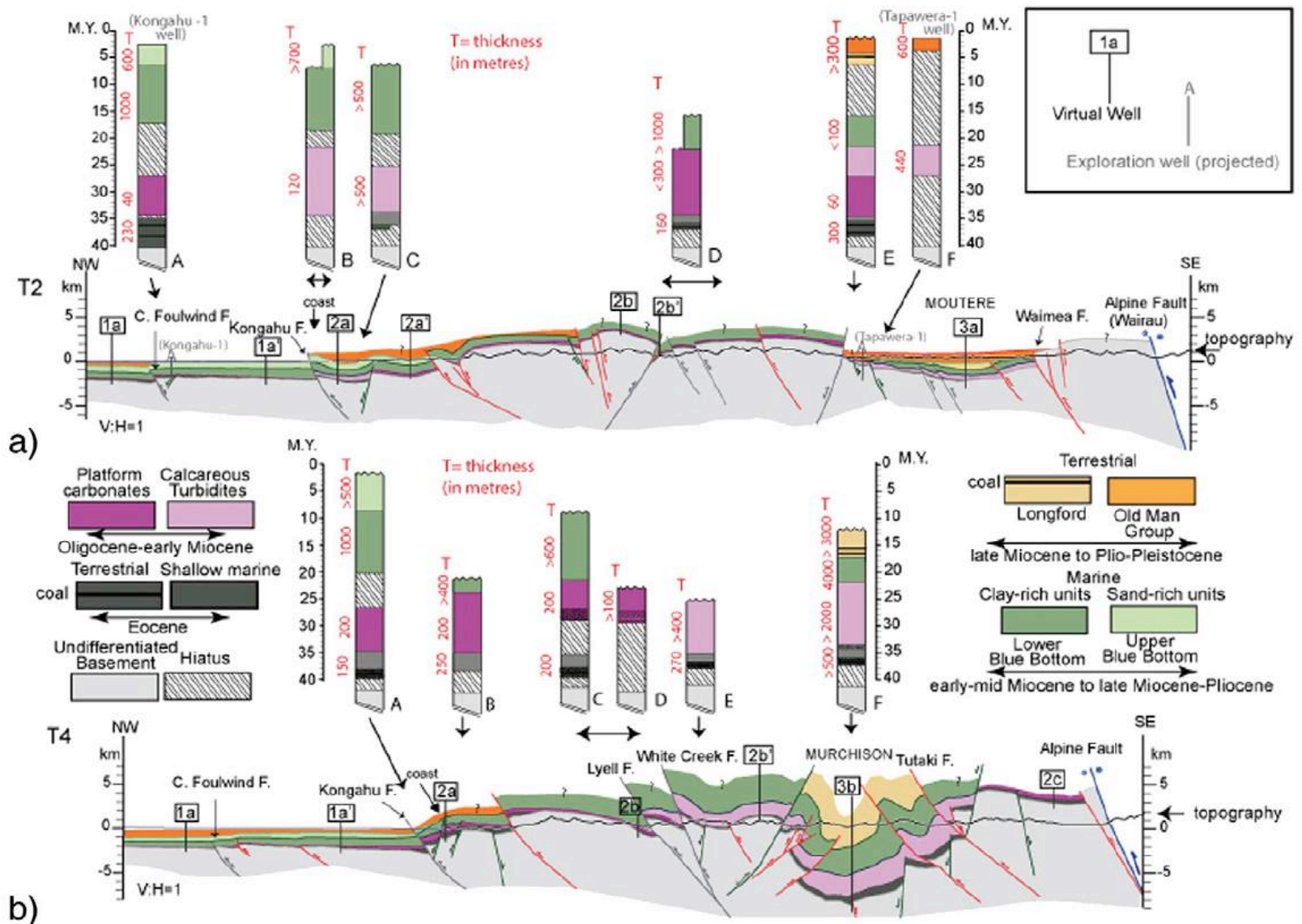
V:H=1 for all sections

Contours on Top Basement Unconformity, NW South Island

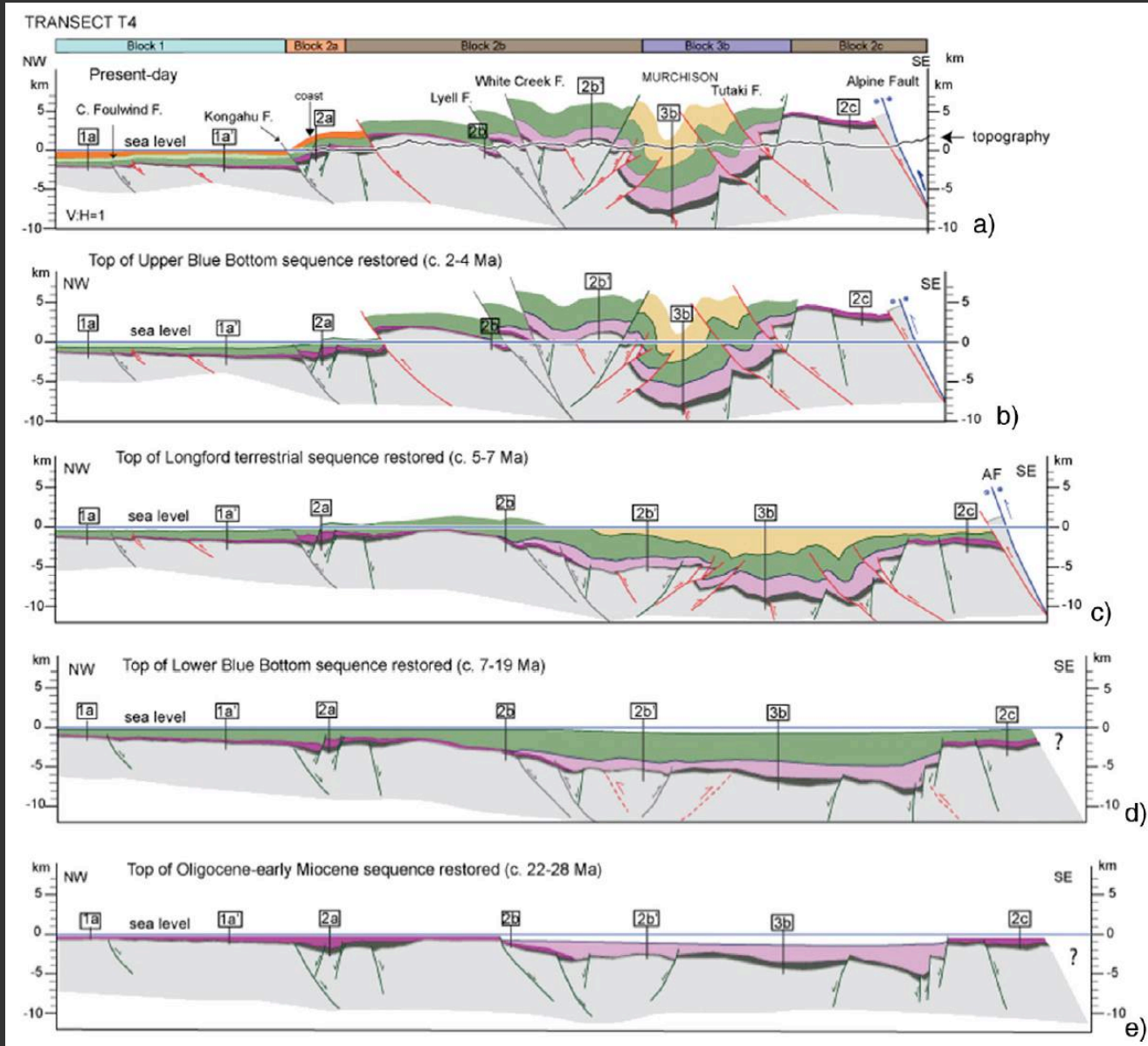
- *THICK-SKINNED* deformation
- WNW-ESE finite shortening locally <40% or more
- TBU ranges from 6500 m b.s.l. to 4500 m a.s.l.



Stratigraphy and Structure, NW South Island



Progressively Restored NW-SE Cross-Sections, NW South Island



3. FRICTIONAL MECHANICS OF COMPRESSIONAL INVERSION

Stress Ratio for Frictional Reactivation (2D)

- for a cohesionless fault

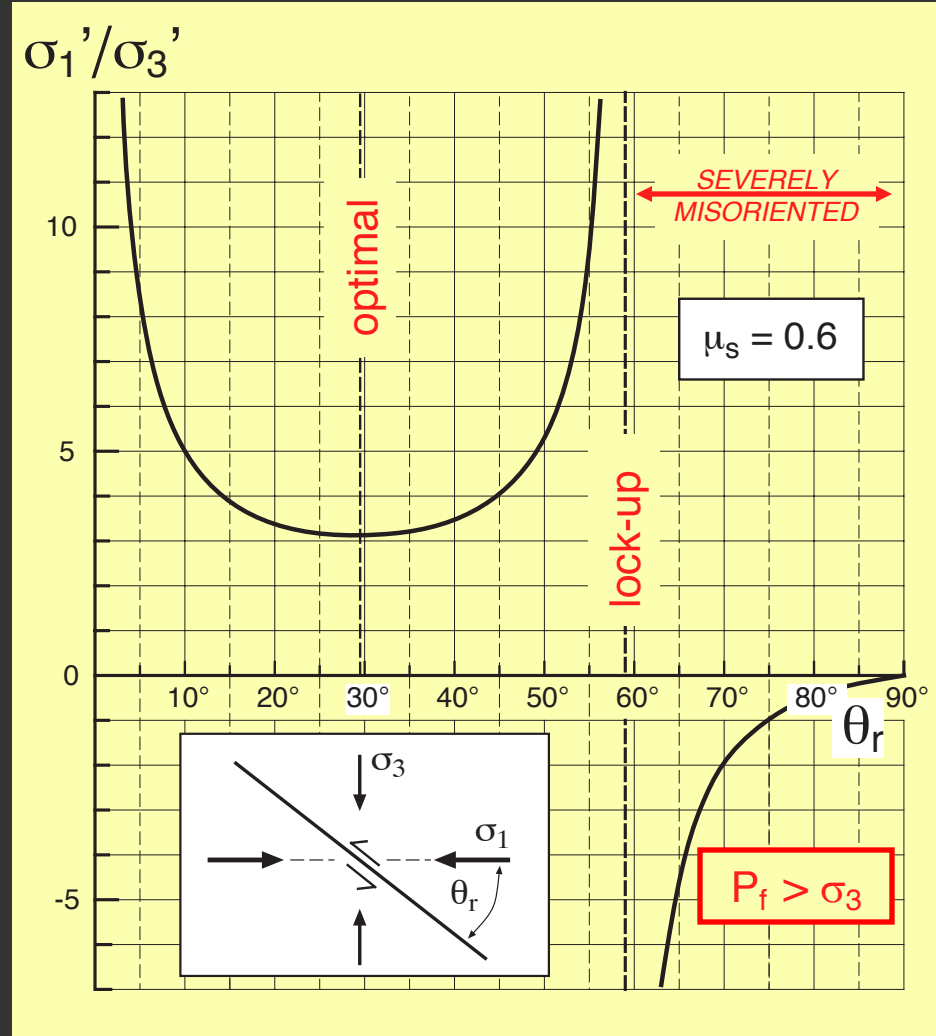
$$\tau = \mu_s \cdot \sigma_n' = \mu_s(\sigma_n - P_f)$$

$$\frac{\sigma_1'}{\sigma_3'} = \frac{(\sigma_1 - P_f)}{(\sigma_3 - P_f)} = \frac{(1 + \mu_s \cot \theta_r)}{(1 - \mu_s \tan \theta_r)}$$

OPTIMAL - $\theta_r^* = 0.5 \tan^{-1}(1/\mu_s)$

LOCK-UP - $\theta_r = 2\theta_r^* = \tan^{-1}(1/\mu_s)$

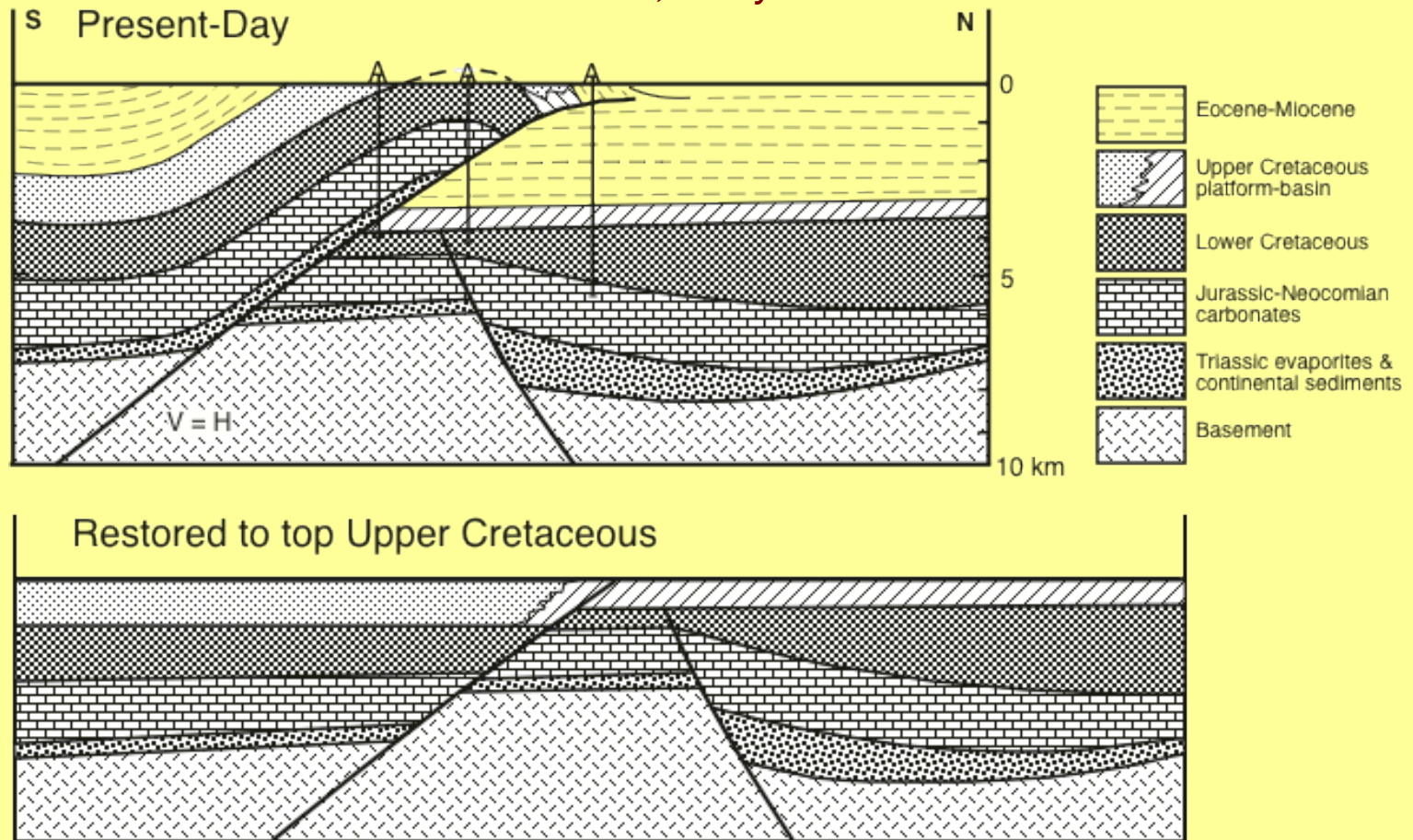
As $P_f \rightarrow \sigma_3$, $(\sigma_1'/\sigma_3') \rightarrow \infty$,
allowing badly oriented faults
to reactivate in the absence
of well-oriented structures



- for Byerlee friction, optimal reactivation occurs at $25^\circ < \delta_r = \theta_r < 30^\circ$

Preferential Reactivation During Compressional Inversion

St. Suzanne Anticline, N. Pyrenees

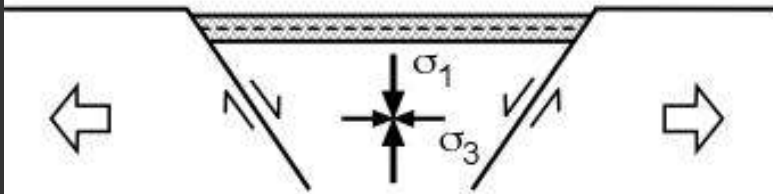


COMPETITION - Steep Reverse Faults vs. Thrusts in Compressional Regimes

Compressional Inversion of Inherited Normal Faults ($\theta_r < 60^\circ$?)

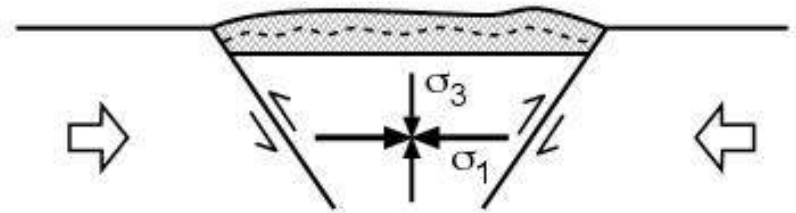
EXTENSIONAL RIFTING

$$\sigma_v = \sigma_1$$



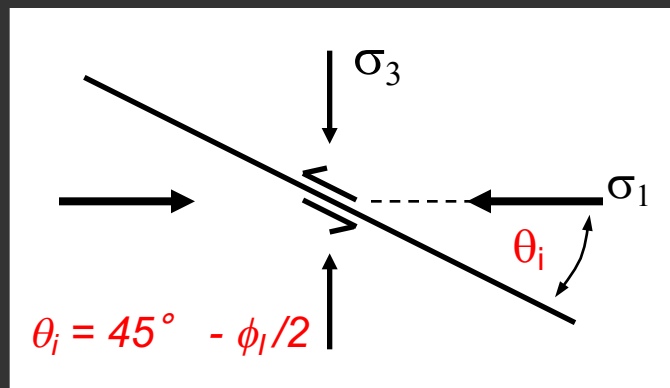
COMPRESSIONAL INVERSION

$$\sigma_v = \sigma_3$$



Reverse-Slip reactivation at $\delta = \theta_r > 45^\circ$
requires $P_f \rightarrow \sigma_3$

New-Forming
'Andersonian' Thrust
($\theta_i < 45^\circ$)

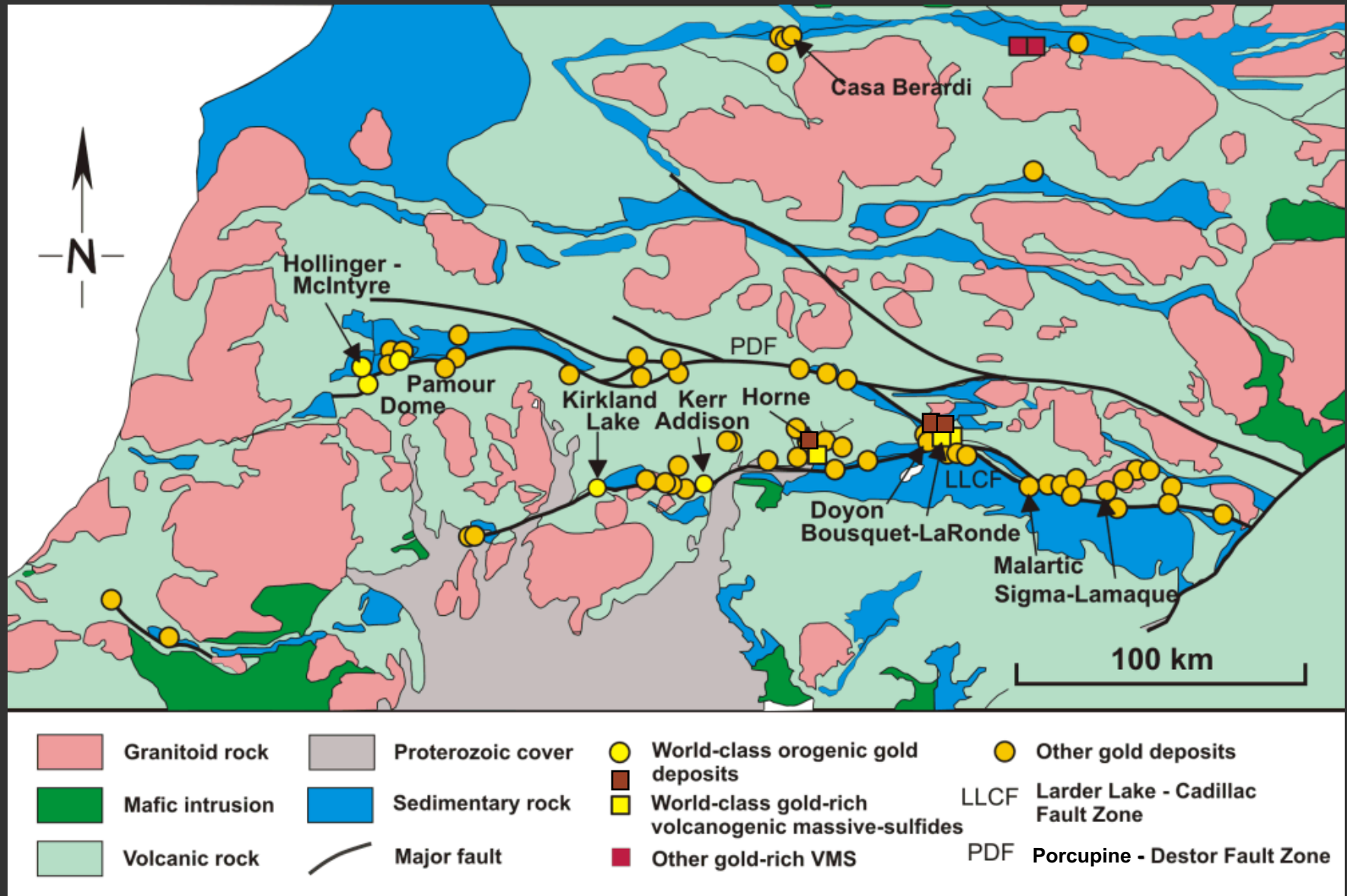


4. A BRIEF DIVERSION TO THE BASE OF THE SEISMOGENIC ZONE

“To a shower of gold most things are penetrable”

- Thomas Carlyle

Exhumed Base of the Seismogenic Zone at c. 10 km - the Late Archean Abitibi Granite-Greenstone Belt



P-T Environment for Mesozonal Lode Gold

TEMPERATURE RANGE - 270-400 ° C

PRESSURE / DEPTH - 2-4 kbar?? ~ 7-14 km??

FLUID COMPOSITION - low salinity, H₂O-CO₂

INCREMENTAL VEIN DEPOSITION – fluid inclusions - repeated episodes of fluid-pressure cycling and phase separation

METAMORPHIC ENVIRONMENT - low-mid-greenschist facies with carbonate alteration haloes around veins

DEFORMATION STYLE - mixed brittle-ductile character (discrete shears and vein fractures as well as an L-S schistose shear zone fabric)

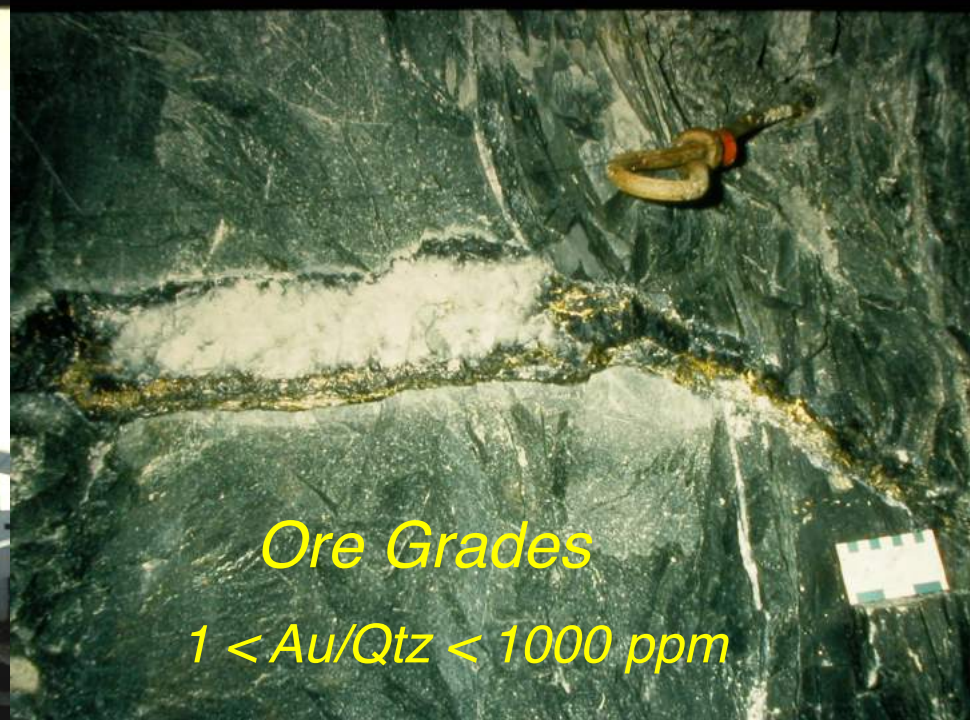
- vein systems have mostly developed on REVERSE FAULTS within the lower seismogenic zone in deforming continental crust

Val d'Or District

Transport Solubilities

$$\text{H}_2\text{O} / \text{Qtz} \sim 10^3 - 10^4$$

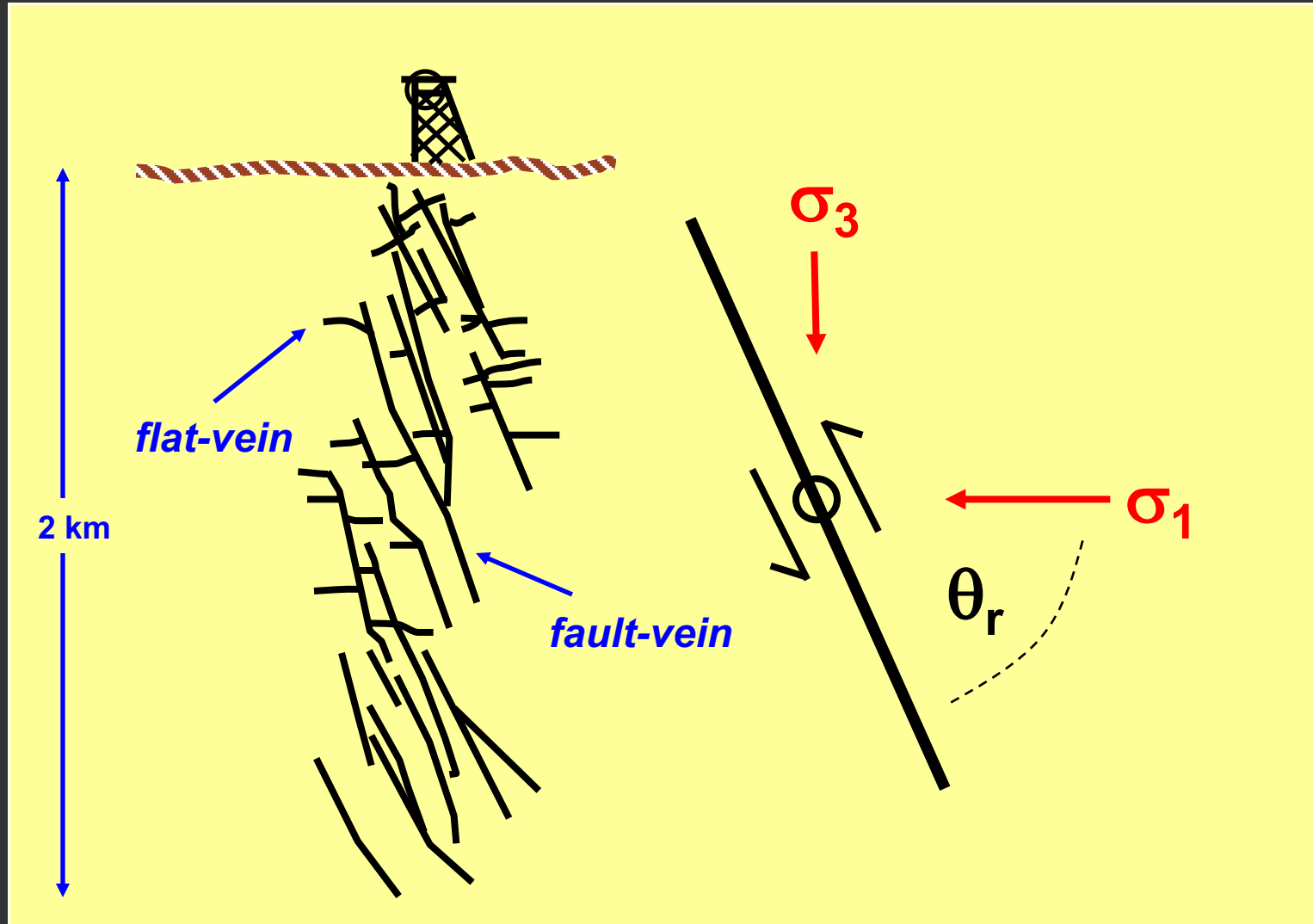
$$\text{H}_2\text{O} / \text{Au} \sim 10^7 - 10^9$$



Ore Grades

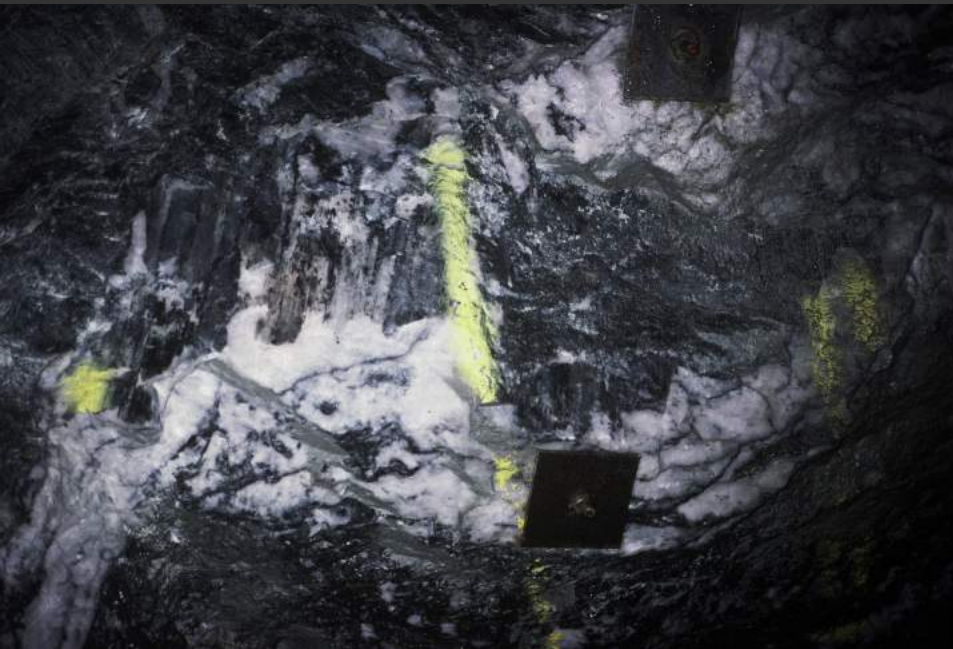
$$1 < \text{Au/Qtz} < 1000 \text{ ppm}$$

Sigma Mine, Val d'Or



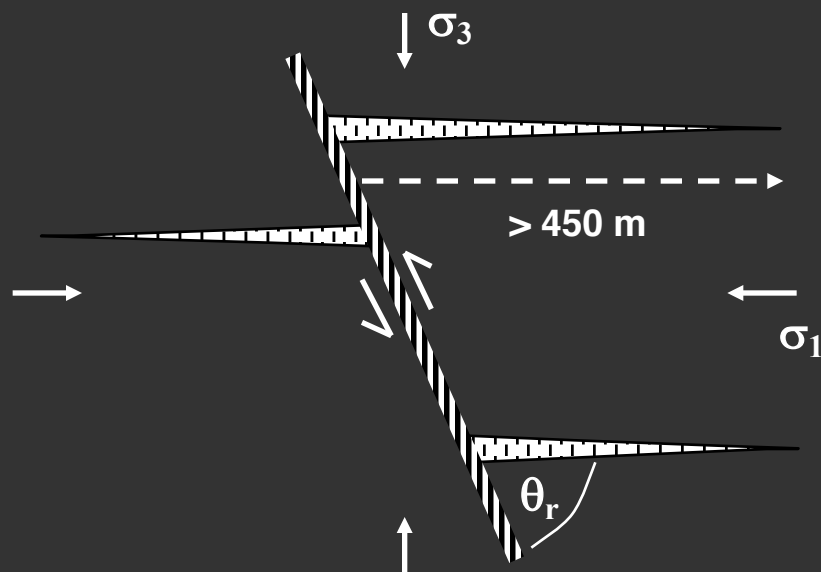


Sigma Mine - Au-Quartz Veins Hosted on Reverse Faults with Associated Flat-Lying Extension Veins

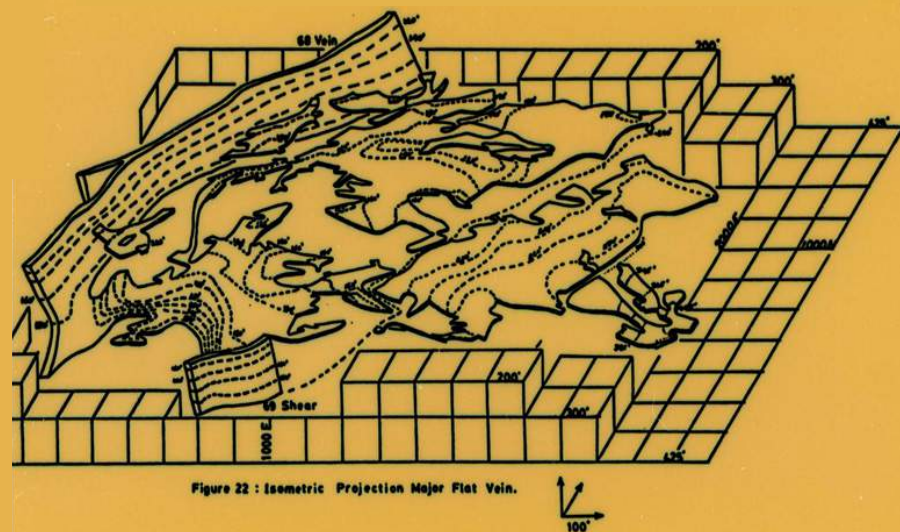


*Mutually Cross-Cutting Flats & Fault-Veins,
Giant Mine, Yellowknife*





Hollinger Mine (from Hall, 1985)



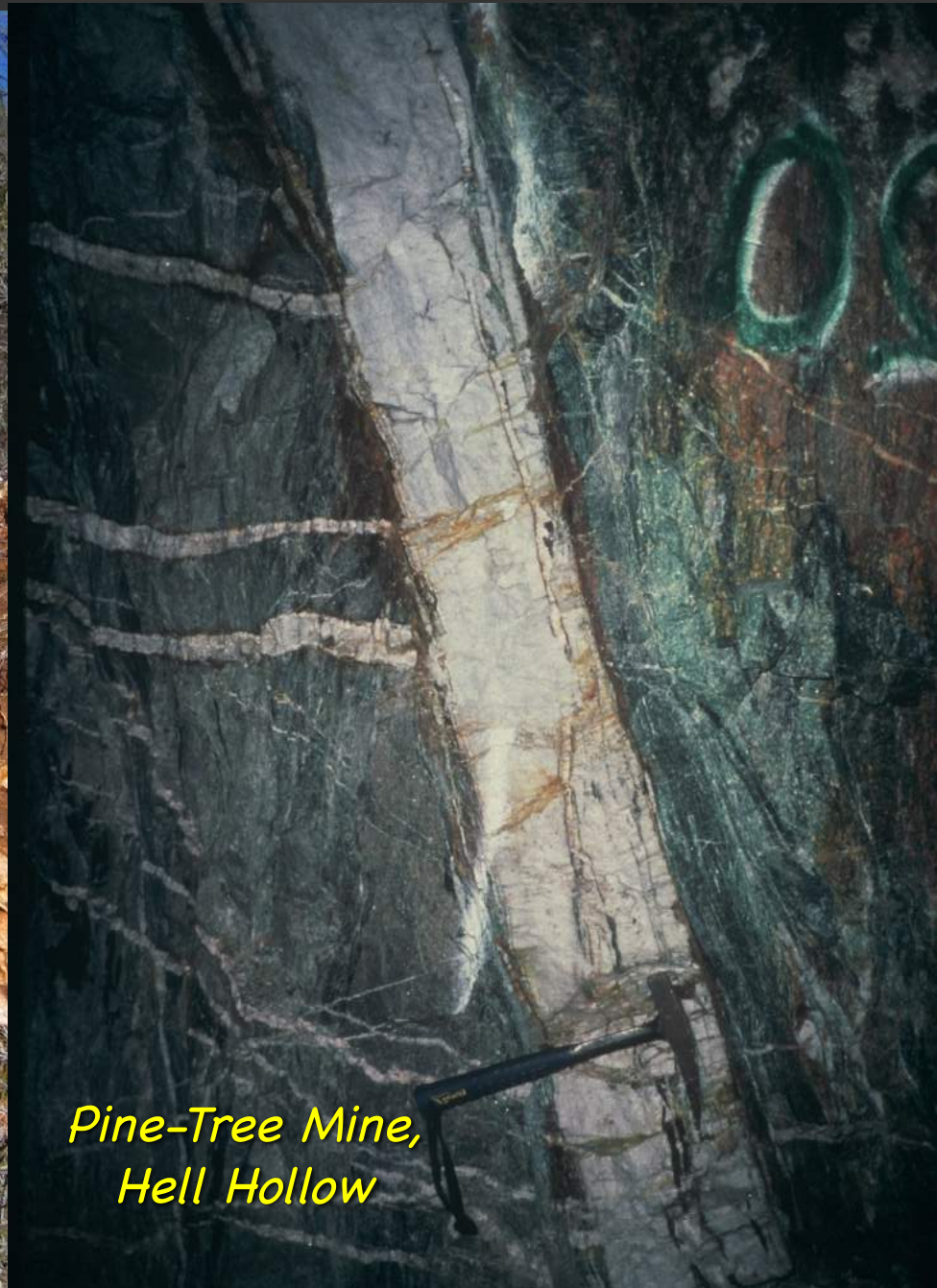
Flat Extension Veins Associated with Steep Reverse Faults



Mesozoic Orogenic Gold-Quartz, Mother Lode Belt, CA



*Penon Blanco,
Coulterville*



*Pine-Tree Mine,
Hell Hollow*

Stress Ratio for Fault Reactivation (2D)

- for a cohesionless fault

$$\tau = \mu_s \cdot \sigma_n' = \mu_s (\sigma_n - P_f)$$

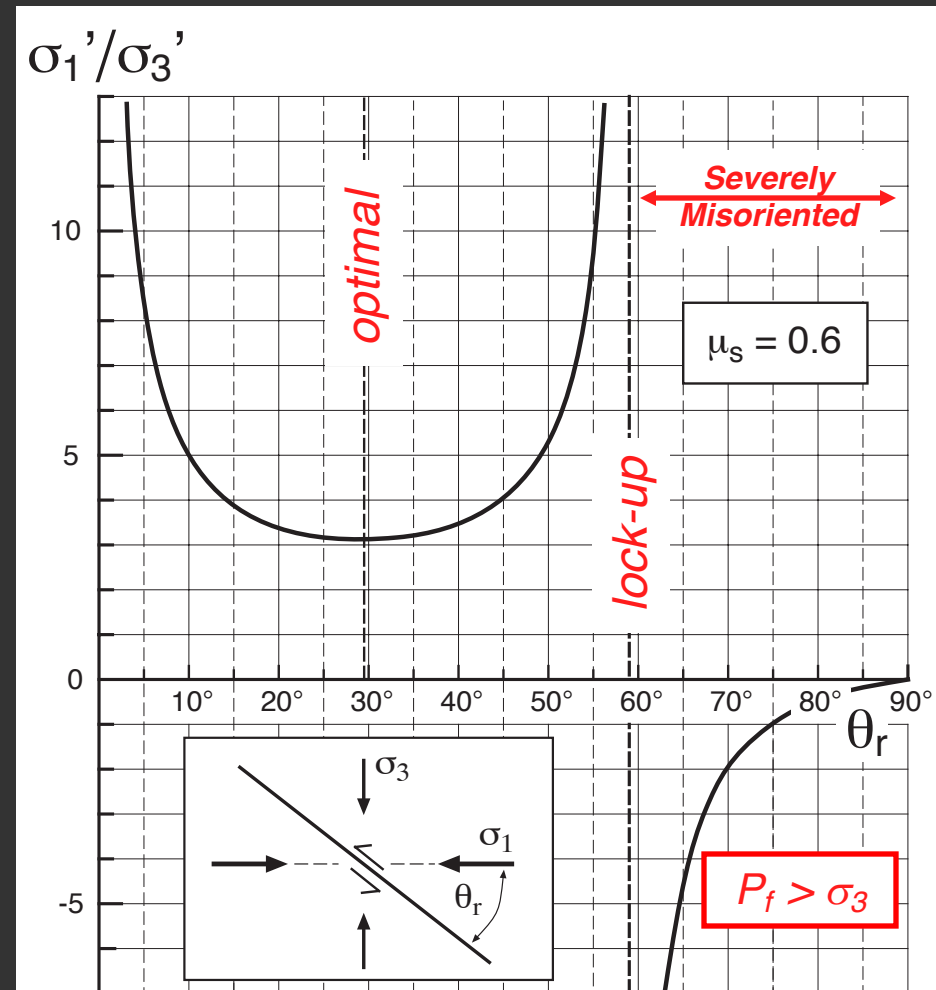
$$\frac{\sigma_1'}{\sigma_3'} = \frac{(\sigma_1 - P_f)}{(\sigma_3 - P_f)} = \frac{(1 + \mu_s \cot \theta_r)}{(1 - \mu_s \tan \theta_r)}$$

OPTIMAL - $\theta_r^* = 0.5 \tan^{-1}(1/\mu_s)$

LOCK-UP - $\theta_r = 2\theta_r^* = \tan^{-1}(1/\mu_s)$

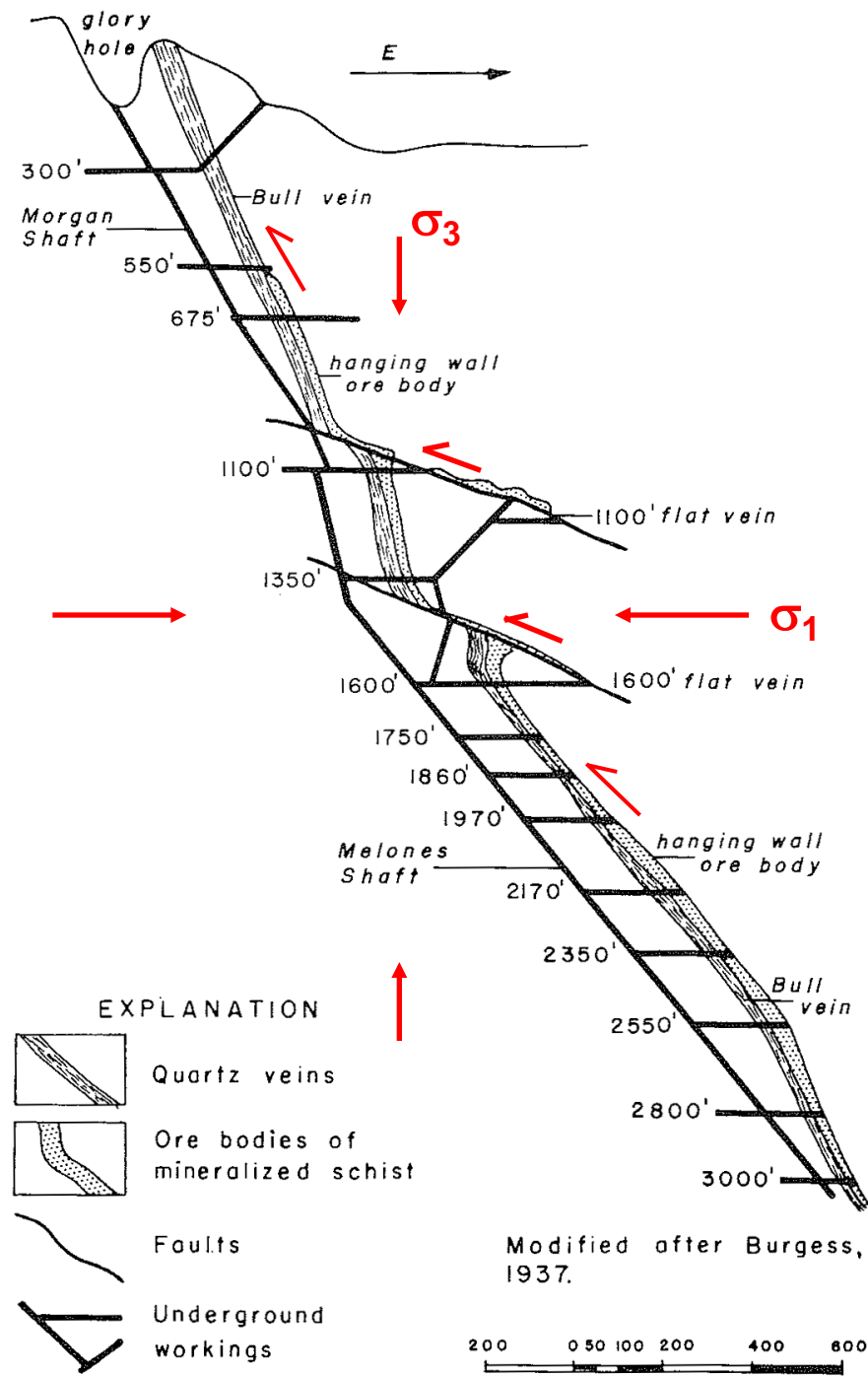
$$\sigma_1' / \sigma_3' \rightarrow \infty \quad \text{if } \sigma_1 \gg \sigma_3$$

$$\text{or if } \sigma_3' \rightarrow 0 \quad \text{i.e. } P_f \rightarrow \sigma_3$$

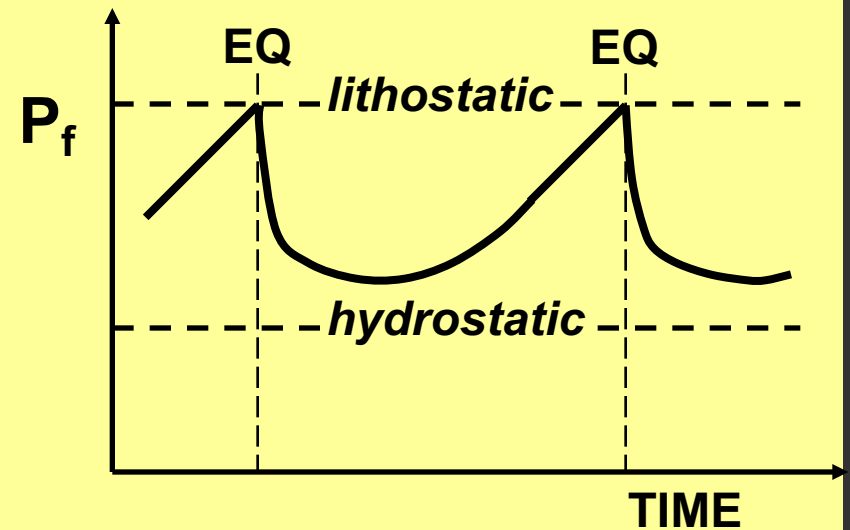
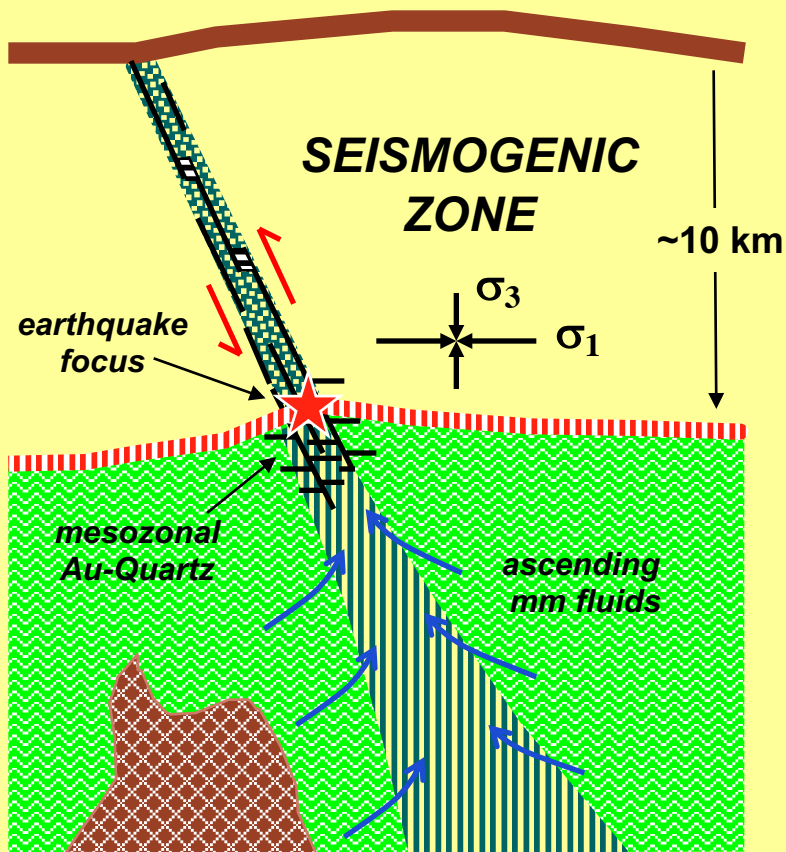


Carson Hill Mine, Mother Lode belt, California

COMPETITION!



Extreme Fault-Valve Action on a Steep Reverse Fault

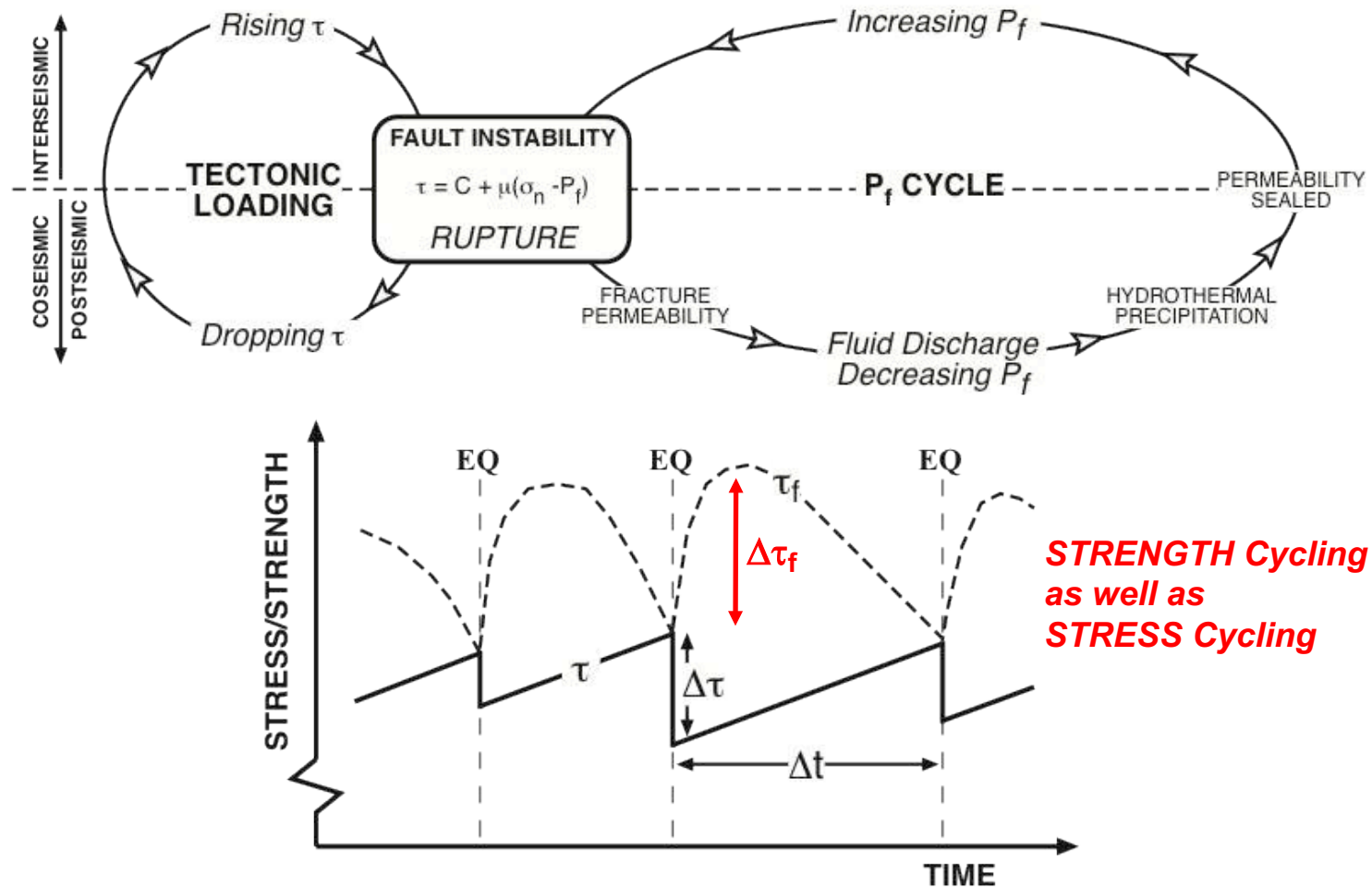


- extreme valving action
likely to be of short duration

What is Fault-Valve Action?

- *A fault may behave as a **fluid-pressure activated 'valve'** because of the dramatic postfailure increase in fault zone permeability*
- *Valving occurs when an earthquake rupture **transects steep fluid-pressure gradients** at the boundaries of overpressured portions of the crust*
- ***Extreme valve-action** (involving episodic discharge of large fluid volumes) commonly associated with steep reverse faults in the lower seismogenic zone*

Fault-Valve Action Affecting Earthquake Nucleation and Recurrence

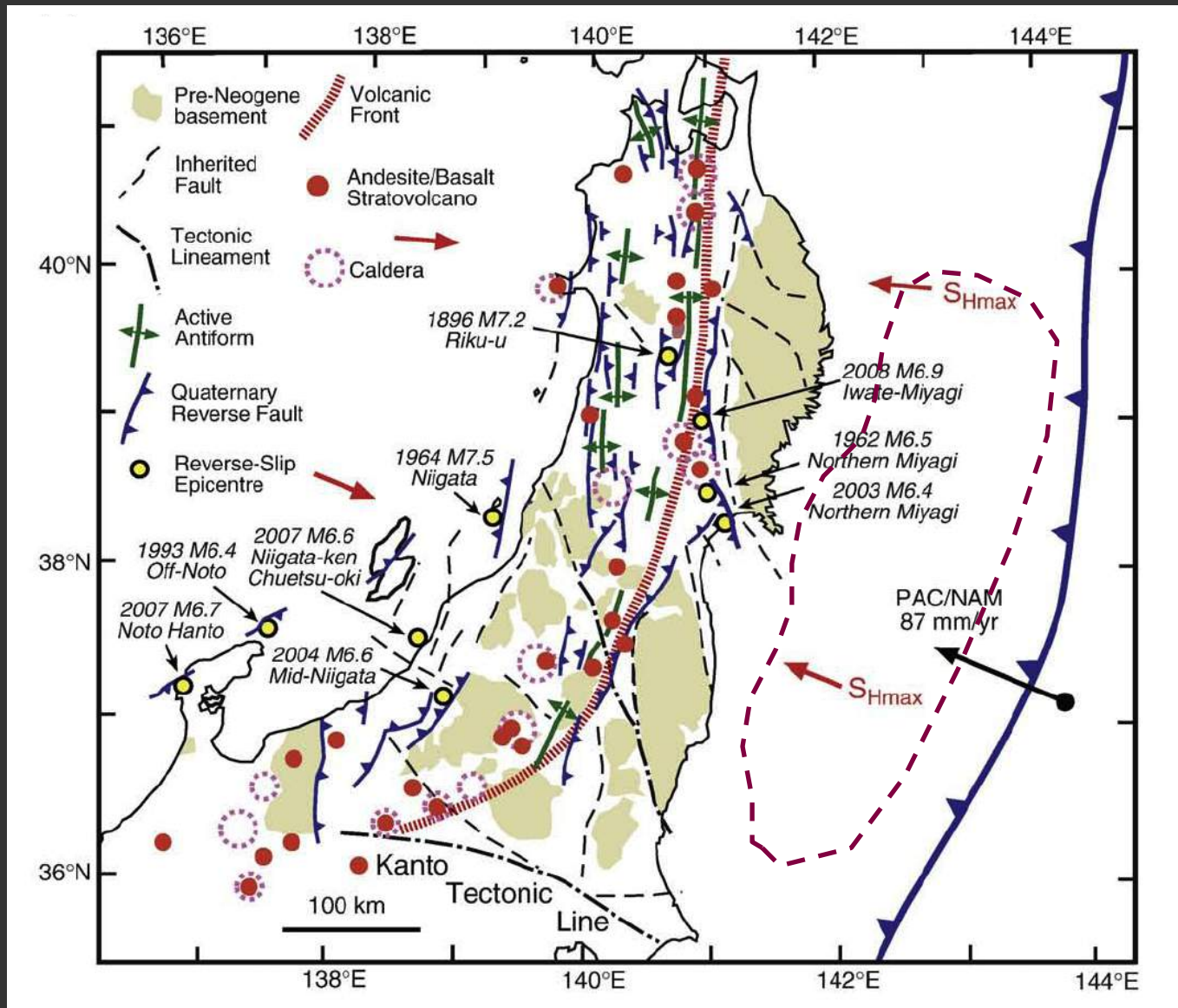


How Faults Get Loded – Are Rupture Nucleation Sites Special??

- *Mesozonal vein systems develop towards base of the seismogenic zone ($270^{\circ} < T < 400^{\circ} \text{ C}$; $7 < z < 14 \text{ km}$)*
- *Vein systems demonstrate that the P_f conditions for reactivation of misoriented faults were locally satisfied*
- *Typical dimensions $< 2 \text{ km}$ along strike and down-dip*
- *? **NUCLEATION SITES** ? for reverse-slip ruptures ?*
- *Can rupture nucleation sites be identified on non-misoriented faults?*

*5. WHERE MAY 'FAULT-VALVE' ACTION
BE OCCURRING TODAY?*

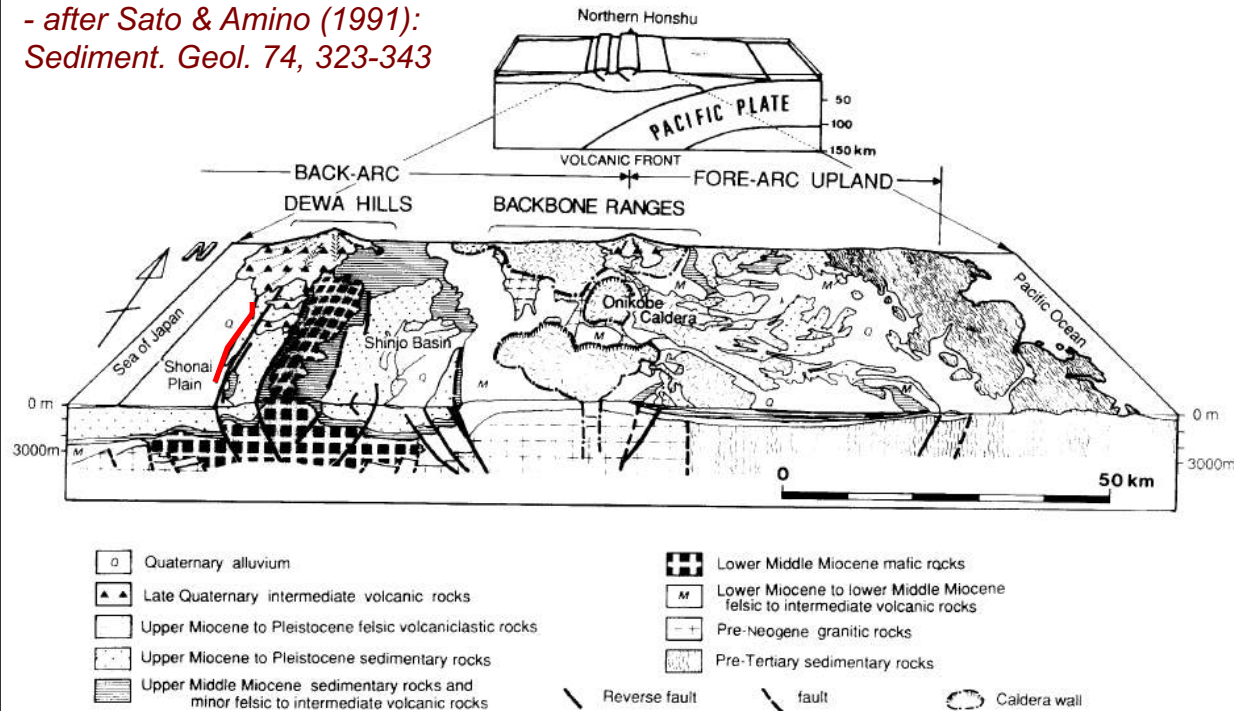
NE Honshu – a Magmatic Arc under Compression



- after H. Sato, 1994: J. Geophys. Res. 99, 22,261-22,274

Active Compressional Inversion in NE Honshu

- after Sato & Amino (1991):
Sediment. Geol. 74, 323-343

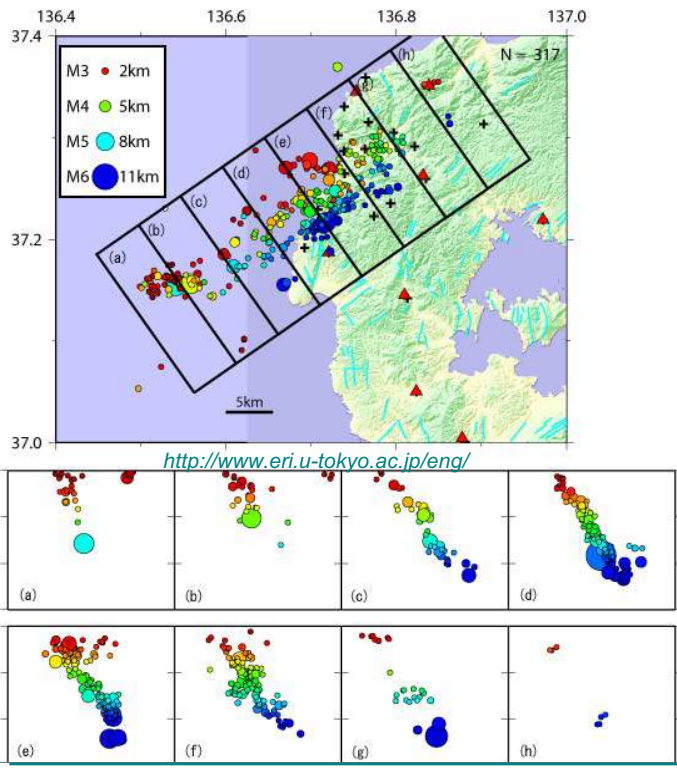


IV. COMPRESSSIONAL INVERSION - < Late Pliocene < 3-4 Ma to Present

III. PRE-INVERSION PHASE - Late Miocene to Pliocene

II. POST-RIFT PHASE - Middle to Late Miocene

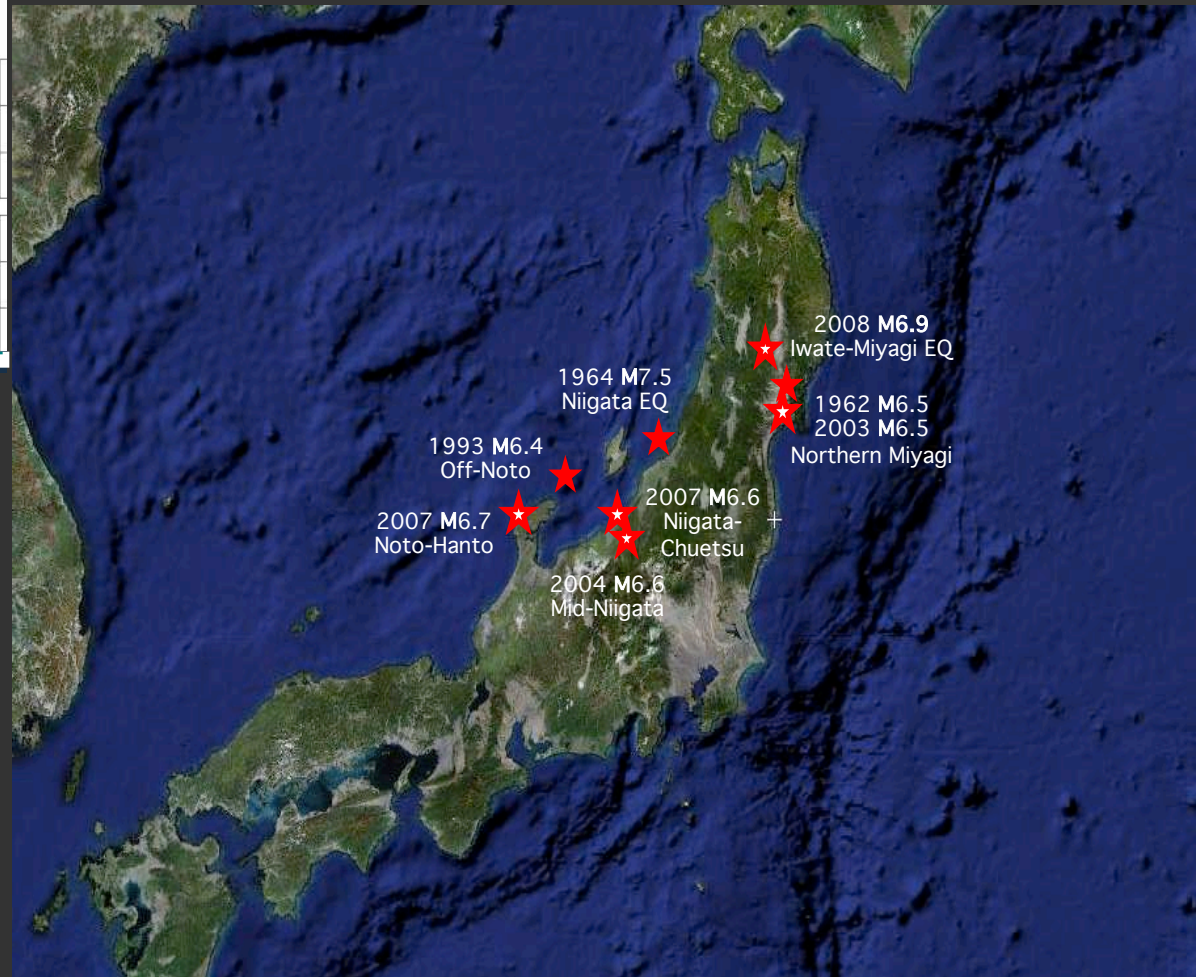
I. RIFT PHASE - Early to Middle Miocene (22-15 Ma) (opening of Japan Sea)



March 25, 2007, M6.7 Noto Hanto
Reverse Slip Rupture - 058° / 60° SE

High proportion of 'Inland Earthquakes' in northern Honshu result from ongoing compressional inversion

Recent Compressional Inversion Earthquakes in NE Honshu

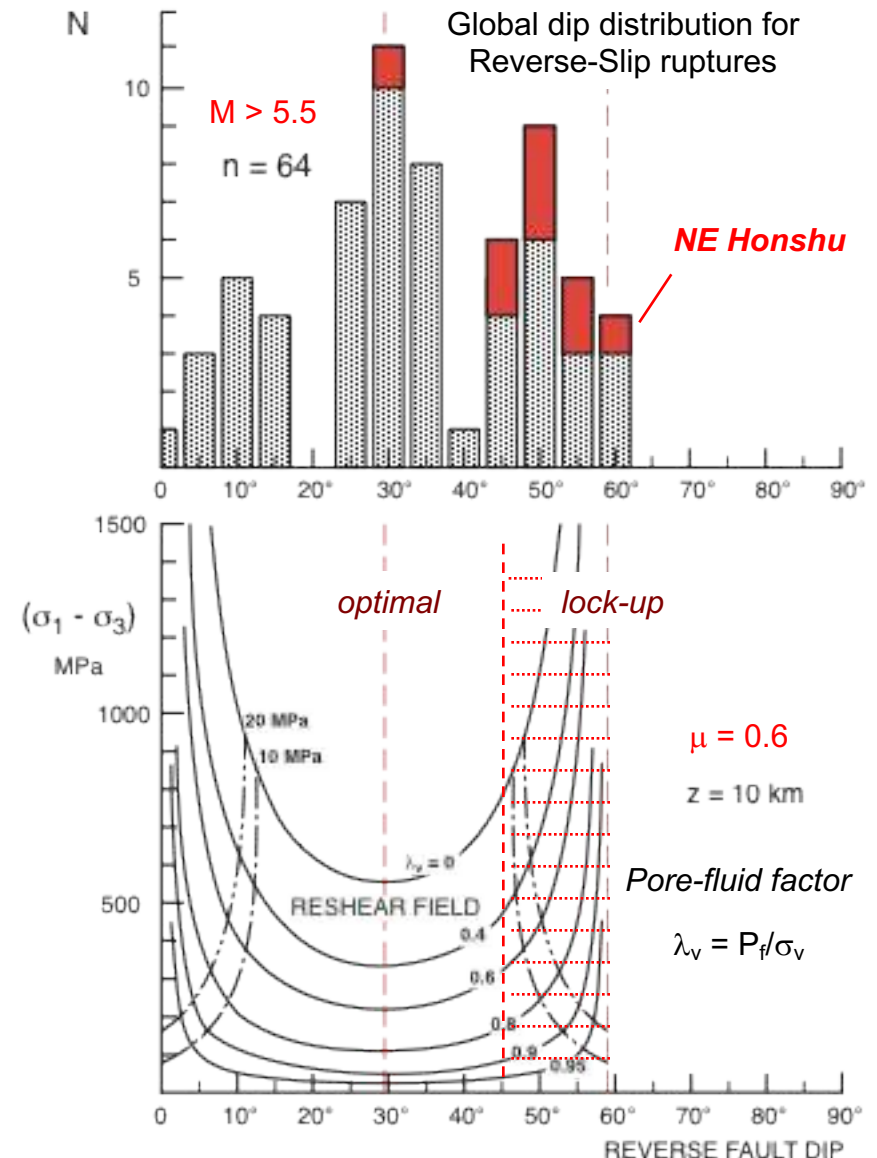


Dip Distribution of Reverse Fault Ruptures

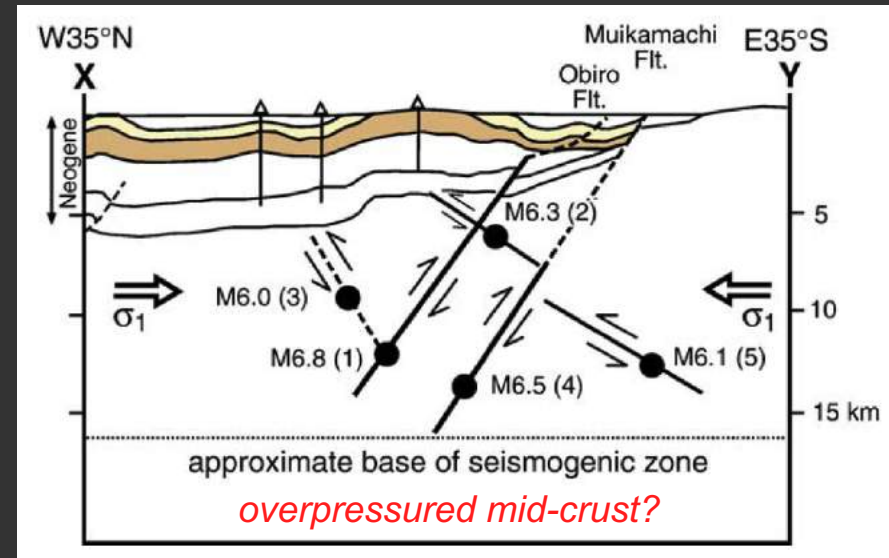
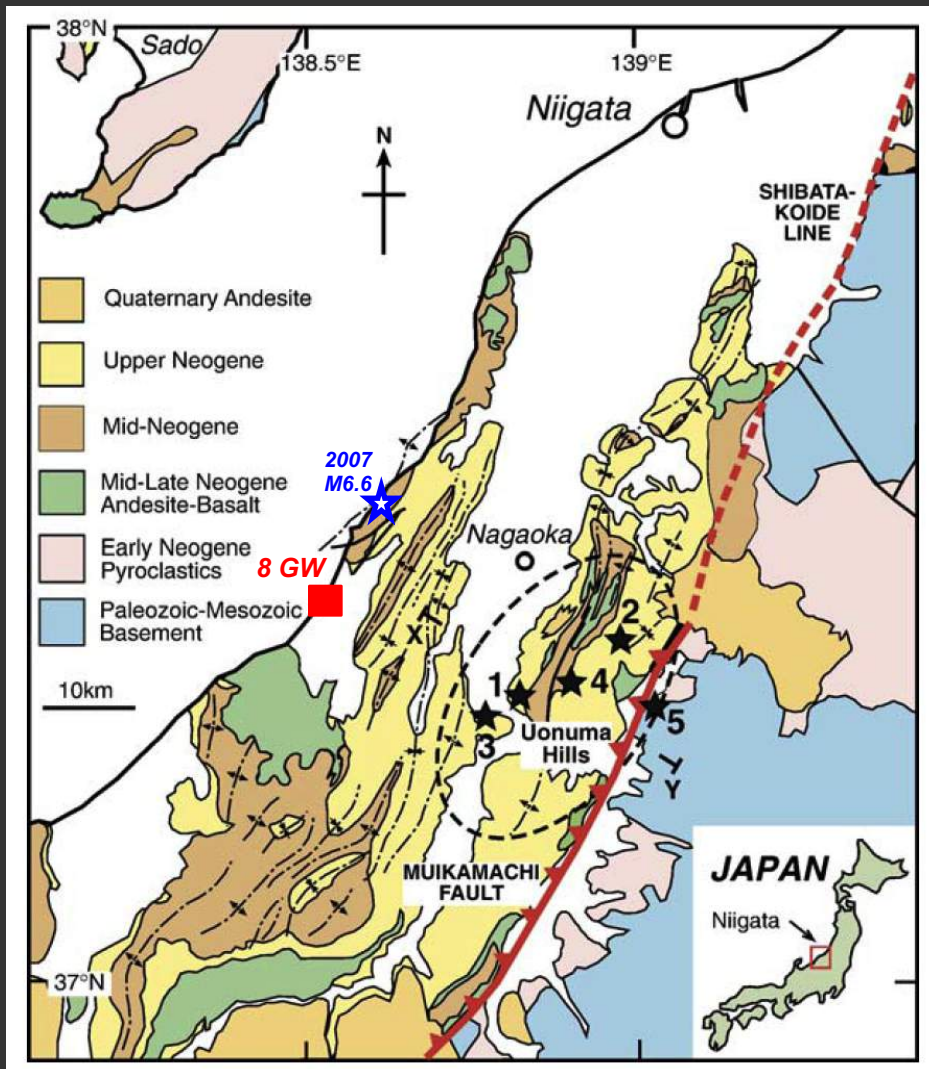
Peak at $\delta \sim 30^\circ$ and apparent 'lock-up' at $\delta \sim 60^\circ$ consistent with $\mu = 0.6$

Differential stress needed for reverse fault reshear at 10 km depth as a function of fault-dip and the state of fluid overpressure (σ_1 assumed horizontal)

Near-lithostatic fluid overpressures needed for reshear of steep reverse faults in preference to formation of new optimally oriented thrusts



2004 Mid-Niigata Earthquake Sequence



COMPETITION!

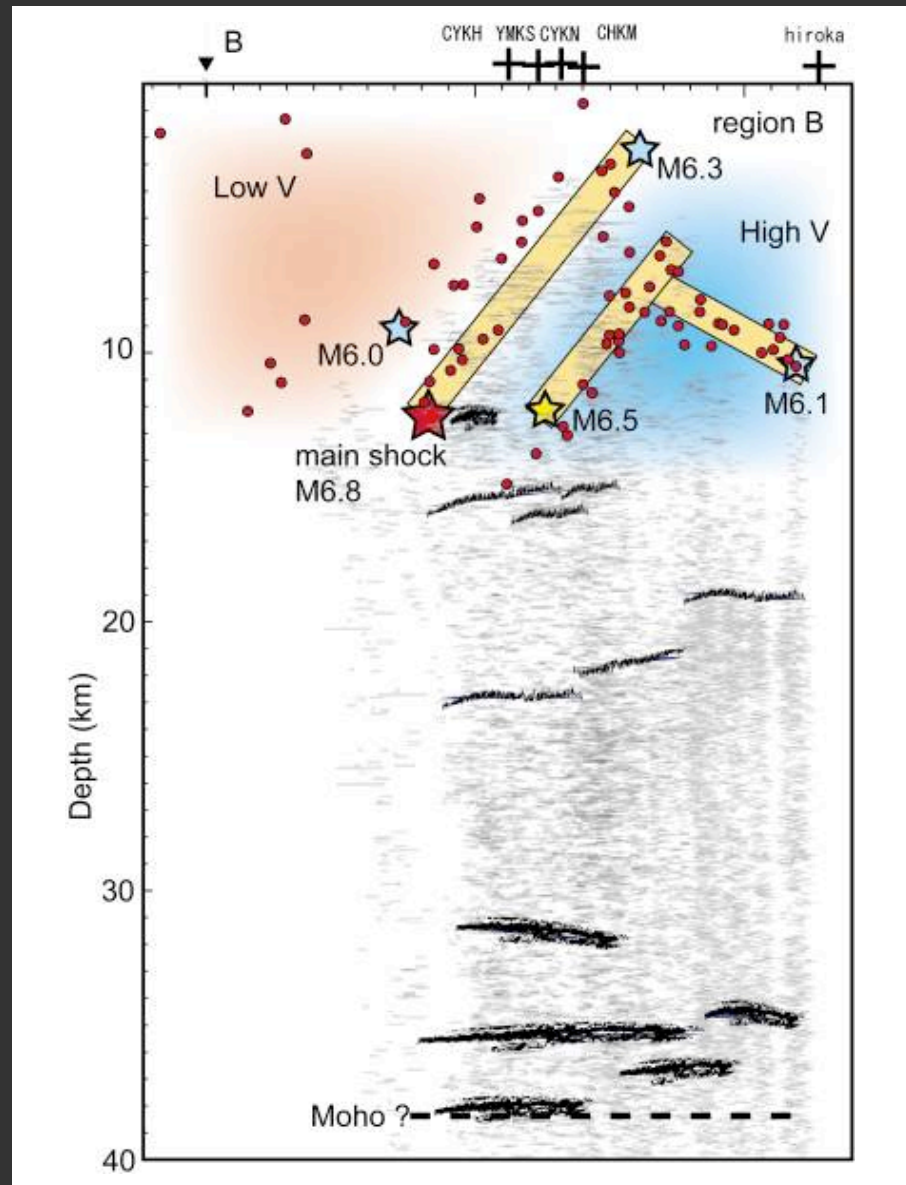
- Sibson (2007): *EPSL* 257, 188-199
after Hirata et al. (2005) and Hikima & Koketsu (2005)

2004 Mid-Niigata Earthquake Sequence

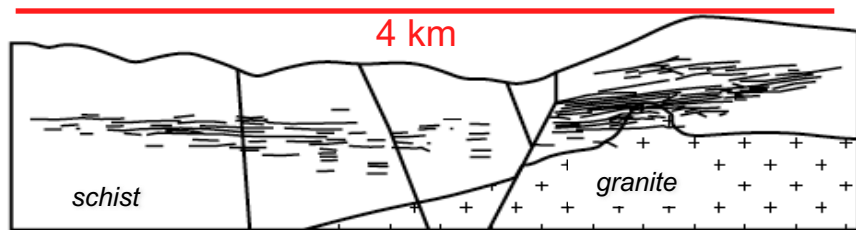
EQ	<u>Date-Time</u>	<u>Strike</u>	<u>Dip</u>	<u>Rake</u> (dev.)	<u>Depth</u>	M _{JMA}	M _W	M _o (x 10 ¹⁷ Nm)
1.	Oct. 23 17.56	216°	53° N W	93° (+3°)	9 km	6.8	6.6	88
2.	Oct. 23 18.03	020°	34° SE	73° (-17°)	7 km	6.3	5.9	8.5
3.	Oct. 23 18.11	020°	58° SE	70° (-20°)	9 km	6.0	5.7	4.1
4.	Oct. 23 18.34	216°	55° N W	94° (+4°)	12 km	6.5	6.3	32
5.	Oct. 27 10.40	039°	29° SE	73° (-17°)	11.5 km	6.1	5.9	7.5

- from Hikima & Koketsu (2005) & Shibutani et al. (2005)

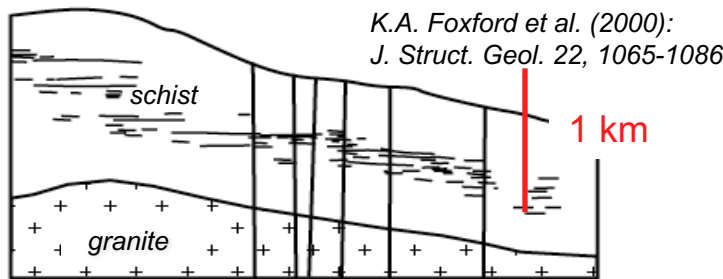
Bright-Spots Associated with 2004 Mid-Niigata Sequence



Fluid-Filled Arrays of Flat-Lying Hydrofractures as Bright-Spot Reflectors



4 km x 3km x 1 km array of W-Sn-Quartz veins, Minas da Panasqueira, Portugal



Hydrofracture Condition

$$P_f = \sigma_3 + T$$

with

$$(\sigma_1 - \sigma_3) < 4T$$

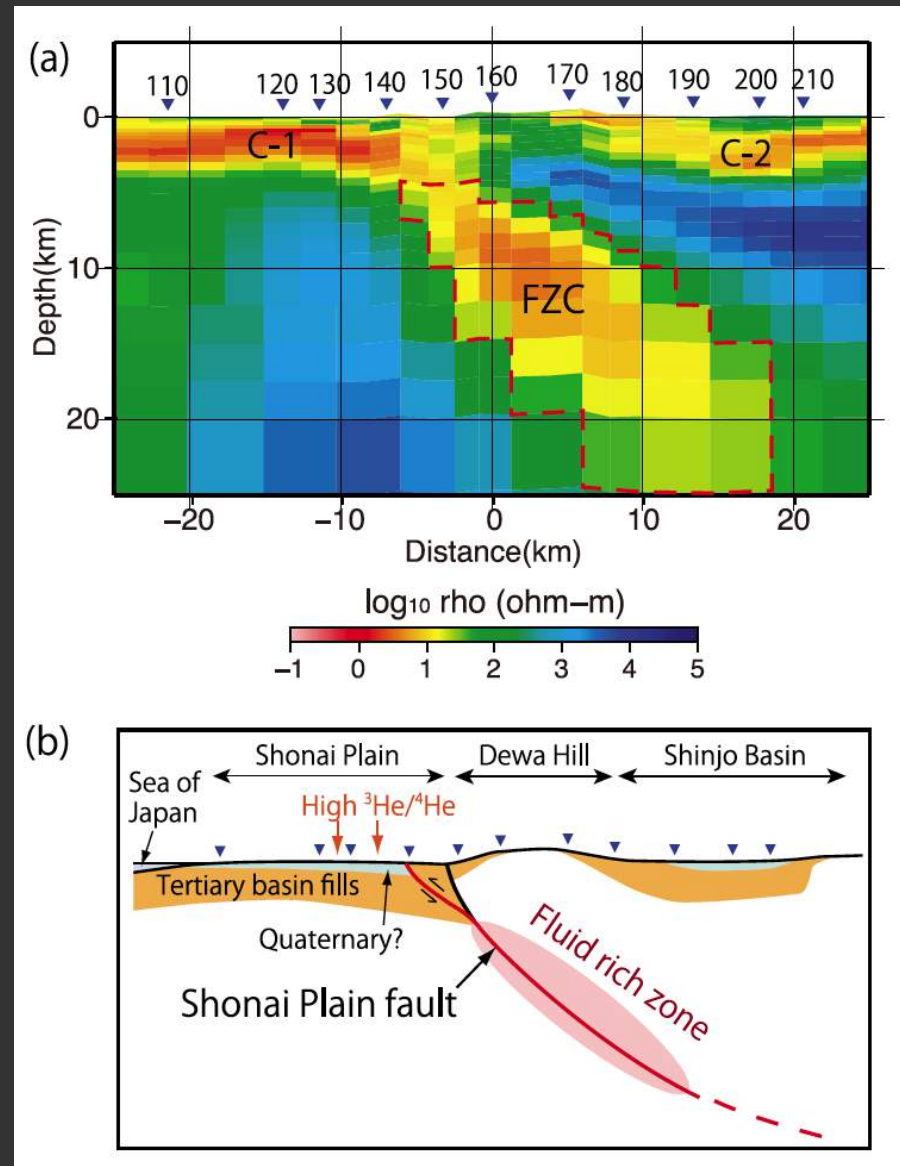
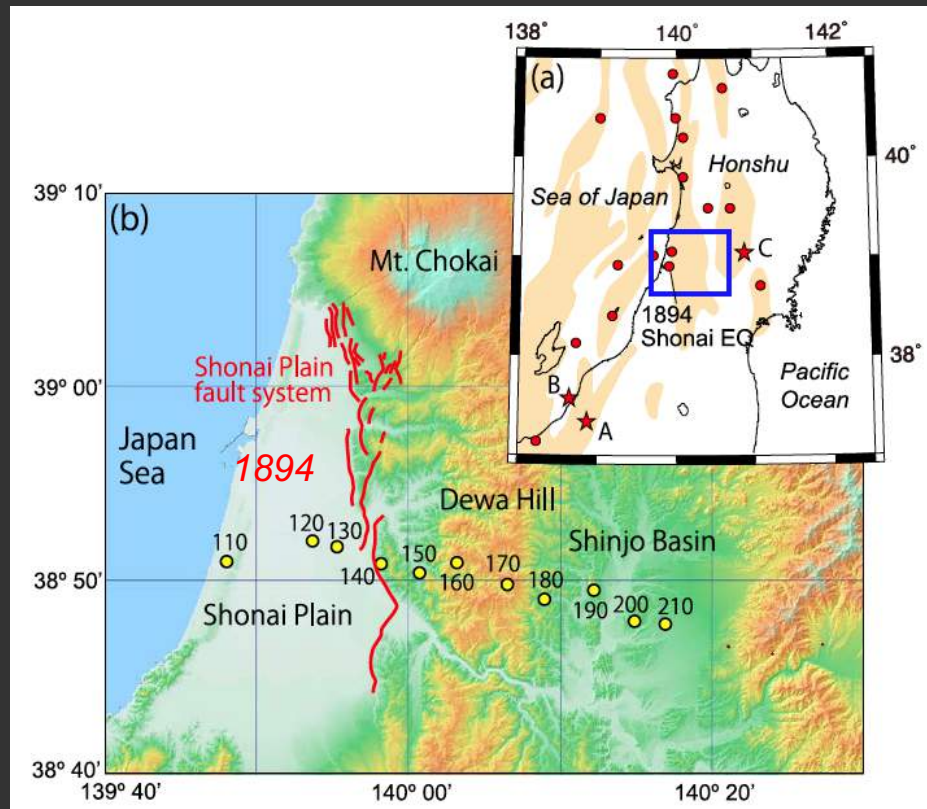
$\Rightarrow > \text{lithostatic } P_f \text{ if } \sigma_v = \sigma_3$

Au-Quartz Vein System, Damang Mine, Ghana



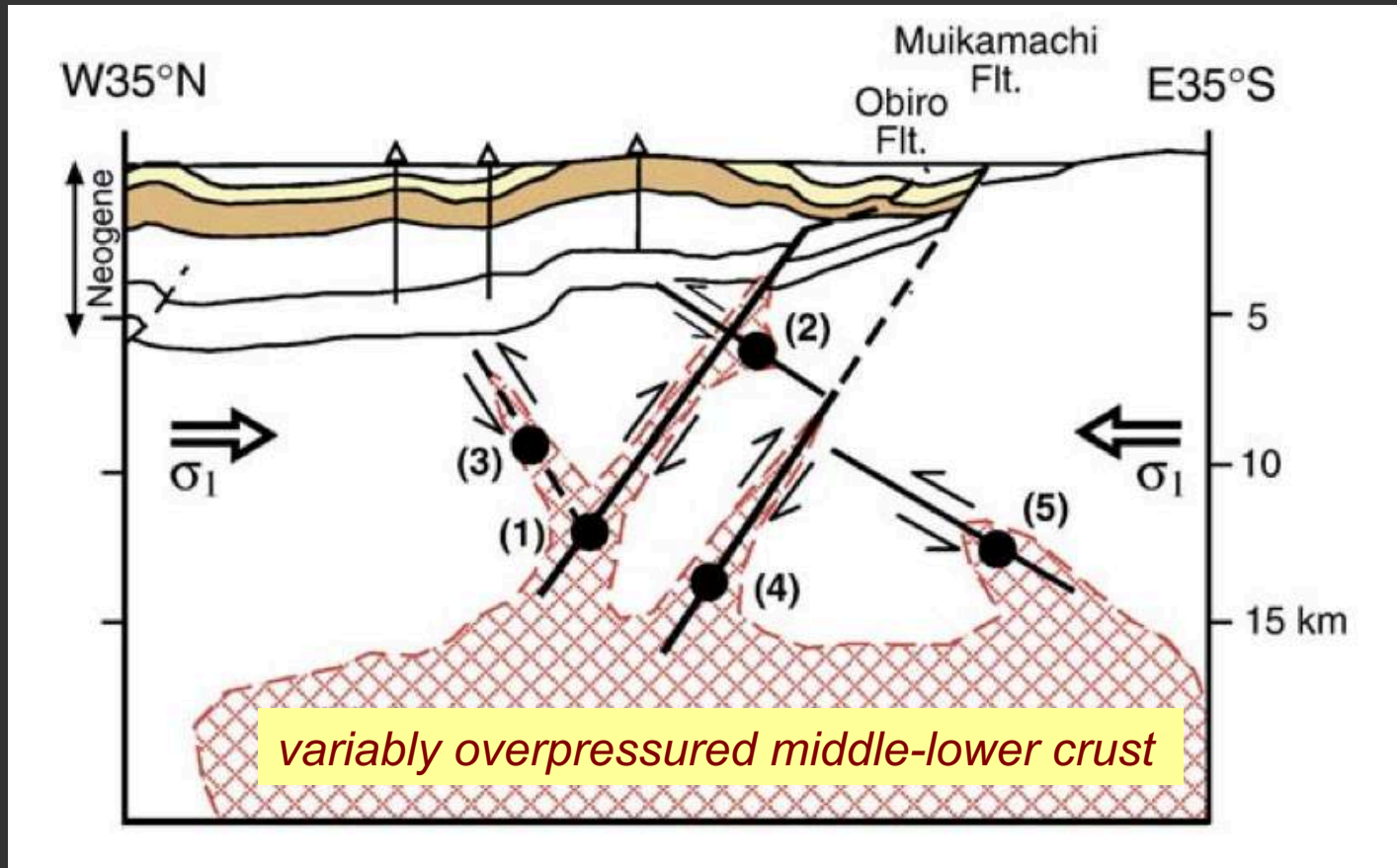
-photo by Andrew Tunks (see Tunks et al.
2004: J. Struct. Geol. 26, 1257-1273)

Shonai Plain Reverse Fault System

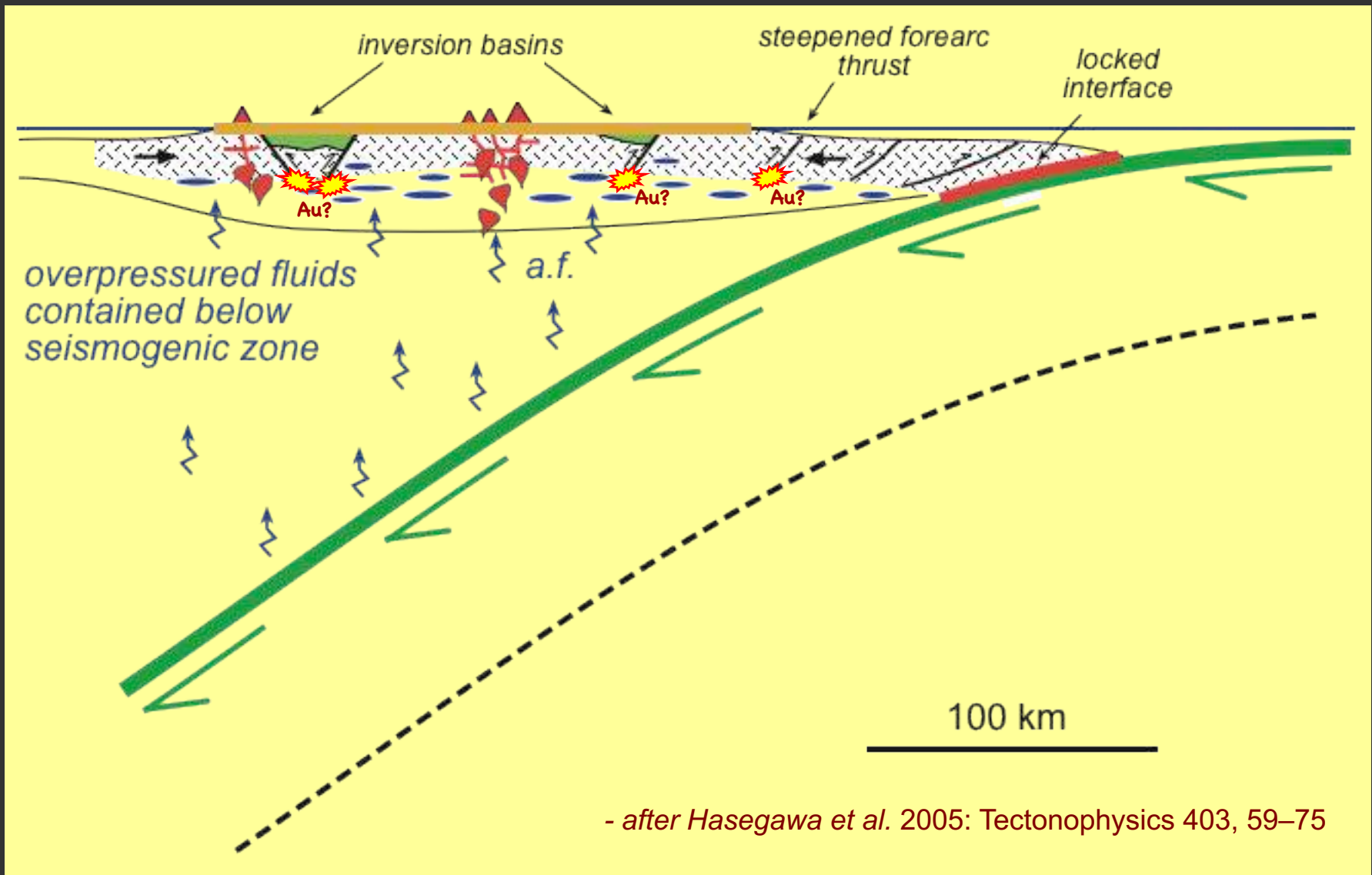


- Ichihara et al. 2011: *Geophys. Res. Lett.*
39, L09301, doi:10.1029/2011GL047382

Localised vs. Distributed Overpressuring?



Magmatic Arc Under Compression

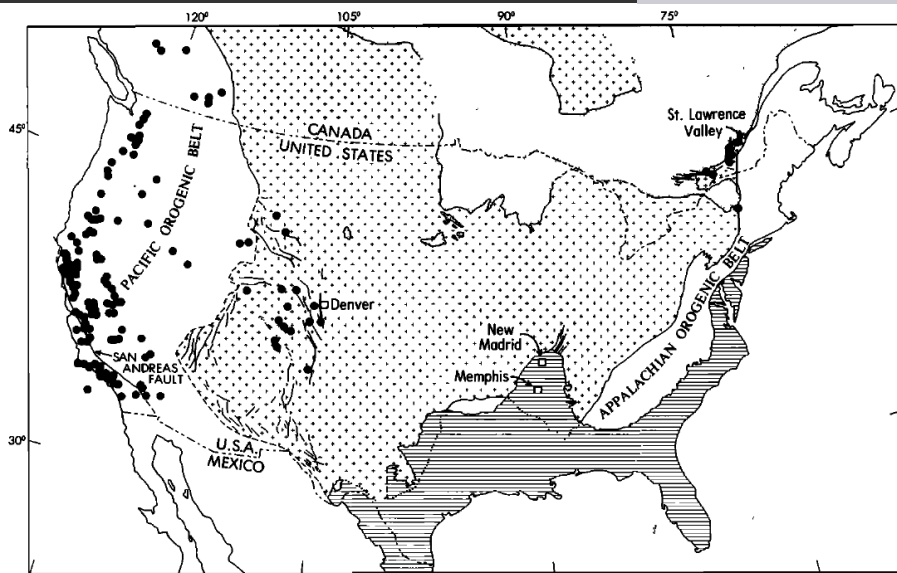
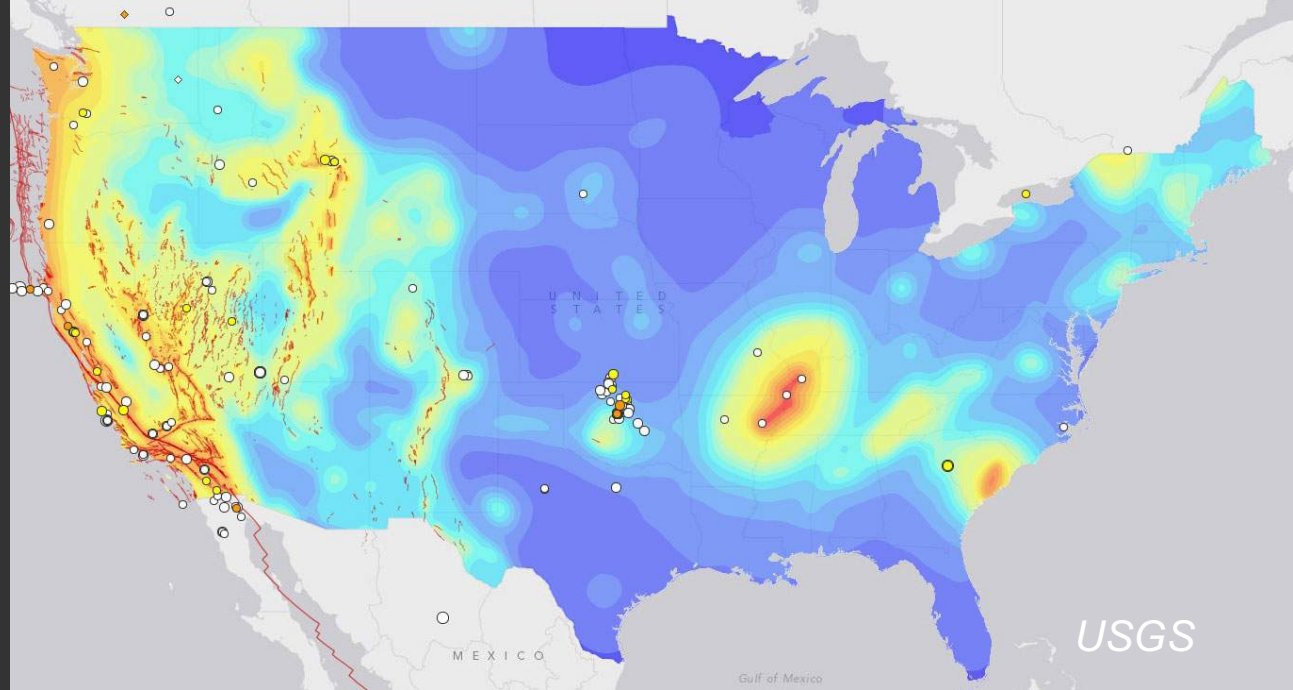


Conditions of Seismogenesis – NE Honshu

- *Compressional regime ($\sigma_v = \sigma_3$) with horizontal σ_1 orthogonal to magmatic arc*
- *Larger ruptures nucleate in lower half of crustal seismogenic zone (commonly, $7 < z < 15$ km)*
- *Dominance of steep reverse faults ($50^\circ < \delta < 60^\circ$) over ‘Andersonian’ thrusts ($\delta \sim 25\text{-}35^\circ$) suggests near-lithostatic overpressure in rupture nucleation sites*
- *Lower seismogenic zone with $150^\circ < T < 350^\circ$ C is hydrothermally active - electrical and tomographic studies support presence of overpressured fluid in interconnected pore space around the active faults*
- *($\sigma_1 - \sigma_3$) $< 40\text{-}80$ MPa if bright spot reflectors are fluid-filled hydrofracture arrays with $P_f > \sigma_v = \sigma_3$*

*How many EQs are
are wholly or partly
fluid-driven?*

- Anthropogenic vs. Natural?



- EXPLANATION
- Precambrian rocks
 - Platform deposits on Precambrian basement; Paleozoic and younger strata
 - Platform deposits; Mesozoic and Cenozoic strata
 - CO₂ locality

Seismicity and CO₂ rich springs

*Irwin & Barnes, 1980: J. Geophys.
Res. 85, 3115-3121*

Intraplate EQs along the Atlantic Seaboard

- *1982 Miramichi , New Brunswick, sequence – m_b 5.7, 5.1, 5.4, 5.0 at c. 7 km depth - predominantly reverse-slip ruptures on NNE-SSW striking conjugate planes dipping $50-65^\circ$ (Wetmiller et al. 1984)*
- *1983 Goodnow, NY - m_b 5.7 – 7-8 km depth, close-to-pure reverse slip on a plane striking NNW-SSE, dipping $60-70^\circ$ WSW*
- *2011 Mineral, Virginia EQ – M_w 5.7 – 6-8 km depth – close-to-pure reverse slip mainshock rupture $033^\circ / 51^\circ$ SE (Wu et al. 2015)*
- *2012 Waterboro, Maine – M_w 4.0 – 6.6 km depth – close-to-pure reverse slip – dip c. 33° SW? or 57° NE?*
- *1886 Charleston, S. Carolina – c. M_w 7.0 ?????*

What Drives Fault Failure?

TWO drivers to failure - $\Delta(\sigma_1 - \sigma_3)$ and ΔP_f



*Failure from INCREASING
DIFFERENTIAL STRESS*

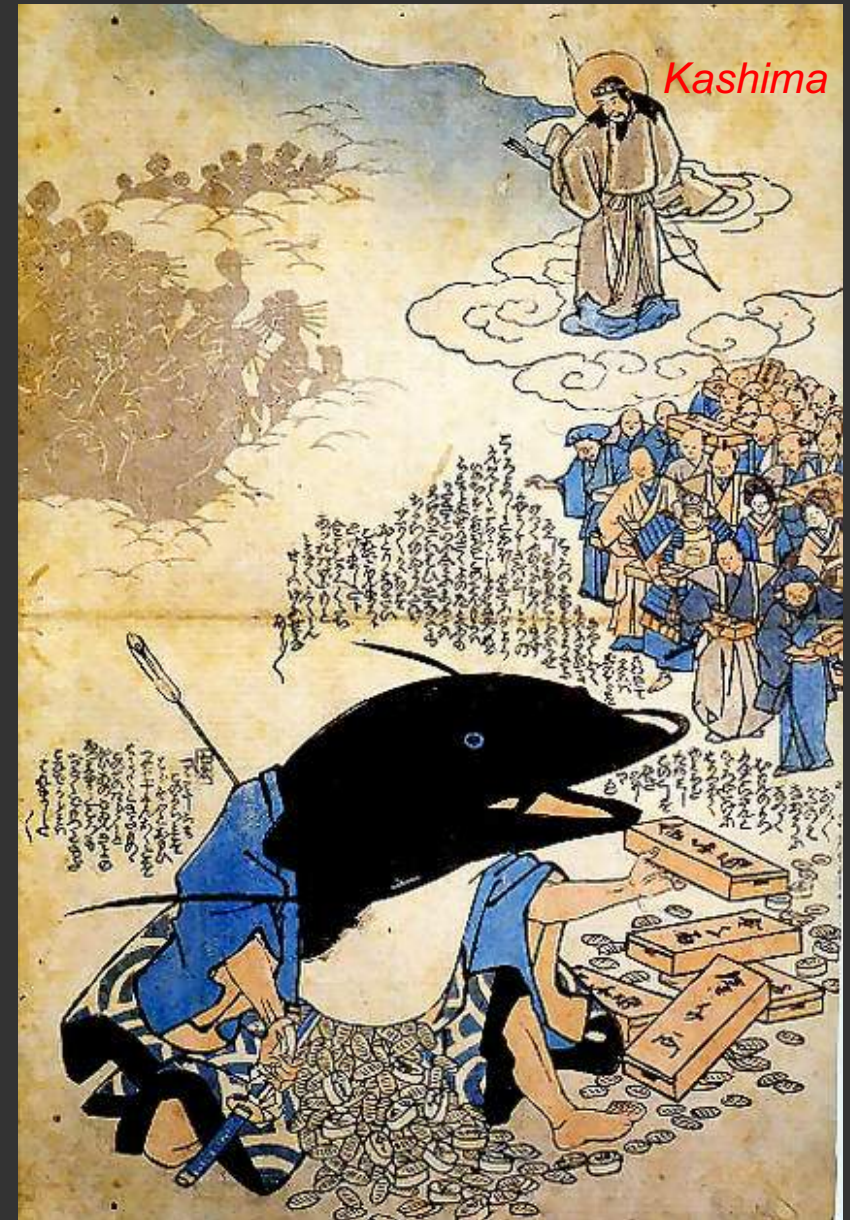
*Failure from DECREASING
FAULT STRENGTH*

WHAT FLUIDS? - H_2O and/or CO_2 ??

CONCLUSIONS

1. Dip distribution of reverse fault ruptures supports $\mu_s \sim 0.6$
2. Compressional Inversion is widespread and accounts for a high proportion of active steep reverse faults (e.g. N. Honshu)
3. Reactivation mechanics suggest \sim lithostatic fluid overpressures needed for rupture nucleation on steep reverse faults
4. Such high overpressures are supported by hydrothermal vein systems developed around steep reverse faults exhumed from the lower seismogenic zone
5. High fluid overpressures in the lower seismogenic zone of areas undergoing active compressional inversion also supported by observations of bright-spot reflectors, anomalously high V_p/V_s , and high electrical conductivity
6. Cycling of fluid-overpressure through 'fault-valve' action changes frictional fault strength, affecting EQ nucleation and recurrence
7. Fault Failure that is at least partly FLUID-DRIVEN may be more widespread than is generally supposed.

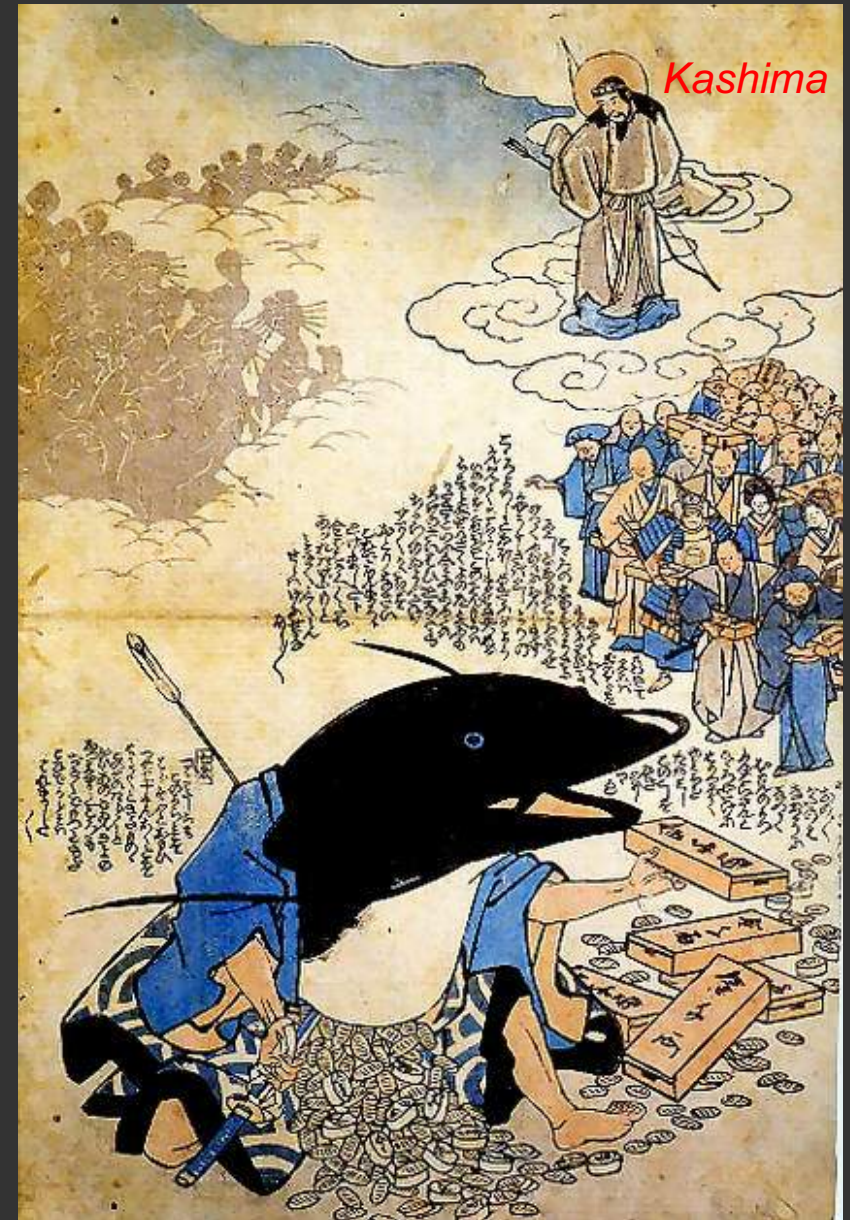
THE GOLDEN NAMAZU



THE GOLDEN NAMAZU



Active Catfish Need Water!



Escarpment of Waimea Fault & Nelson City



*Mathematical
Complexity*

x

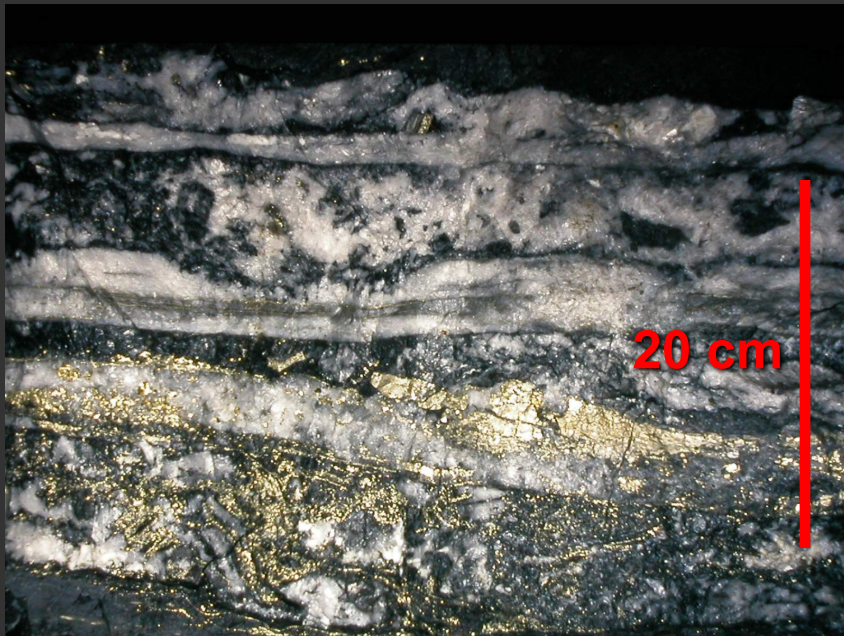
*Geological
Complexity*

~ 1

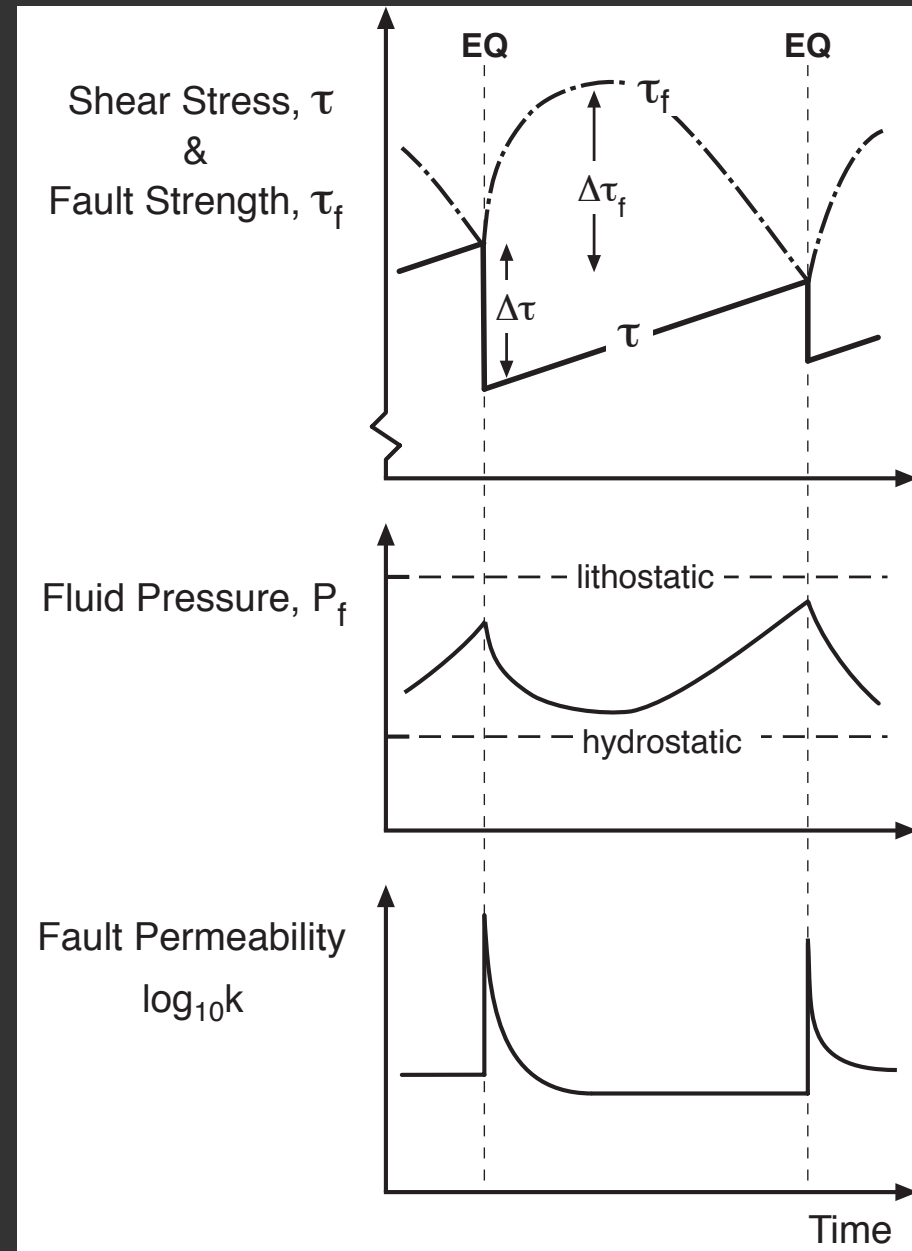
Low-Displacement Normal Faults



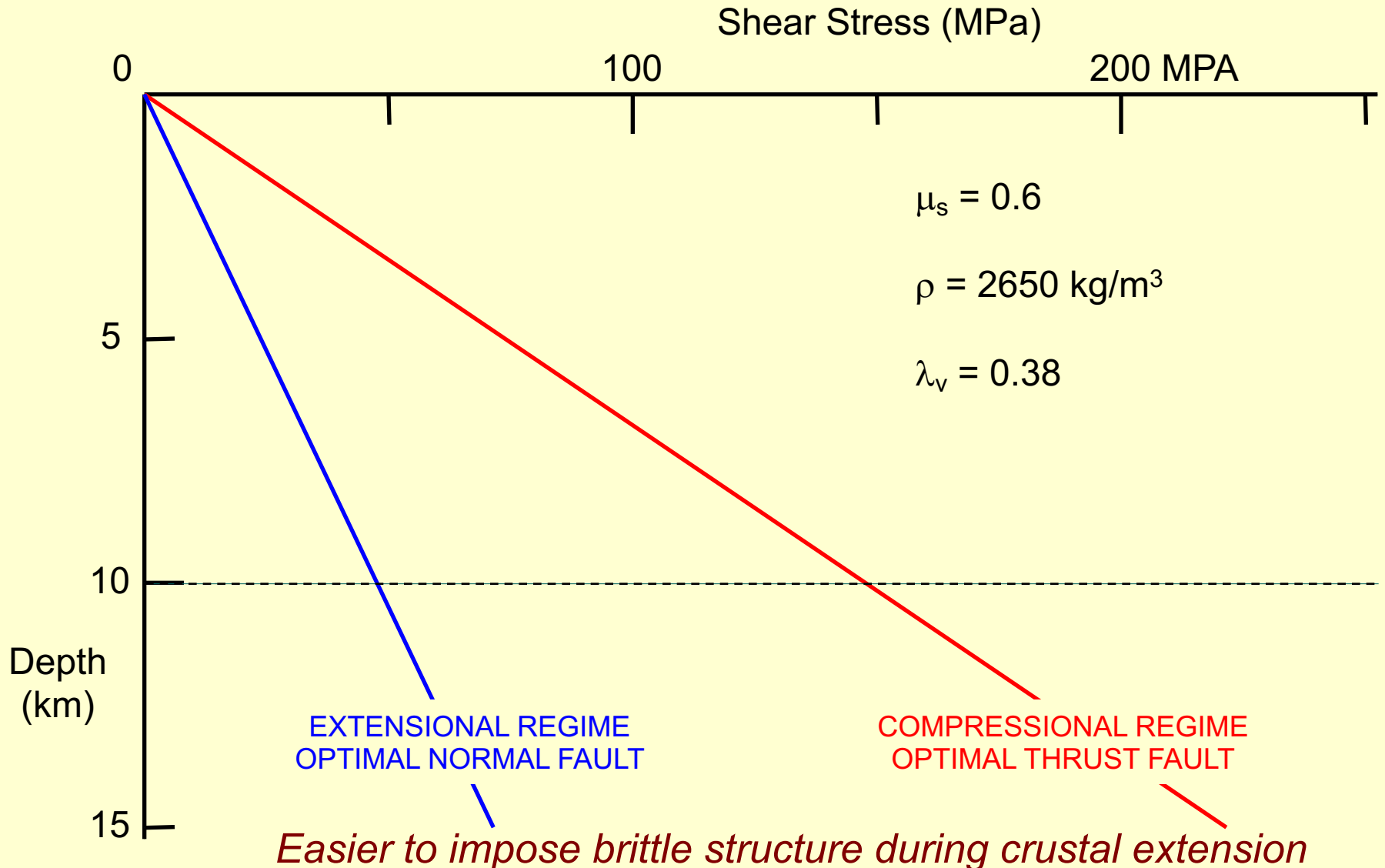
INFERRED FAULT-VALVE CYCLE



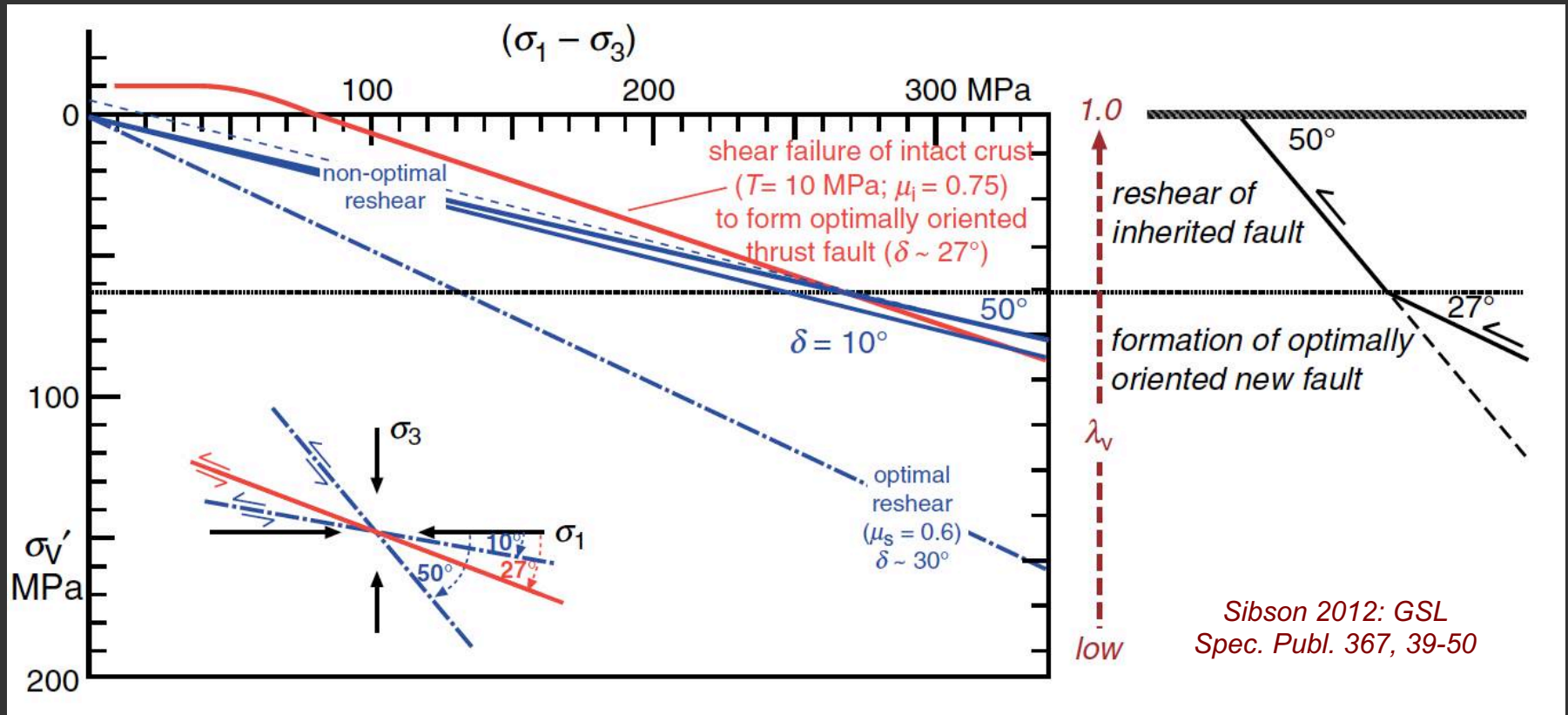
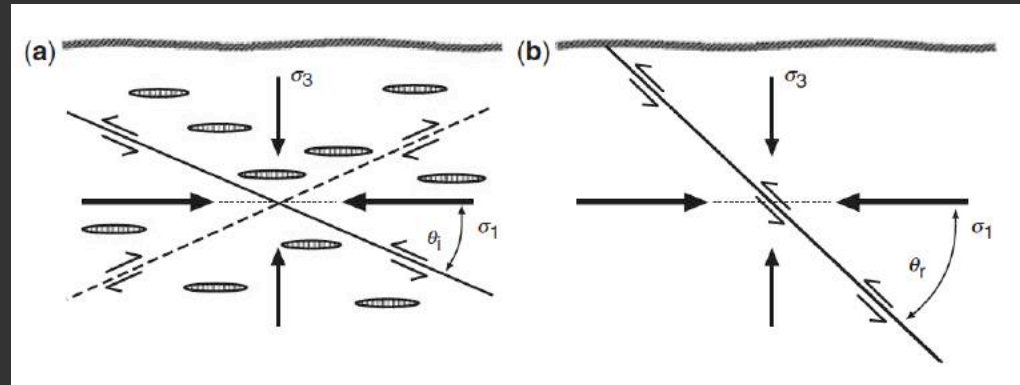
- intense competition between creation and destruction of fracture permeability



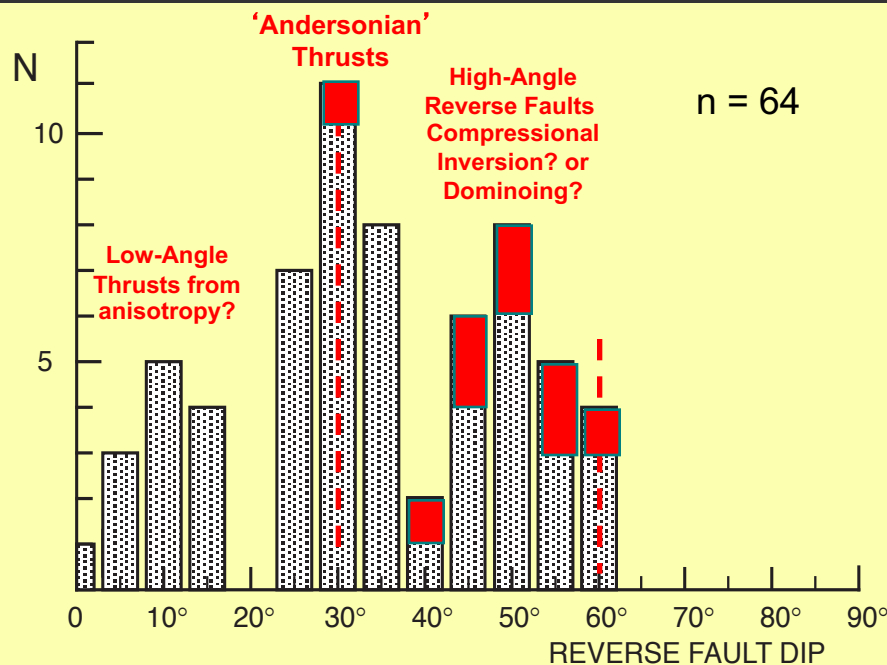
Frictional Strength of Optimally Oriented Faults under Hydrostatic-Byerlee Conditions



Non-Optimal Reshear vs. Formation of New Fault



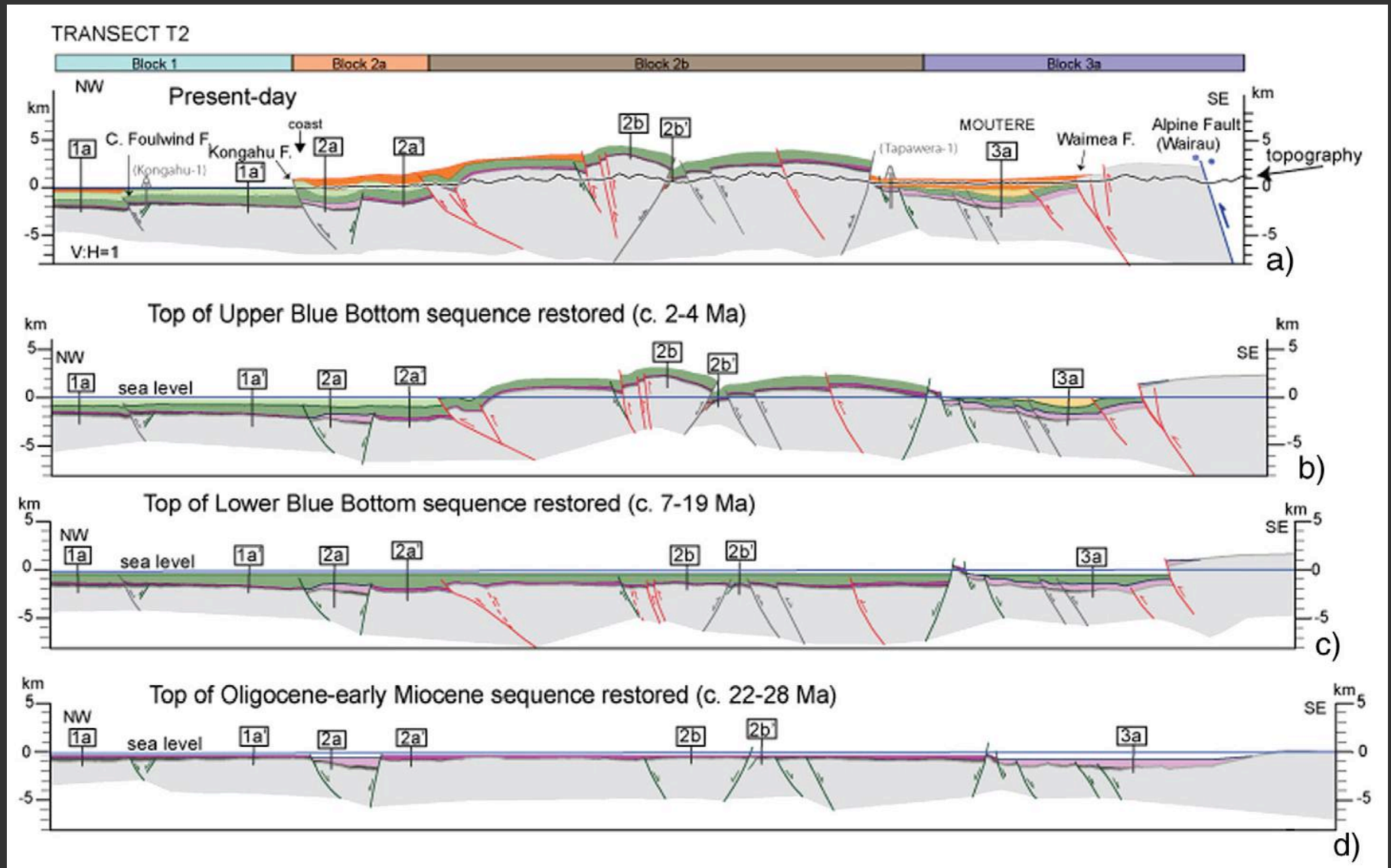
Interpreted Dip Distribution for Reverse Fault Ruptures



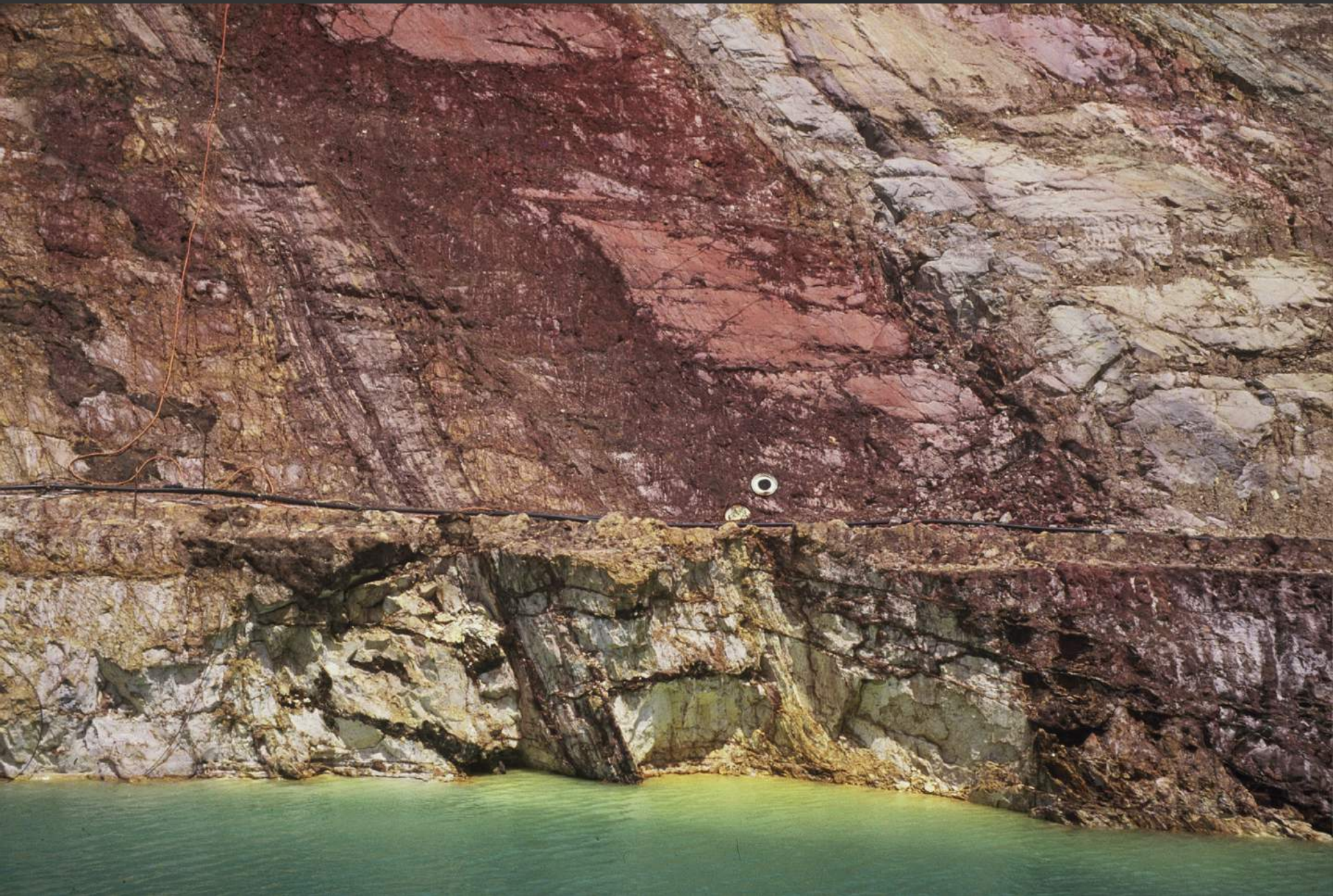
On the assumption of horizontal σ_1

- $30 \pm 5^\circ$ dip cluster may reflect optimal 'Andersonian' orientation for reactivation when $\mu_s \approx 0.6$
- Lack of rupture dips $> 60^\circ$ may reflect frictional 'lock-up' at $\theta_r \approx 60^\circ$, also consistent with $\mu_s \approx 0.6$
- Dip clusters at $10 \pm 5^\circ$ and $50 \pm 5^\circ$ represent unfavourably oriented reverse faults

Progressively Restored NW-SE Cross-Sections, NW South Island



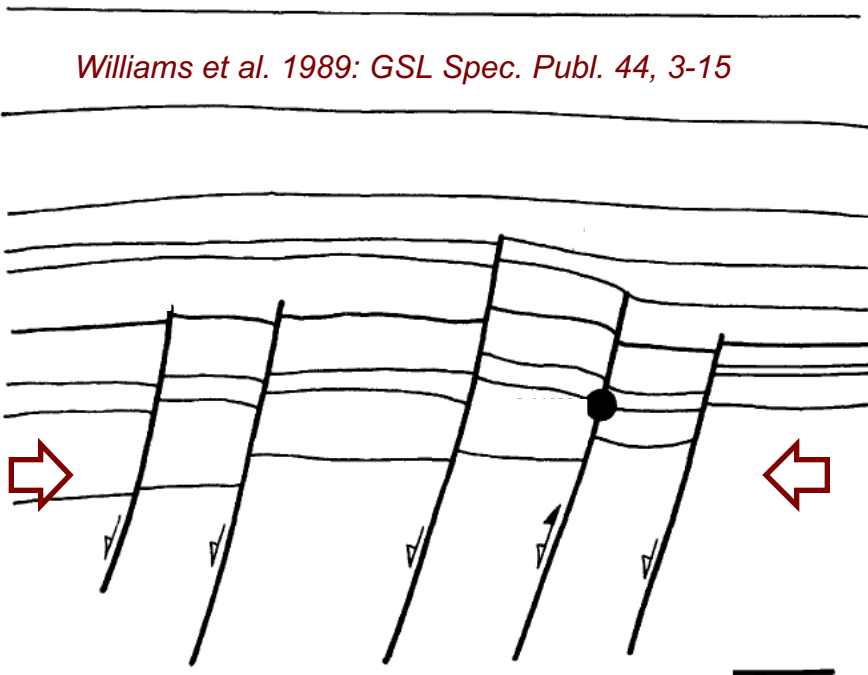
Paddington North Pit, W.A.



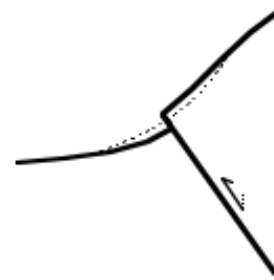
Near-Surface Structural Complications

Incipient Inversion – seismogenic structures lurking below sediment cover along margins of former extensional basins

Williams et al. 1989: GSL Spec. Publ. 44, 3-15



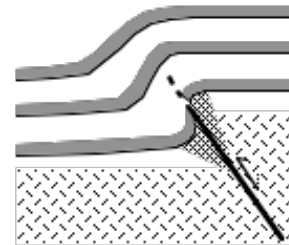
(a) Collapse of Rupture Scarp



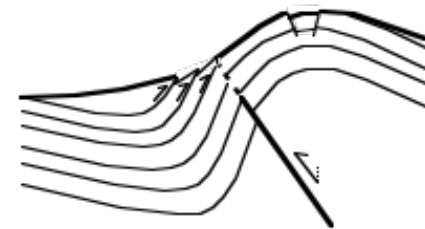
(b) Rockfalls & Landslides



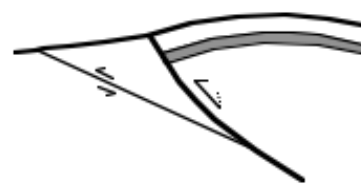
(c) Monoclinal Drape-Fold in Cover



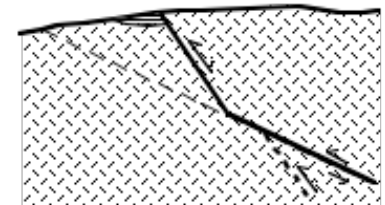
(d) Distributed Folding Deformation (flexural slip and bending) in Cover



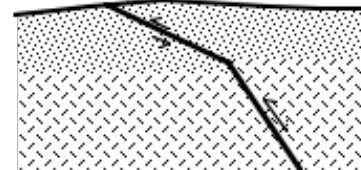
(e) Listric Reverse Fault - High-Level Folding with Development of a Footwall Short-Cut at Depth



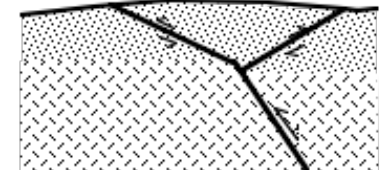
(f) Decapitation in Basement by Short-Cut Thrust



(g) Reverse-Fault Refracting to Low-Dip in Young Cover Sediment

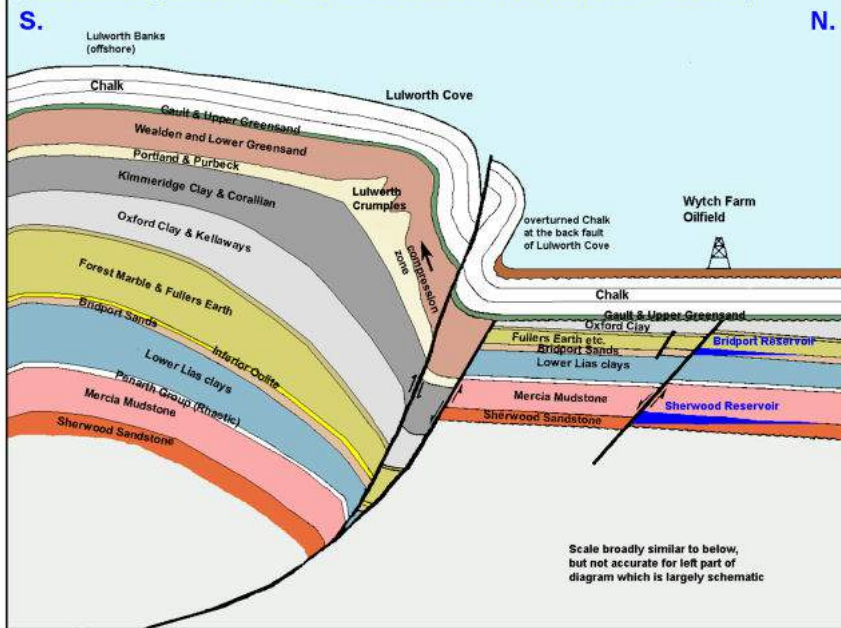


(h) Reverse Fault 'Pop-Up' in Young Cover Sediment

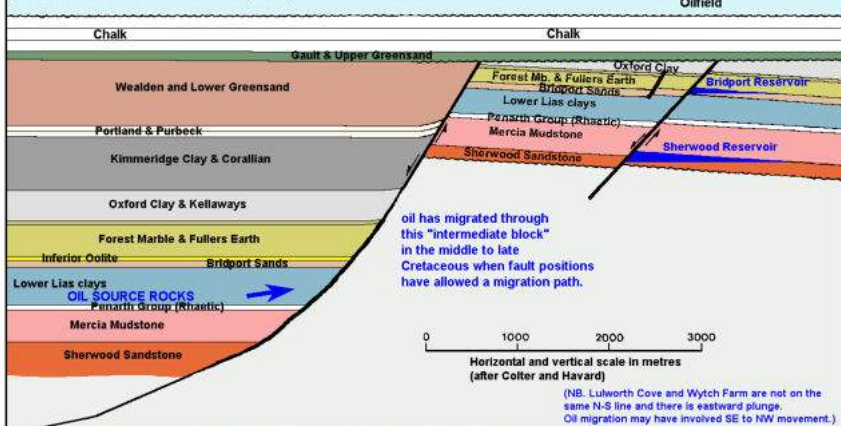


Progressive Inversion

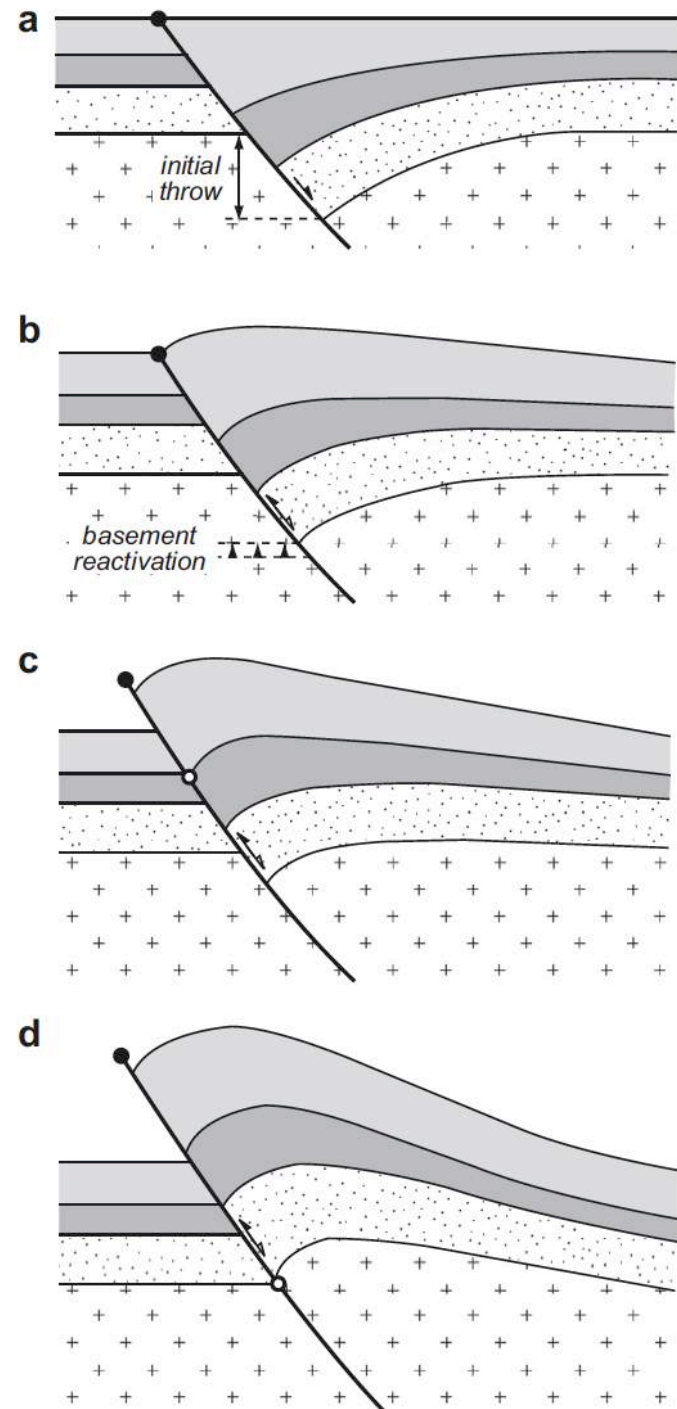
ALPINE, TERTIARY, COMPRESSIONAL PHASE AT THE PURBECK DISTURBANCE (FAULTED MONOCLINE)
(Schematic and exaggerated on the left, and without the Middle Eocene and later unconformities shown)



LATE KIMMERIAN EXTENSIONAL FAULTING BENEATH THE SUB-ALBIAN UNCONFORMITY
(modified after Colter and Havard, 1981)



EXPLANATION OF STRUCTURES AT LULWORTH COVE AND WYTCH FARM, DORSET (MARGIN OF CHANNEL INVERSION).
This is schematic and simplified, and is based on Colter and Havard (1981), House (1993), and observations on the analogous inversion margin at Bincombe (Weymouth Relief Road). It is hypothetical above cliff level at Lulworth Cove and it omits Tertiary unconformities. See also Underhill and Stoney (1998) for more information.
Ian West (c) 2010.



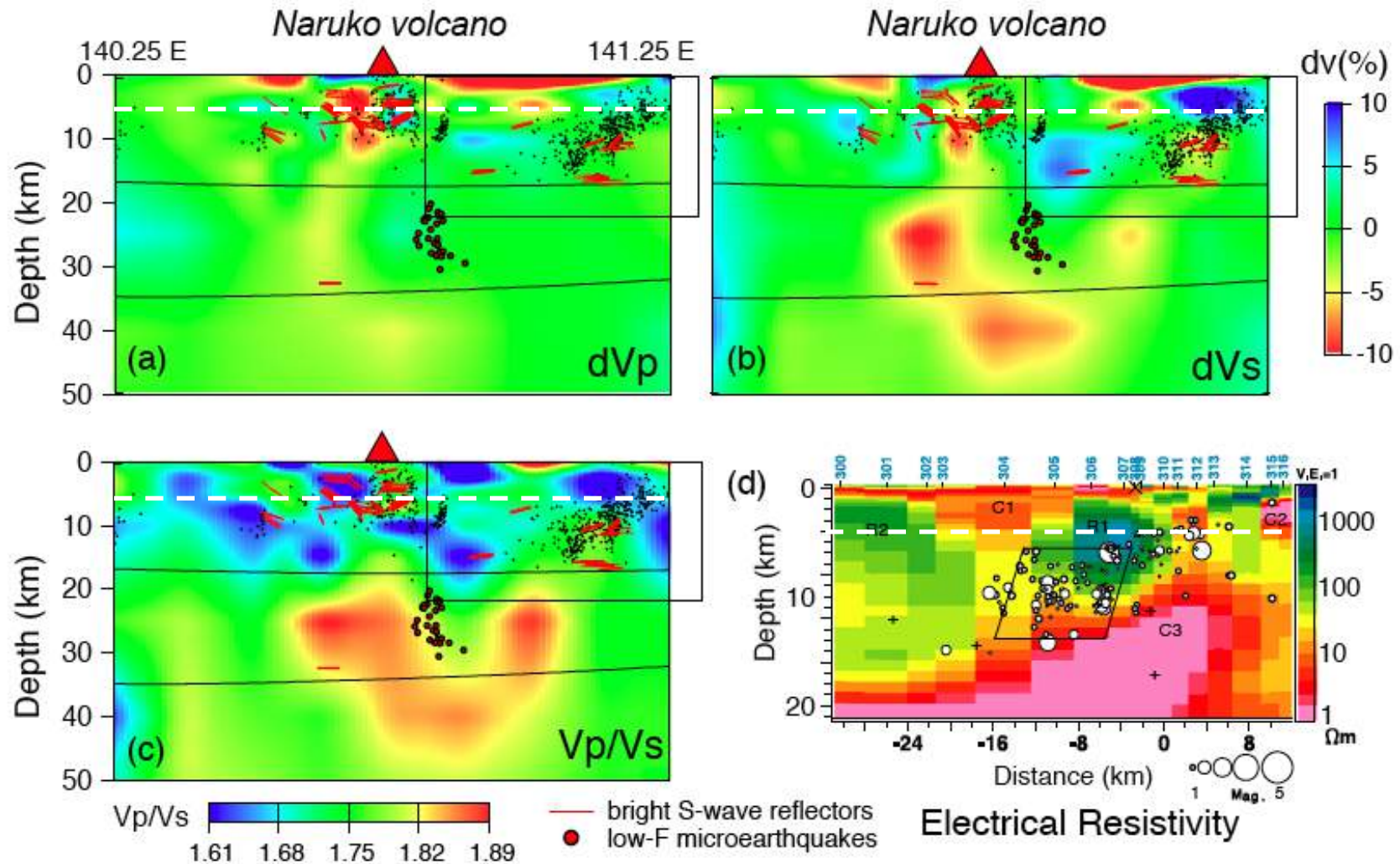


*Harvard Mine,
nr. Jamestown,
Mother Lode Belt*



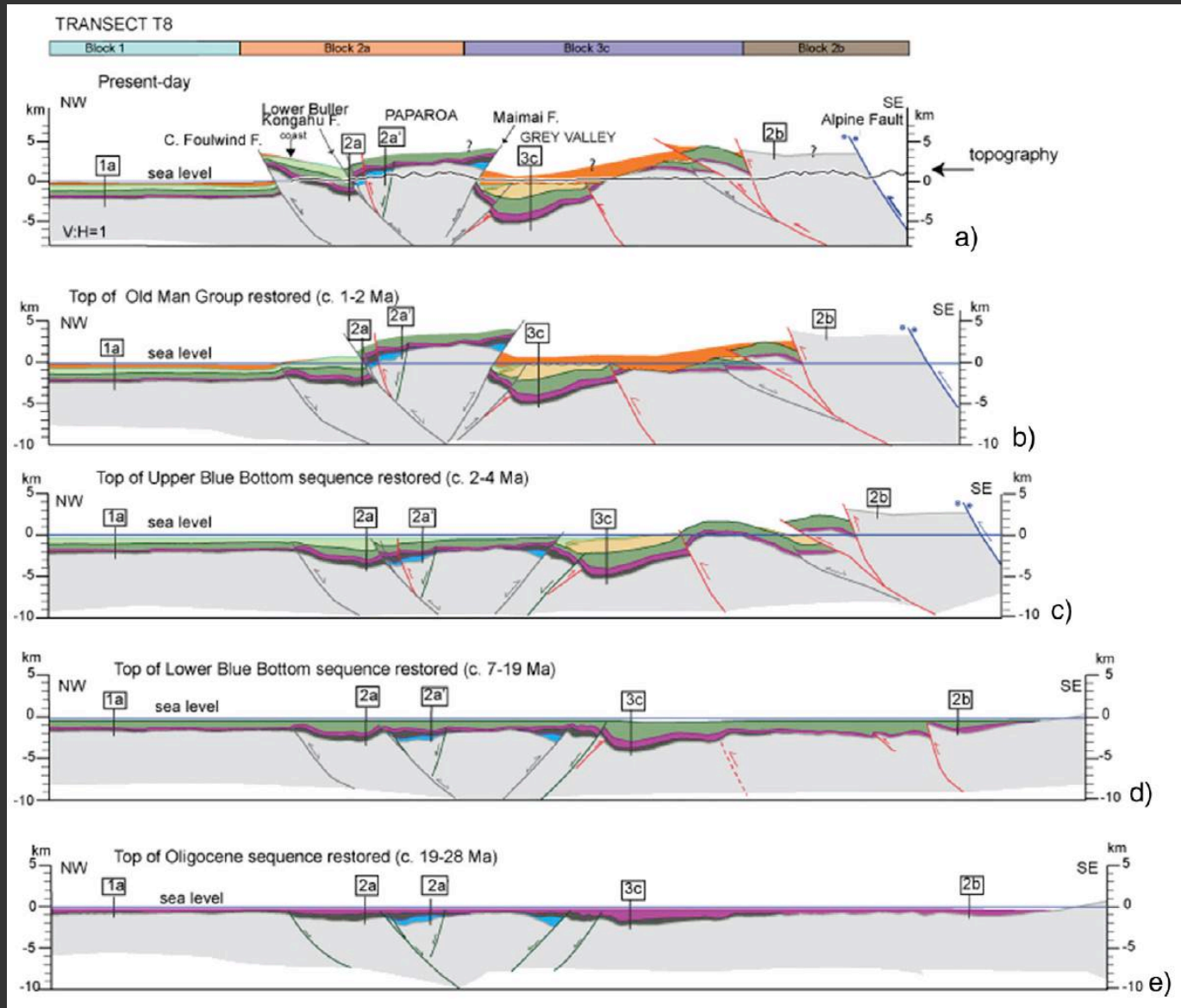
*Pine-Tree Mine,
Hell Hollow,
Mother Lode Belt*

Bright-Spot Reflectors, NE Honshu

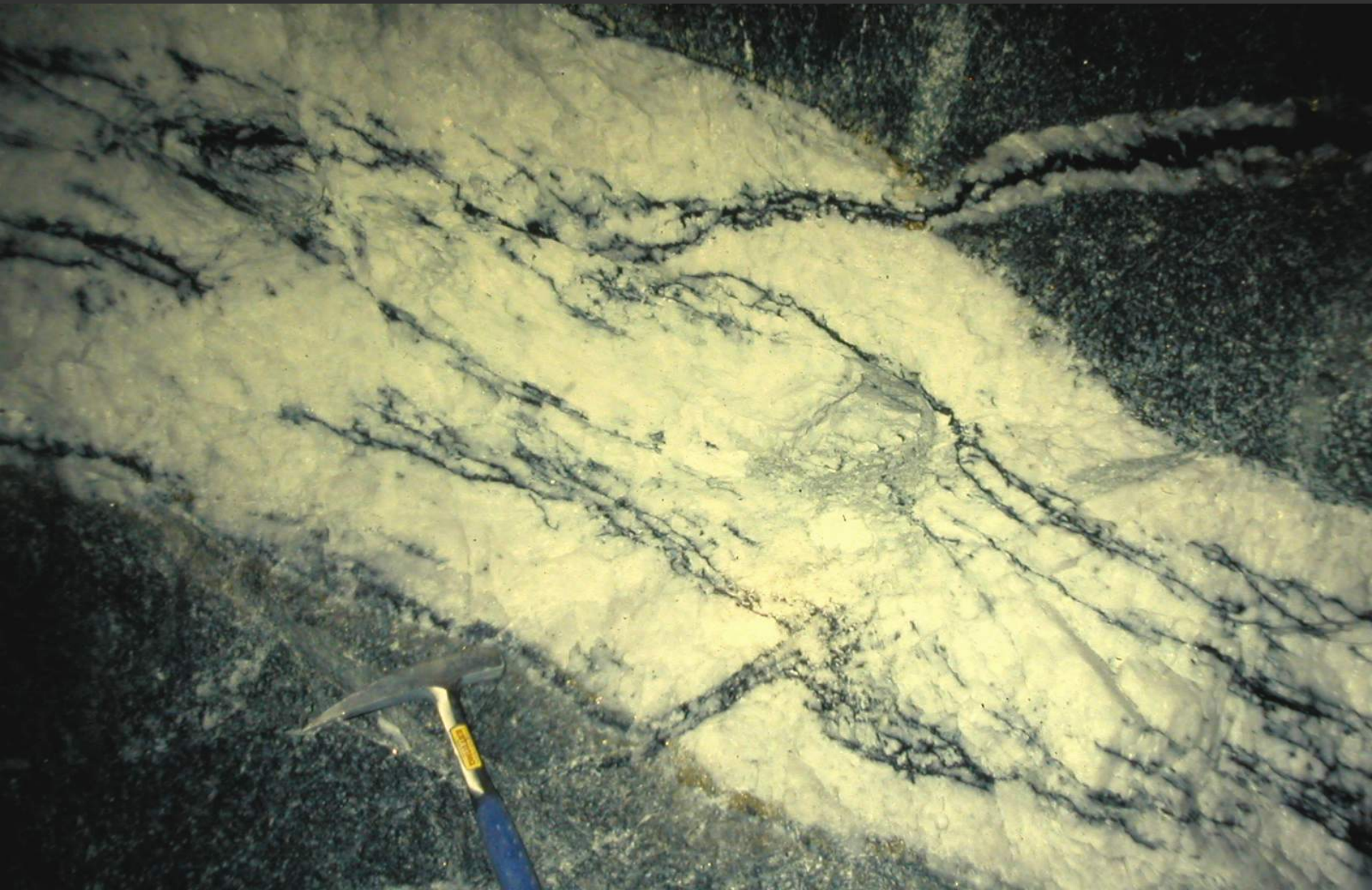


A. Hasegawa et al. (2005): *Tectonophysics* 403, 59–75

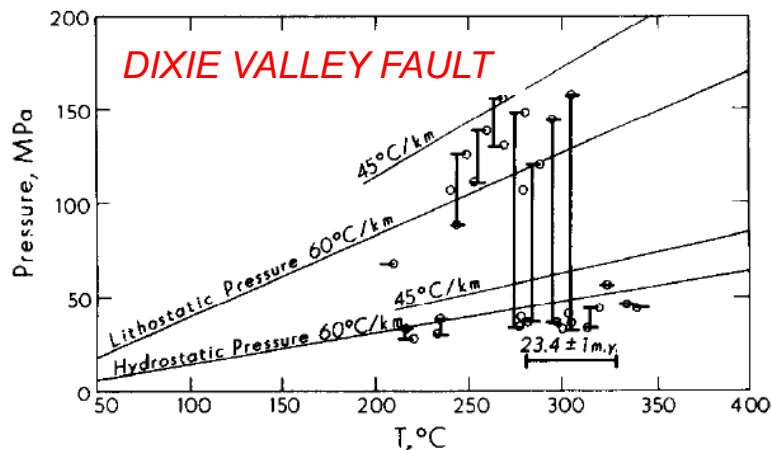
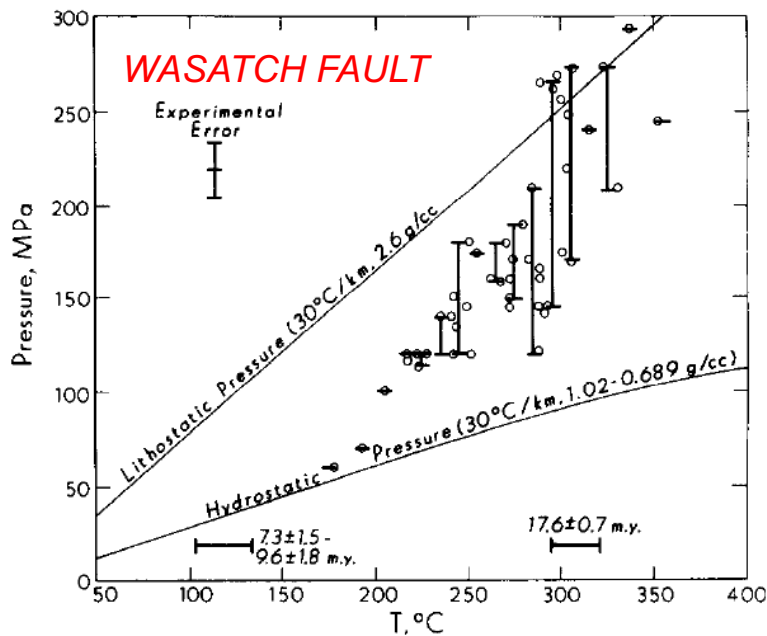
Progressively Restored NW-SE Cross-Sections, NW South Island



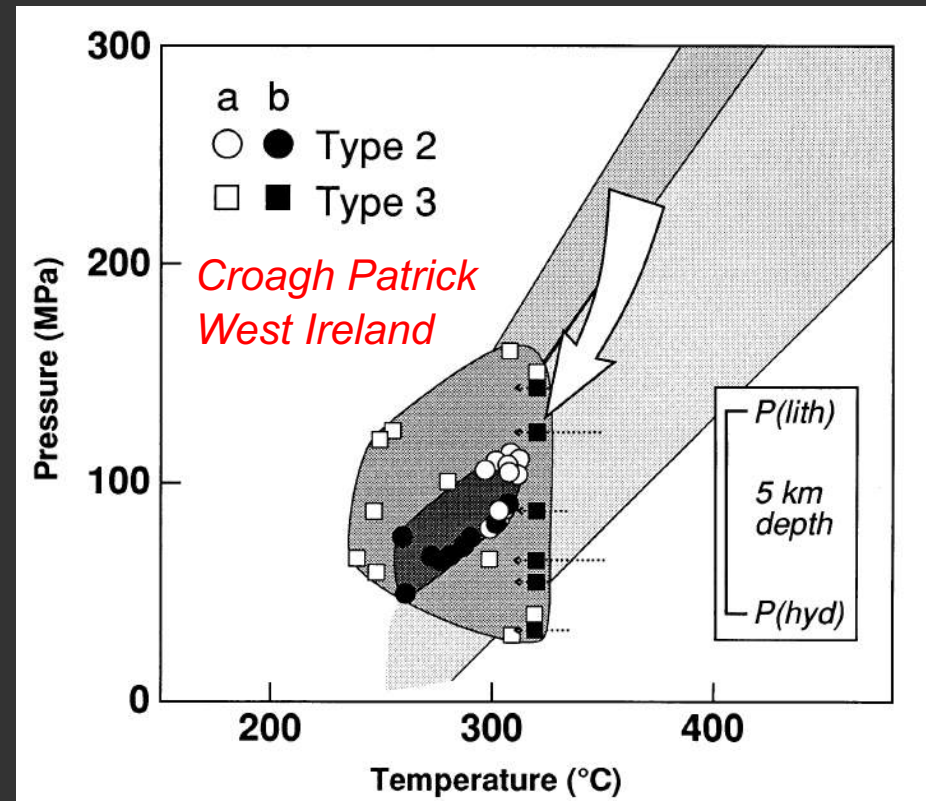
*Cross-Cutting Flats & Fault-Veins,
Pascal Nord Mine, Abitibi Belt*



Fluid Inclusion Records of Pressure Cycling

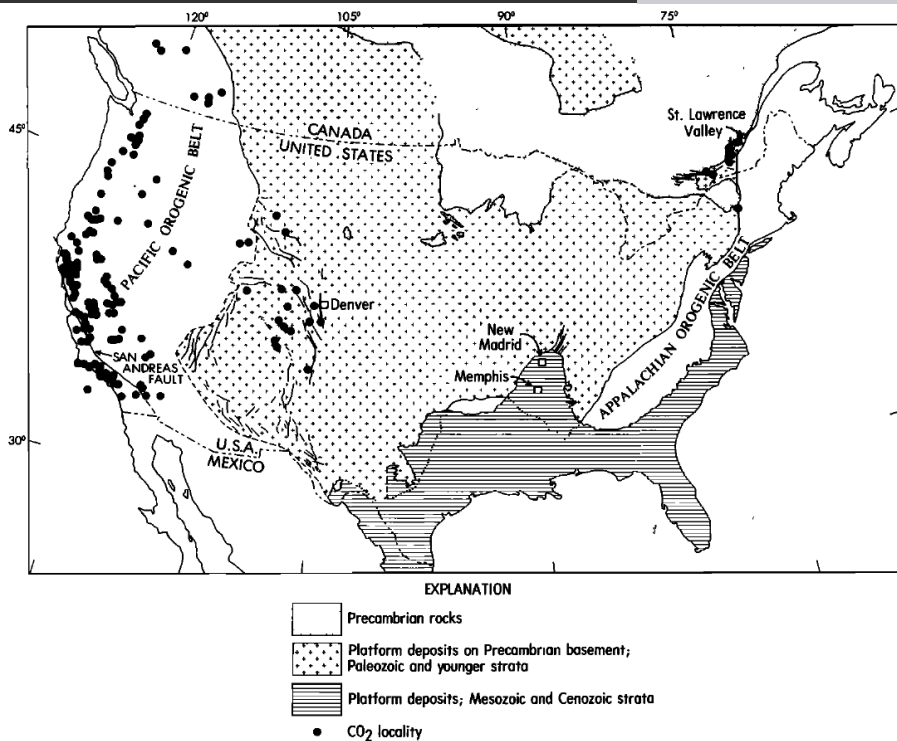
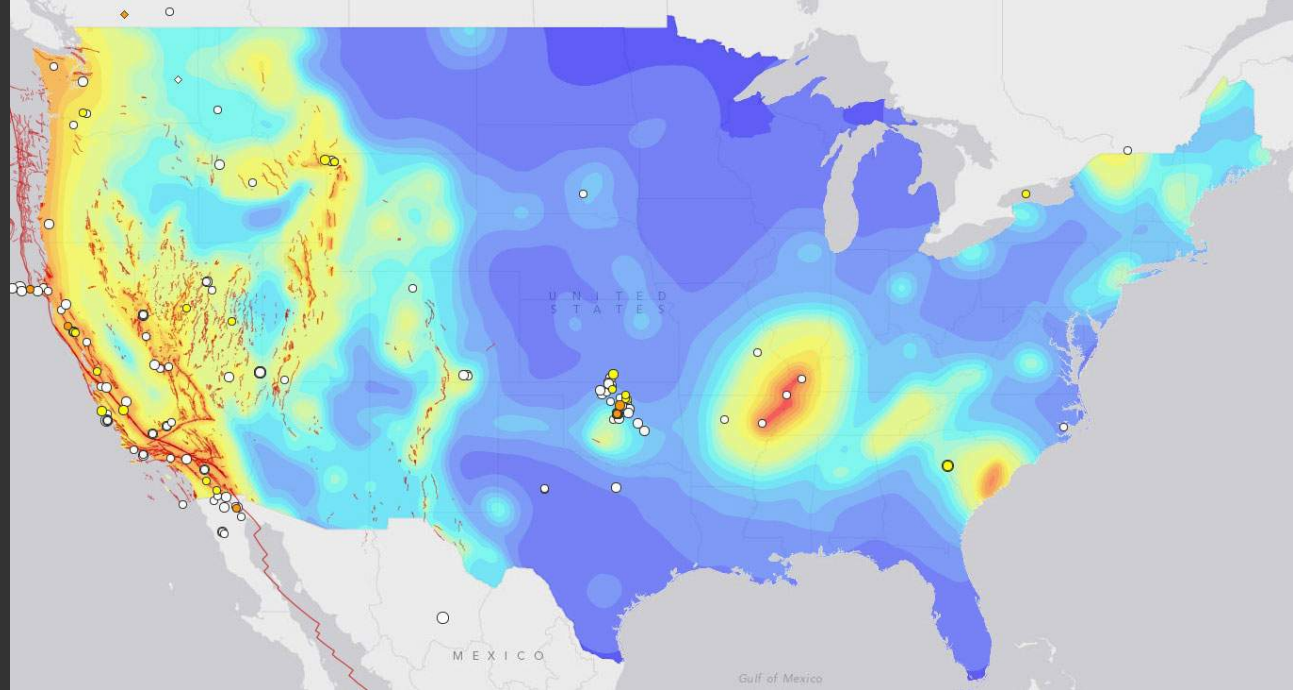


- Parry and Bruhn, 1990:
Tectonophysics 170, 335-344



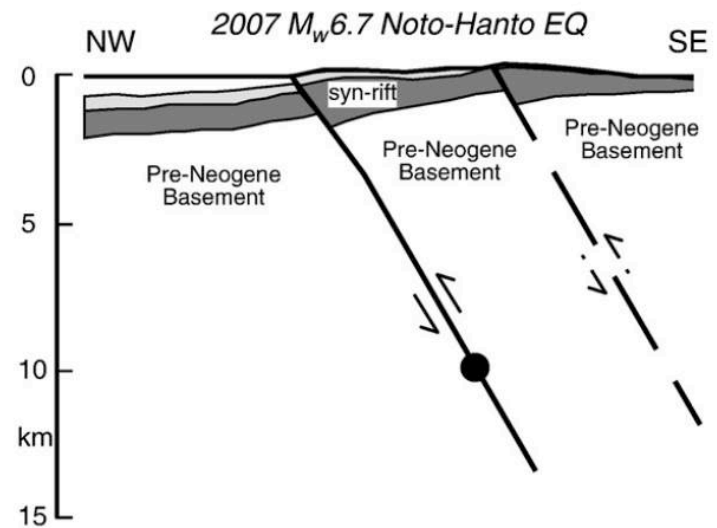
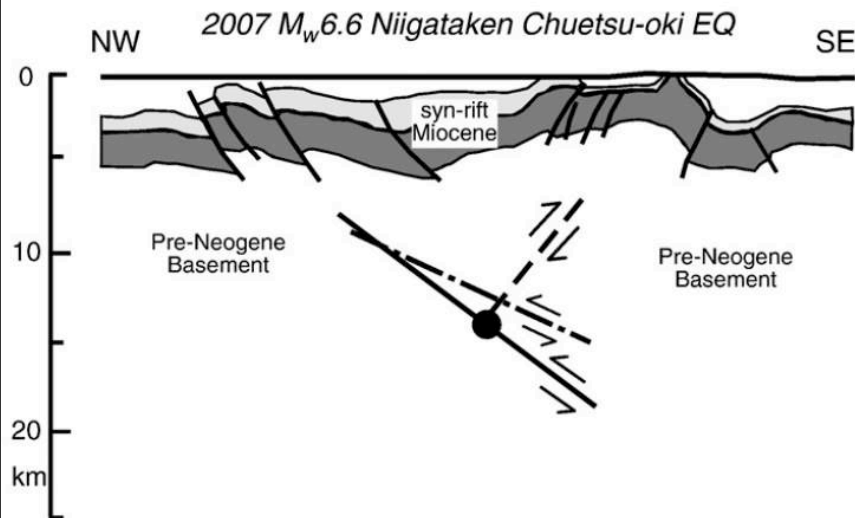
- Wilkinson and Johnston, 1996:
Geology 24, 395-398

Seismicity and CO_2 rich springs

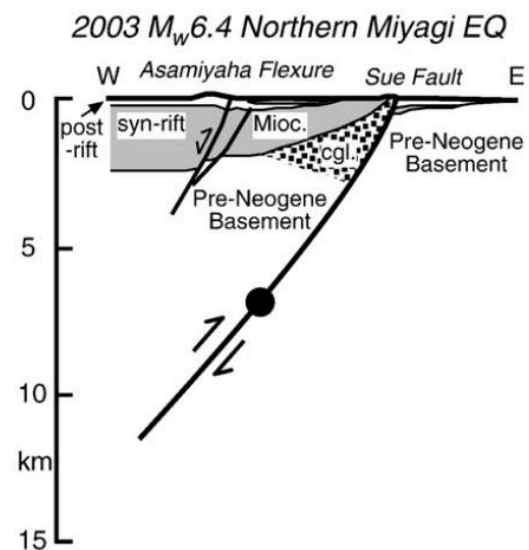
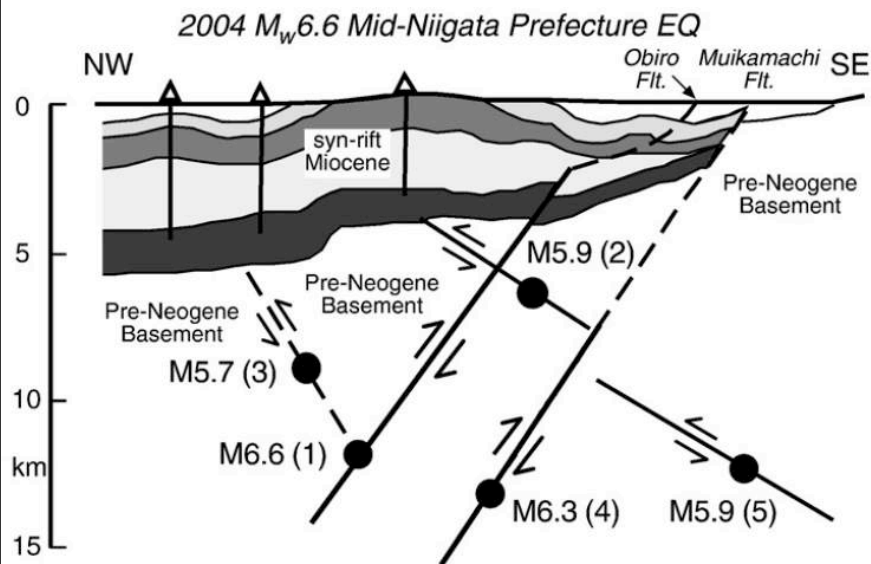


Irwin & Barnes, 1980: *J. Geophys. Res.* 85, 3115-3121

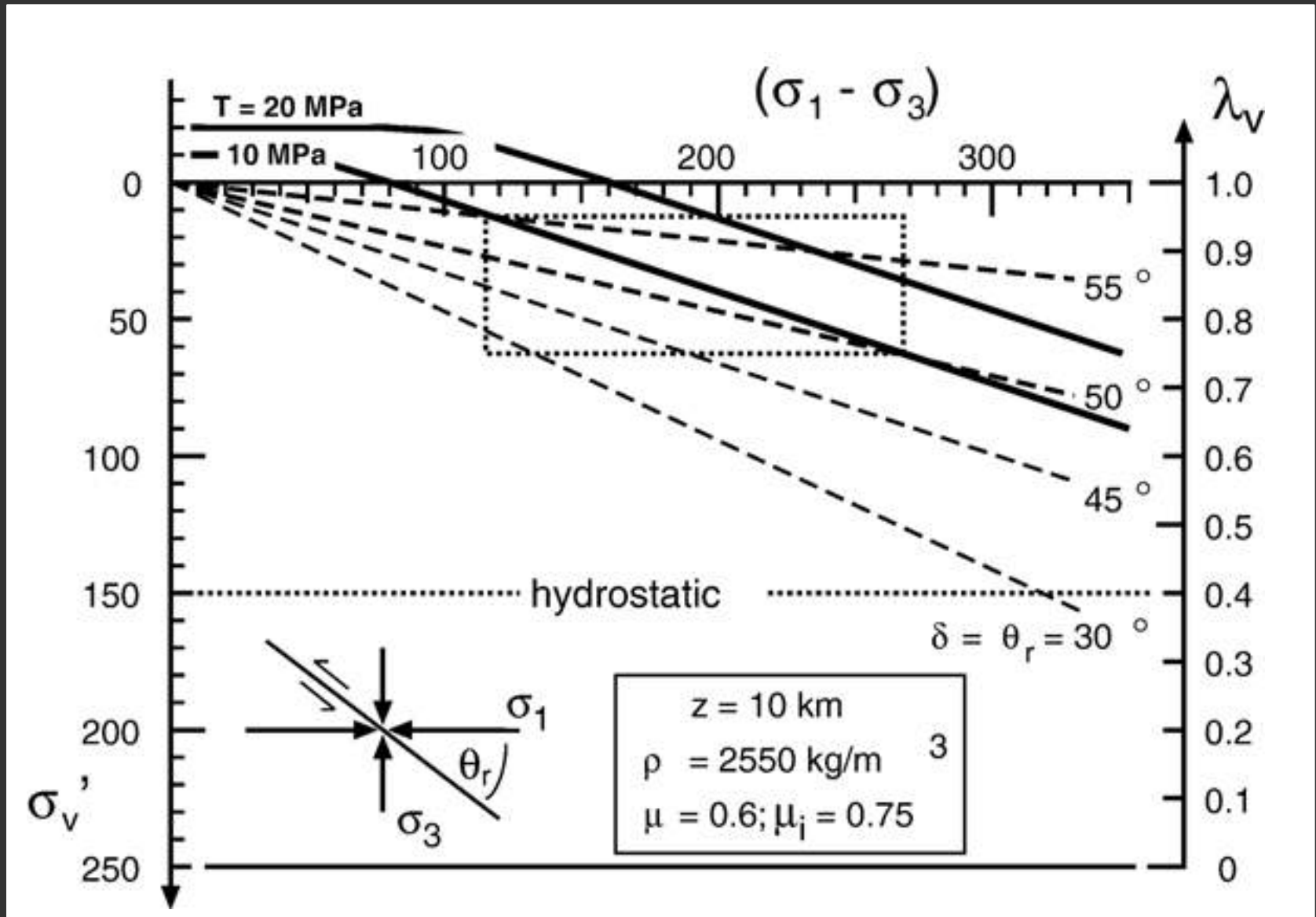
Northern Honshu Inversion Earthquakes



- Sibson, 2009: *Tectonophysics* 473, 404-416

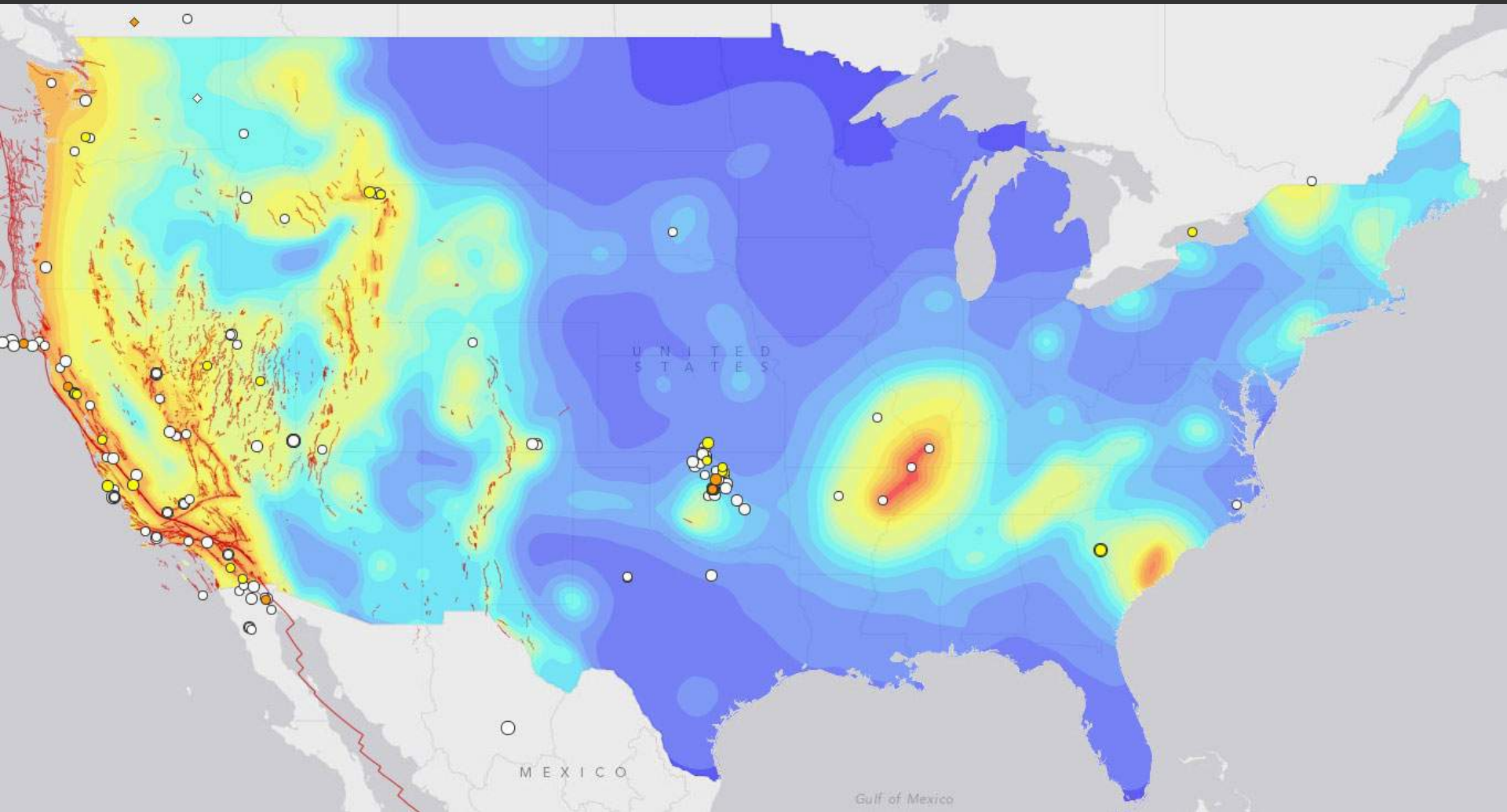


Competition between Inherited and New-Forming Reverse Faults

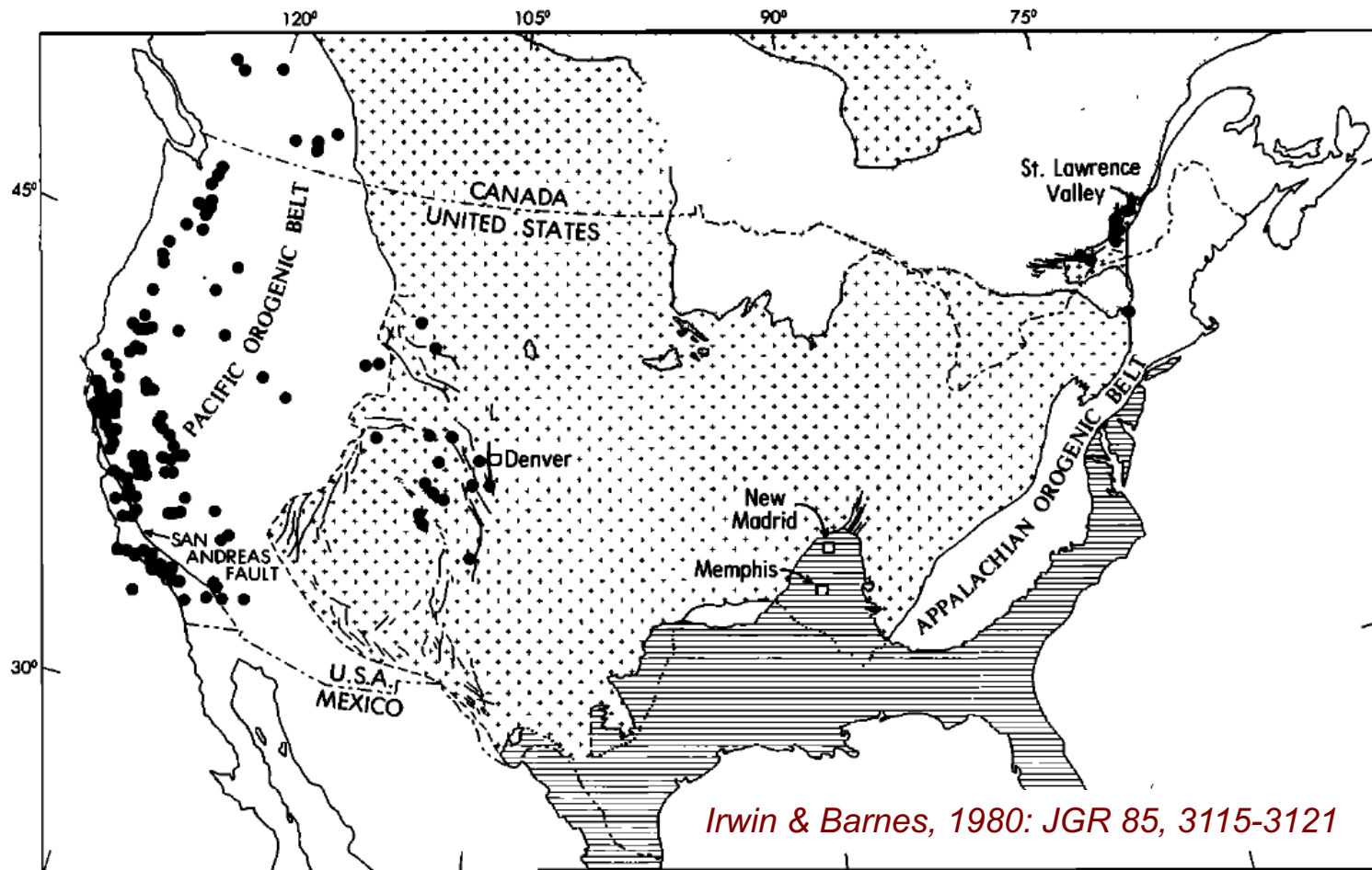


How many EQs are fluid-driven?


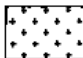


- Anthropogenic vs. Natural?



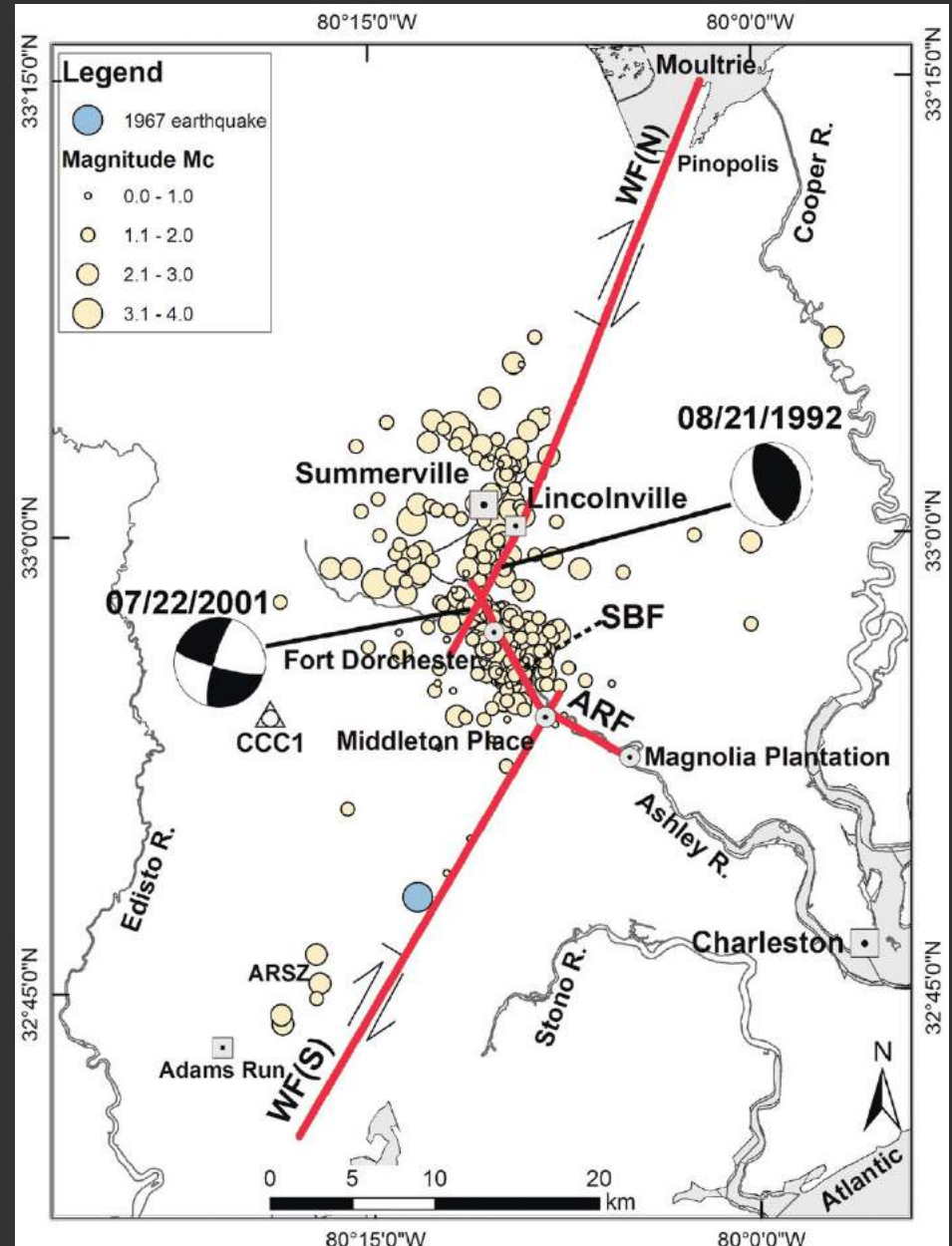
Seismicity and CO₂ rich springs



EXPLANATION

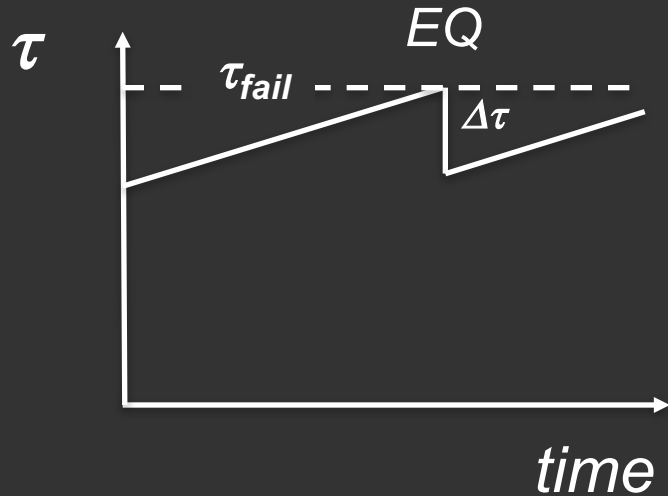
-  Precambrian rocks
-  Platform deposits on Precambrian basement; Paleozoic and younger strata
-  Platform deposits; Mesozoic and Cenozoic strata
-  CO₂ locality

1886 Charleston EQ Source Mechanisms



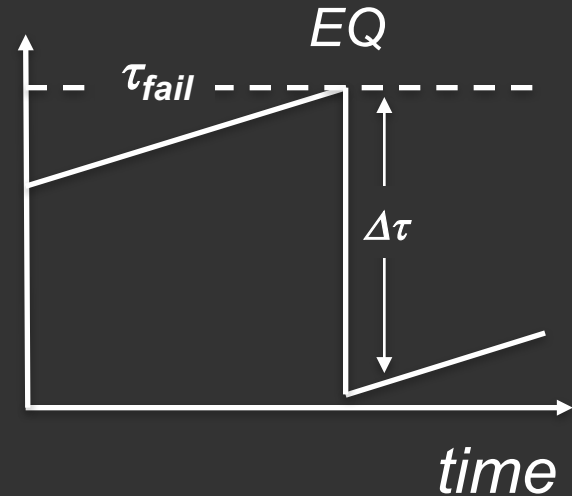
Dura-Gomez & Talwani, 2009

Partial vs. Near-Total Stress Relief



$$\Delta\tau/\tau_{fail} \rightarrow 10\%$$

hydrostatically pressured faults ?



$$\Delta\tau/\tau_{fail} \rightarrow 1$$

approaching lithostatic overpressures ?

$$\Delta\tau/\tau_{fail} \rightarrow 1$$

implies

$$\Delta\tau \approx \tau_{fail}$$

requiring either

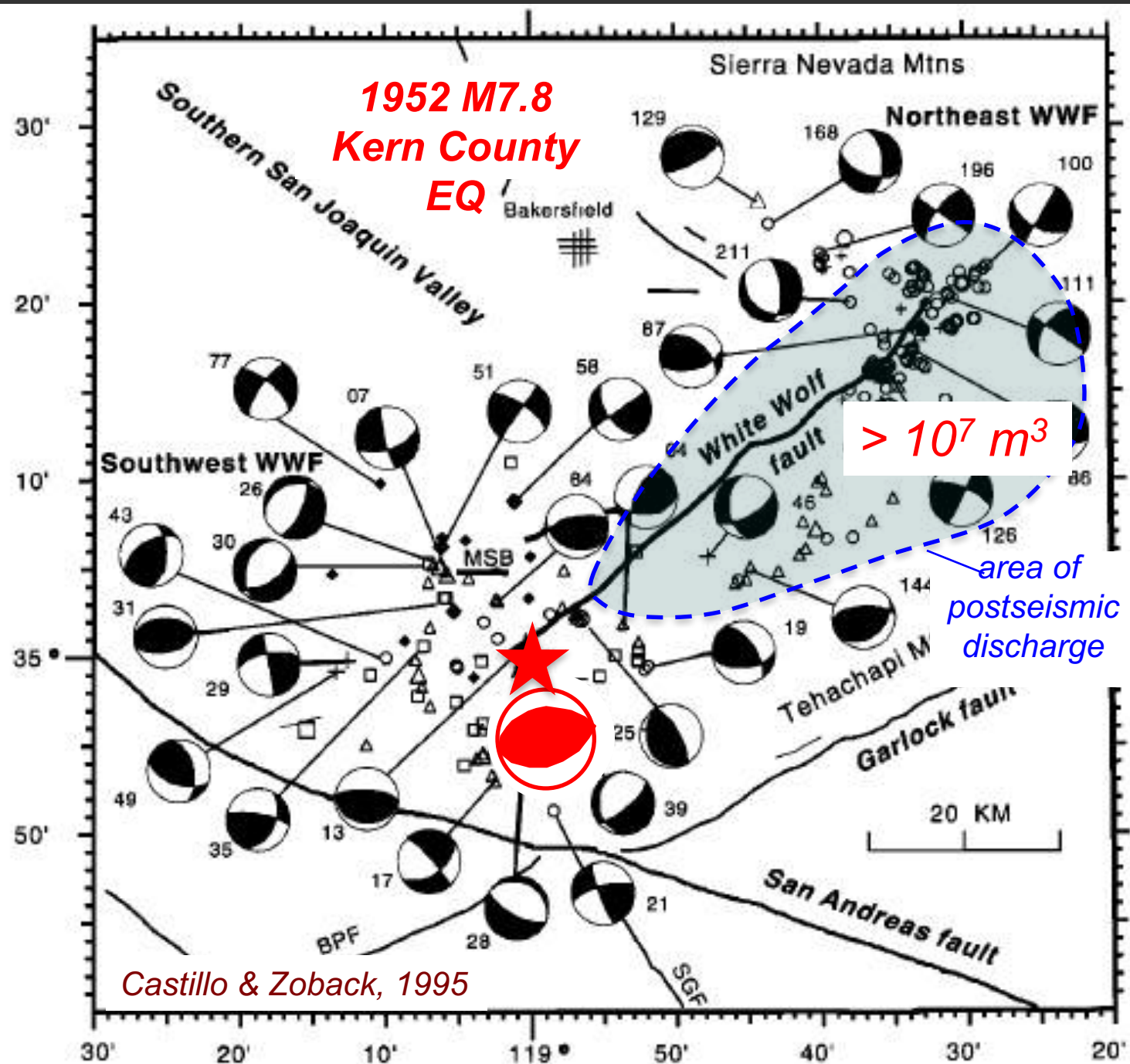
$$\mu_s < 0.1$$

or

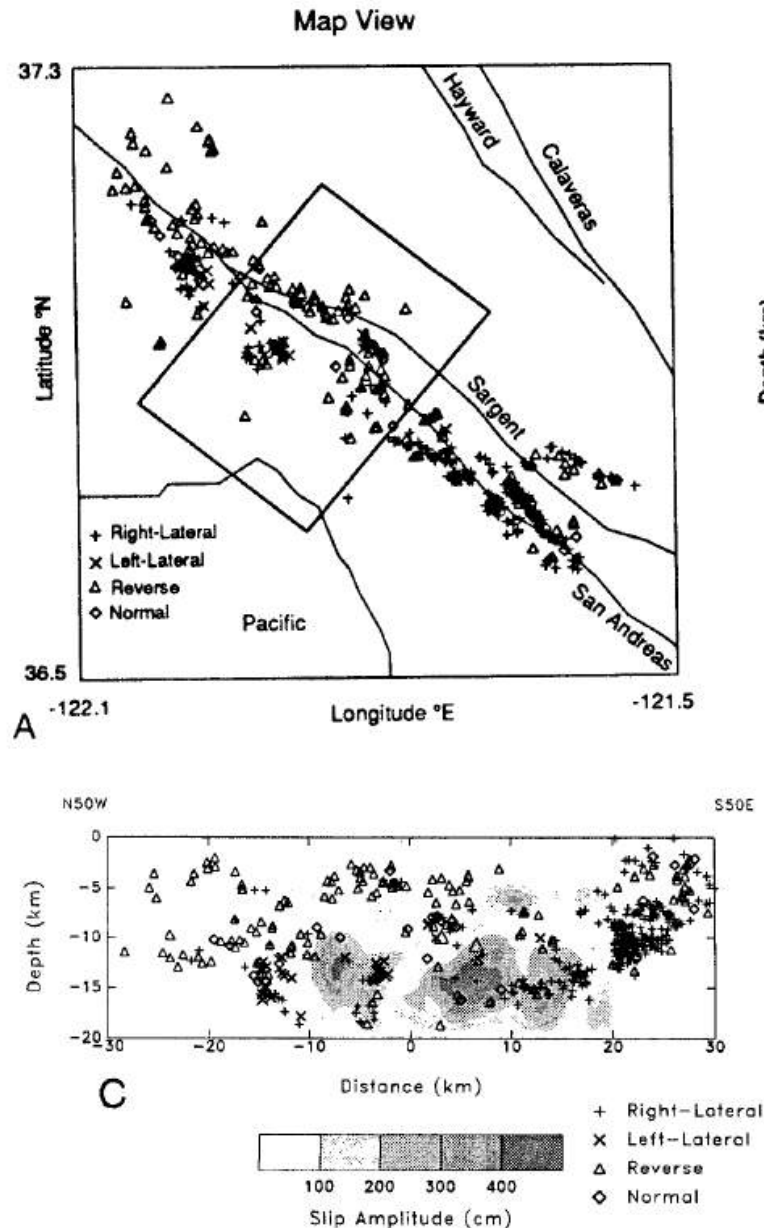
$$P_f \rightarrow \sigma_n \quad (\text{i.e. } \lambda_v \rightarrow 1.0)$$

EQs with Near-Total Shear Stress Drop

1952 M7.7 Kern County EQ	Steep Reverse	Castillo & Zoback, 1995
1989 M6.9 Loma Prieta EQ	Dextral > Reverse	Zoback & Beroza, 1993
2002 M7.9 Denali EQ	Dextral SS	Wesson & Boyd, 2007
2008 M7.2 Iwate-Miyagi-Nairiku EQ	Reverse	Yoshida et al., 2014
2011 M6.6 Fukushima-Hamadori EQ	Normal	Yoshida et al., 2015
2011 M9.0 Tohoku-Oki EQ	Megathrust	Hasegawa et al., 2012



1989 M6.9 Loma Prieta EQ



*Zoback & Beroza, 1993:
Geology 21, 181-185*

Figure 1. Loma Prieta aftershocks occurring in first 21 months after October 17, 1989, main shock with well-determined mechanisms and with one nodal plane subparallel ($\pm 30^\circ$) to main-shock fault plane. Symbols show sense of slip on nodal plane subparallel to main-shock plane as well as relative sizes of aftershocks. Shown are 517 earthquakes for which focal mechanisms are determined within $\sim 30^\circ$ at 90% confidence (D. Oppenheimer, 1991, personal commun.). A: Map view of events located within 30 km of main-shock hypocenter (along strike) and within 10 km of fault plane. B: Cross-section view of aftershocks that occurred within 10 km along strike of hypocenter projected onto N50°W. Limits of this projection are shown in A. C: Longitudinal view of fault zone as viewed from southwest and centered laterally on main-shock hypocenter. Gray shading indicates amount of slip in main shock (after Beroza, 1991). Main-shock hypocenter occurred at depth of 18 km.